N° of order: 40946

Université Lille1 Sciences et Technologies

LILLE 1 UNIVERSITY - SCIENCE AND TECHNOLOGY

Doctoral school: Sciences Pour l'Ingénieur n° 72

THESIS

in order to become

Doctor

Subject: Micro and Nanotechnologies, Acoustics and Telecommunications

defended by

GU Wei

Robustness against interference in Internet of Things

Defended on 14th November, 2012

Dissertation committee:

DUFLOS	EMMANUEL	Professor, Lille 1 University/Ecole centrale de Lille	Chairman
GELLÉ	GUILLAUME	Professor, University of Reims Champagne-Ardenne	Reporter
GOALIC	ANDRÉ	Senior lecturer, University Bretagne Occidentale/TELECOM Bretagne	Reporter
PETERS	GARETH	Associate professor, University College London (UK)	Examiner
ZANELLA	ALBERTO	Senior Researcher, National Research Council of Italy (Italy)	Examiner
BENOÎT	DENIS	Research Engineer/Project Manager, CEA-LETI Minatec	Examiner

Ph. D. thesis supervised by:

LAURENT	CLAVIER	Professor, Lille 1 University/TELECOM Lille 1
NATHALIE	ROLLAND	Professor, Lille 1 University

N° d'ordre: 40946

Université Lille1
Sciences et Technologies

UNIVERSITÉ LILLE 1 - SCIENCES ET TECHNOLOGIES

École doctorale : Sciences Pour l'Ingénieur n° 72

THÈSE

pour obtenir le grade de

docteur

Discipline : Micro et nano technologies, acoustique et télécommunications

présenté par

GU Wei

Robustesse aux interférences dans l'Internet des objets

Soutenue le 14 novembre 2012

Jury :

DUFLOS	EMMANUEL	Professeur, Université Lille 1/Ecole centrale de Lille	Président
GELLÉ	GUILLAUME	Professeur, Université de Reims Champagne-Ardenne	Rapporteur
GOALIC	ANDRÉ	Maitre de conférence, Université Bretagne Occidentale/TELECOM Bretagne	Rapporteur
PETERS	GARETH	Professeur associé, University College de Londres (UK)	Examinateur
ZANELLA	ALBERTO	Chercheur en chef, National Research Council of Italy (Italy)	Examinateur
BENOÎT	DENIS	Ingénieur de recherche/Manager du projet, CEA-LETI Minatec	Examinateur

Thèse dirigée par :

CLAVIER	LAURENT	Professeur, Université Lille 1/TELECOM Lille 1
ROLLAND	NATHALIE	Professeur, Université Lille 1

Keywords: Sensor networks, Multiple-Access-Interference, stable distribution, turbo codes, cooperative communications, distributed channel coding

Mots clés : réseaux de capteurs, interférences d'accès multiple, distribution stable, turbo-codes, communications coopératives, codage canal distribué

This thesis was prepared in

Institut de Recherche sur les Composants logiciels et matériels pour l'Information et la Communication Avancée
Parc Scientifique de la Haute Borne
50, avenue Halley
B.P. 70478
59658 Villeneuve d'Ascq, France
☎ + 33 (0) 3 62 53 15 00
FAX +33 (0) 3 20 71 70 42
✉ secretariat@ircica.univ-lille1.fr
Site http://www.ircica.univ-lille1.fr/

I dedicate this work
to my parents and my wife,
who supported me all the time during the writing.

"I just wondered how things were put together."

Claude SHANNON

Acknowledgements

First of all, I would like to thank sincerely my supervisor Dr. Laurent Clavier, professor at IEMN - IRCICA and TELECOM Lille 1 institute, for his kind support and help throughout the work of my thesis. He was always keen and patient to answer my questions and proof-read my work. He has motivated me a lot and led me in the right direction, providing in the same time some freedom to carry out my research. His guidance, his encouragement and his belief in me were precious and valuable to my future work.

My gratitude is extended to Pr. Nathalie Rolland, director of CSAM group in IEMN, and Pr. Paul-Alain Rolland, former director of CSAM group of IEMN, former director of IRCICA laboratory, as well. They supported me all along my project and offered me an excellent research environment with well equipped facilities. As two of my master teachers, they also gave me a very solid theory foundation which was so helpful for my thesis work.

I must appreciate the cooperation work with Dr. Garath Peters, lecturer at University of New South Wales, Dr. Ido Nevat, research fellow at CSIRO, and Dr. François Septier, assistant professor at TELECOM Lille1. They have enlightened me in one part of my work and helped me find an efficient solution to some difficulties. Thanks to their help, my research has been greatly broadened and enriched.

My appreciation is also extended to my colleagues Kouakou Koussi, Benoit Bensahla Tani, Aymeric Pastre, and some former colleagues Dr. Jiajia Chen, Dr. Mingdong Li, Dr. Lin Jin, Dr. Hassen Ben Maad and Dr. Abdelbasset Massouri, for their kind help and valuable discussions which corrected and extended my learning in the communications domain.

I am also grateful for the service provided by Michel Soulage, Ahmed Ben Abdeselam, Peggy.Stankowski and other staff at IRCICA laboratory. They have resolved a lot of problems for me and furnished me a comfortable working environment.

At last, I should give my great thanks to my parents and my wife. They always had trust and confidence on my decisions and encouraged me throughout my work of thesis. Without their support, I cannot have such an achievement.

This work was also supported by the ERDF (European Regional Development Fund) and the Nord-Pas-de-Calais Region (France).

Abstract

Internet of Things brought great interests in recent years for its attractive applications and intelligent structure. As a part of the "Internet", the implementation of sensor networks still presents some important challenges such as interference rejection and energy cost. The multiple-access-interference (MAI) generated by other nodes in a sensor network exhibits an impulsive nature. Both the MAI and the thermal noise should then be considered due to the strong impairments each may cause on the reception quality at destination nodes. We use stable distributions to model the MAI, due to their heavy-tail property, and employ Gaussian distribution to model the thermal noise. Employing the conventional decoder and receiver will generate significant performance degradation. We first study the performance of turbo codes in the direct link and we propose the p-norm as a decoding metric to replace the conventional Euclidean distance metric. Simulation results show that the p-norm allows a considerable error correction improvement compared with other alternative metrics such as Euclidean distance or Huber function, and the performance appears to be close to the optimal decoder. We then investigate cooperative communications. We consider optimal receiver design and develop an importance sampling approach to perform the estimation of the optimal receiver in the presence of stable and Gaussian noises. Such an approximation approach to the optimal receiver is computationally expensive. Hence we also develop several suboptimal linear and non-linear receivers, including an approximation approach based on the Normal Inverse Gaussian (NIG) distribution. We demonstrate that the NIG receiver provides a computationally efficient solution close to the optimal receiver. In addition we show that the p-norm receiver appears to have robust performance no matter what kind of noise is dominant. At last we combine the channel coding and cooperative communication works to establish a distributed channel coding strategy, with a mixture of distributed turbo and MRC coding techniques. Through some simulation assessment, an energy saving strategy can be realized by choosing an appropriate distributed channel coding scheme based on the direct channel quality and target bit error rate level.

Résumé

L'Internet des objets a attiré beaucoup d'attention ces dernières années du fait du nombre de ses applications et de la structure intelligente. Comme une partie de l'Internet, la mise en œuvre des réseaux de capteurs soulève encore de nombreuses difficultés, comme le rejet des interférences et le coût énergétique. Les interférences d'accès multiple (MAI) générées par les autres nœuds dans un réseau de capteurs présentent un caractère impulsif. Les MAI et le bruit thermique doivent être considérés simultanément car ils influencent fortement la qualité de la réception au niveau des nœuds de la destination. Nous utilisons des distributions stables pour modéliser les MAI du fait de leur queue lourde, et employons la distribution gaussienne pour modéliser le bruit thermique. L'utilisation du décodeur et du récepteur classique conduit à une dégradation importante des performances. Dans un premier temps, nous étudions les performances des turbo codes en lien direct, proposant la norme-p comme une métrique de décodage pour remplacer la distance euclidienne. Les résultats des simulations montrent que la norme-p permet une amélioration considérable de correction d'erreur par rapport à d'autres métriques telles que la fonction de Huber, et sa performance apparaît être proche du décodeur optimal. Ensuite nous étudions les communications coopératives, considérant la conception du récepteur optimal et nous développons une approche d'échantillonnage importance pour effectuer l'estimation des performances du récepteur optimal en présence des bruits stable et gaussien. Une telle approche pour mettre en œuvre le récepteur optimal est coûteuse en calcul. Nous développons donc également plusieurs réalisations sous-optimales pour les récepteurs linéaires et non linéaires, y compris une approche basée sur l'approximation de la distribution stable par la distribution gaussienne inverse normale (NIG). Nous démontrons que le récepteur NIG fournit une solution de calcul efficace pour approcher le récepteur optimal. Nous montrons également que la norme-p a des performances robustes, quel que soit le type de bruit dominant. À la fin nous combinons les travaux du codage canal et des communications coopératives, établissant une stratégie de codage canal distribué. Une stratégie d'économie d'énergie peut être mise en place en choisissant un schéma approprié du codage canal distribué, basé sur la qualité du canal direct et le niveau du

taux d'erreur par bit.

Contents

List of Tables

List of Figures

Introduction

"The concept of Internet of things refers to the transparent connection of apparatuses, sensors, objects, buildings, machines, vehicles, etc. via fixed and wireless networks". It will play in the near future an essential role in the evolution of telecommunications, from an economic as well as a sociological perspective. However many challenges remain before making possible an effective and widespread use of these sensors and their implementation. Energy and cost constraints are critical for the development of economically sustainable applications. Besides, it appears clear that applications with a strong potential will appeal to active technologies, meaning they will use objects that are able to spontaneously transmit and give accurately localized information. Hence it is important that technological solutions can anticipate the environmental evolution. Particularly, interference between objects will rise sharply due to the high increase of simultaneous transmissions and the unavoidable reduction of transmitted power per object. It will become a fundamental limitation to the future systems. This Ph.D. thesis aims at bringing innovating solutions, especially at the physical layer, in digital communications and signal processing, to better address against such interference.

With respect to network interference, the modelling problem has been raised in many literatures as an interesting and vital issue [58, 75, 47, 20, 77]. The conventional approach is to model the network interference with Gaussian random variables. This is true if the interference is accumulated by numerous independent and identically distributed (i.i.d.) signals, which leads to a justification with the central limit theorem. However, many circumstances encountered in real system are determined to be non-Gaussian, like underwater acoustic signals, low frequency atmospheric noise, and some man-made noise for instance. Similarly in dense sensor networks, the multiple-access-interference (MAI) is often the main contribution to the noise; it presents an impulsive behaviour and is shown to be non-Gaussian. Significant performance degradation will occur when applying optimized system under the Gaussian assumption in a non-Gaussian environment. Thus a more accurate statistics model is needed and considered in

the first time.

Stable distributions are often evaluated and justified in such environment as an appropriate model for impulsive interference [77, 58, 38, 73, 50]. As the tails of the density functions decay less rapidly than in the Gaussian case [58], stable distribution is proved more suitable for describing signals with sharp but occasional bursts. In addition, stable law is a generalization of the Gaussian distribution and the Gaussian and Cauchy distributions are both special cases. Therefore, stable distributions are employed in this thesis as the network interference model, and their symmetric sub-family is considered and noted as symmetric α-stable (SαS) distribution. One difficulty lies in the interference strength measurement, because the second-order moment of a SαS variable is infinite [58, p.22, theorem 3] when $\alpha < 2$. Some solutions exist and we employ the geometric power framework proposed in [40] as an alternative measurement.

Sensor networks are composed of several nodes which are scattered randomly and effectuate communications in *ad hoc* mode without a control centre. If channel knowledge from such an *ad hoc* network is not available, the channel coding technique should be a rather effective and efficient method in dealing with network interference. Among several channel coding types, the turbo codes are a powerful and excellent candidate, due to their performance close to the Shannon limit [8, 80].

In a first step, we investigate the sensor network from a direct link, with a limited knowledge of the network. Thus turbo codes is firstly considered and evaluated in an impulsive environment where both the Gaussian noise and SαS interference are present. BCJR maximum a posteriori (BCJR MAP) algorithm [2] is employed as decoding method for turbo codes. Since the interference model is changed, the conventional metric used in the decoding algorithm (Euclidean distance) is no longer optimal. In fact, the Euclidean distance used in the decoding algorithm cannot deal with the impulsive interference and gives an unacceptable decoding performance. The distance metric used in the decoder has to take into account that the large amplitudes may be impulsive interference samples rather than highly reliable ones.

However, the difficulty of changing the distance metric in the decoding algorithm lies in the absence of explicit probability density function (PDF) of SαS distributions, which is necessary to decide the log-likelihood ratio (LLR) decision statistics. Some decoding metrics have been proposed such as Huber function [24] or 1-norm metric [21] and used as an alternative distance measurement. A more direct method is based on the numerical inverse Fourier transform of the characteristic function of SαS distributions [67], in respect that the characteristic function is the Fourier transform of the PDF. For the sake of finding a more suitable decoding metric corresponding to SαS model, we propose to use the

p-norm inspired by the fractional lower order moments (FLOMs) and α-stable norm. Since the distance between two SαS random variables measures the p^{th}-order moment of the difference of these two random variables [58], the p-norm should bring a wide adaptation for all kinds of SαS environments, only if the condition $0 < p < \alpha$ is fulfilled. The advantage of the p-norm is that is does not require to estimate all the noise parameters but only to have a rough idea of the characteristic exponent α in order to choose a p such that $0 < p < \alpha$.

The second part of the works concern cooperative communications and robustness to interference. Receiver design is an arduous task due to some existing constraints, as communication impairments resulting from wireless propagation effects, network interference and thermal noise [77]. We consider a slow-fading channel for the propagation effects. The channel coefficients are constant for each time slot and change independently from one time to another. We still adopt SαS models to capture the effects of network interference. Additional to and independent from this interference is the thermal noise at the destination, caused by receiver equipment, which is commonly modelled as a Gaussian distribution. Hence, the combined noise is captured by the convolution between an independent, symmetric stable distributed network interference and a Gaussian thermal noise, the result of which is not in general stable distributed.

We improve the robustness against interference by the cooperation of network nodes, referred to as cooperative communications, the helping nodes serving as relays. We study a two-hop decode-and-forward relaying scheme: a set of relays is selected among all possibilities. The selected relays are the ones with the strongest relay-to-destination channel. When considering optimal receiver in this context, one faces a challenge for an efficient design due to its inherent intractability, arising from the convolution between network interference and thermal noise. Some proposed receivers [50, 13, 73] give feasible but complex solutions. We provide several ideas for designing either optimal or suboptimal receivers which are efficient alternatives, and a global comparison of the proposed approaches. A careful study of the decision strategy is developed in a cooperative communication in the presence of non-Gaussian network interference and Gaussian thermal noise; An original strategy by developing a Normal Inverse Gaussian (NIG) receiver is proposed. We compare it to a novel adaptation of the p-norm strategy, noting that the p-norm has already been proposed in other contexts, especially with generalized Gaussian distributions [5]. Performance of these two suboptimal strategies is studied as a function of the noise-to-interference ratio, comparing with the optimal receiver which is computationally inefficient but studied through importance sampling approach. Other conventional receiver design strategies such as linear (Gaussian) receiver, maximum ratio combiner [59], Cauchy receiver [38], hole puncher and soft limiter

[58] are compared as well,

The p-norm approach and the NIG approximation method appear to be attractive solutions. The first one does not require any noise parameter estimation (at most only a rough estimation of α is sufficient). The second one has flexible and efficient Moment Matching based closed form solutions for its parameter estimation. They perform both better than the other conventional receiver approaches.

Since energy consumption issue is very sensitive to sensor networks, the massive use of relays will demand a lot of energy cost thus a more intelligent strategy may be welcome. Based on the study of turbo coding in direct link and cooperative communications in the whole network, we proposed a mixture of these achievements by establishing a distributed channel coding strategy, in the sense of minimising network energy consumption. The intervention of relay gives support for the transmission if the source-to-destination link is badly impacted by the network interference.

Compared with repetition algorithms based on amplify-and-forward relaying protocols [27], distributed channel coding allows a more flexible distribution of channel symbols between source and relay nodes. We build some distributed channel coding schemes, taking idea from the distributed turbo codes [14] and recursive systematic convolutional (RSC) codes. BCJR MAP decoding algorithm applied for distributed turbo codes and Viterbi algorithm for RSC codes, a flexible choice can be made among several schemes based on a bit error rate (BER) target level, since the transmission of data costs much more energy than decoding operations. Hence the energy saving problem with the reduction of decoding error in a sensor network is possible and feasible, according to some simulation demonstrations in this thesis.

The rest of this thesis is organised as follows. Chapter 1 introduces the stable distribution used as a statistics model for MAI in sensor networks. Parameter estimation methods and generation process give a first look of stable distributions. A demonstration of the stable model for MAI is then provided. Geometric power framework is discussed and is employed in this thesis as an alternative method for representing SαS interference strength. Then the statistics model is validated by some illustrations. In order to show how the stable distribution is applied in communication works, some receiving strategies with simulation results are finally presented.

Chapter 2 is devoted to the channel coding study in the direct link of sensor networks. Turbo codes are introduced with their encoder and decoder structures. The BCJR MAP decoding algorithm is detailed with LLR calculation procedure. When applying turbo codes in MAI environment, some alternative metrics

adapted to SαS model are presented such as Huber function metric, numerical-base PDF calculation approach and p-norm metric. Simulations have been carried out for BER performance comparison of discussed decoder methods in both stable interference only and stable plus Gaussian noise cases.

Chapter 3 focuses on the cooperative communications. We describe the system scenario and state a detection problem, based on which the optimal receiver in the form of LLR is studied. Then we consider some suboptimal solutions involving both linear and non-linear approaches. The NIG distribution is introduced and the Method of Moments based approximation is provided, with analytical solutions after restriction to a symmetric sub-family, but no restriction required for the kurtosis. We finally compare these receiver design approaches with simulations, introducing an importance sampling (IS) approach for the optimal decision statistics calculation.

Chapter 4 addresses the distributed channel coding technique in cooperative communications. In the sense of minimising energy consumption based on an expected level of BER in sensor networks, some distributed channel coding schemes are provided, using distributed turbo codes and RSC codes. The energy consumption amount for each scheme is then assessed, which leads to a scheme choice study based on some simulation results.

We finish this report by drawing a general conclusion with some perspectives stimulated by the works of this thesis.

Chapter 1

Multiple-Access-Interference environment

In this chapter, we will describe the noise environment and its mathematical model. Traditionally, digital communication problems are studied under the Gaussian model. Gaussian assumption is reasonable in a lot of circumstances and can be justified by the Central Limit Theorem: the noise is considered to be the sum of numerous independent and identically distributed (i.i.d.) random variables with finite variance [58]. The most attractive fact is that under the Gaussian model, many problems can have analytically tractable solutions. For the decoder or receiver design in wireless networks, if the channel is assumed to be embedded in an Additive White Gaussian Noise (AWGN), optimal solutions lead directly to linear approaches, which greatly simplifies the implementation work.

However, some works have been carried out in non Gaussian environment, like in dense sensor networks where multiple access interference (MAI) is often the main contribution to the noise. The MAI presents an impulsive behaviour [38], which shows totally different characteristics compared to Gaussian noise. We will introduce stable distributions in the following sections as a network interference model.

1.1 Interference model

Interference from undesired active users in a network will be a strong limitation in future networks performance. The interference model has been studied widely in information theory [17, 41, 65, 11]. If the exact capacity is not

known, some close approximations have been derived. The question on how to deal with interference is however still an open problem. In this regard a lot of works on multi-user detectors for instance have been proposed [74] but also, more recently, some new schemes for interference alignment [11] or amplifying interference [25] have been considered. However, those works aim at avoiding the interference and generally require some costly channel learning mechanisms or synchronization techniques.

An alternative perspective is to consider that a certain amount of interference will be unavoidable. Under such an assumption, a robust interference model can allow an effective design of receivers and networks to limit the resulting impact of such interference, be a powerful tool to study outage probability or connectivity in networks. For instance several works on stochastic geometry are based on similar interference models as we present in this thesis [37, 48]. If we consider κ_R to be a random variable representing the number of active interferers, in a rather general framework, the total interference is a random variable expressed according to $Y = \sum_{k=1}^{\kappa_R} A_k \psi_k$ where $(\psi_k)_{k=1,\cdots,N}$ are independent, identically distributed and bounded random variables with even probability density function that depends on the physical layer design (see [71, 78, 38] for different examples). The $(A_k)_{k=1,\cdots,N}$ are positive, independent, identically distributed random variables that depend on the channel characteristics and determine the statistical properties of the total interference Y.

To proceed, the most intuitive statistical approach would be to consider the asymptotic behaviour of the distribution of the total interference $Y \sim F(y)$ and to determine under what conditions such an interference would belong to the domain of attraction of a Gaussian family of distributions, denoted $\mathcal{D}_G(F)$. Such an approach involves considering an asymptotic regime where the number of interferers grows to infinity while the contribution of each interferer to Y becomes infinitesimal. In non-impulsive, non-sub exponential distributional settings, this would typically result in application of a form of the celebrated Central Limit Theorem: Y converges in law to a Normal distribution, such that $F(y) \in \mathcal{D}_G(F)$. However, in the general case in which impulsive noise is present it is well known that this asymptotic regime is not easily reached (see for example an in-depth study in [34] for impulse radio ultra wide band signals). Instead, the domain of attraction of impulsive noise models from the sub-exponential family, which are convolved to create the total interference $Y \sim F(y)$ can belong to the domain of attraction of a stable family of distributions, denoted $\mathcal{D}_S(F)$, for which $\mathcal{D}_G(F) \subset \mathcal{D}_S(F)$.

A common requirement for convergence of such a sequence of i.i.d. interferences to converge to the Gaussian domain of attraction, involves a restriction on the variance of such summands in the sequence. This is not present in im-

pulsive noise processes. One could argue that this feature may seem natural since it represents a channel attenuation, which by its very nature must be finite. However, the interference which is being modelled is actually compared to the desired link attenuation and can, in comparison, be "very large" and impulsive in nature. Such large impulsive realizations of the interference happen infrequently in practice but are sufficient to give an impulsive nature to interference. To capture these situations, heavy tailed distributions with infinite variance can be well suited while models with finite second order will fail to adequately capture such impulsive attributes observed. The generalized central limit theorem has then to be used (see [58, p. 22] or [64, p. 9]) and states that interference (for large κ_R) falls in the domain of attraction of a random variable with a stable distribution, $F(y) \in \mathcal{D}_S(F)$.

A general framework is proposed in [61] and application to cognitive radio with a modified law (truncated α-stable although the term truncated is slightly misleading) is presented in [63]. Here the truncation refers to a form of soft "tempering" of the stable distribution tails, as opposed to a hard threshold. To prove the validity of the α-stable assumption, the usual solution is to write its $\log$ Characteristic Function (CF) as $\varphi_Y(\omega) = -\sigma|\omega|^\alpha$. This can be done in many situations (users' repartition, channel conditions, physical layer... refer to [78] for more details). One strong advantage of this model over other proposed solutions is its theoretical foundations which we derive in the context of interference modelling from first principles for our domain of modelling, based purely on simple statistical assumptions on the system.

1.2 Stable distribution

1.2.1 Generalities

The α-stable distributions and variables are a direct generalization of Gaussian's and share many of its familiar properties. In particular:

- the convolution stability property, which means that the convolution of two stable distributions is also stable. In other words the sum of two independent stable random variables is also a stable one,
- the central limit theorem, which means that every stable random variable may be expressed as a limit, in distribution, of a normalized sum of independent and identically distributed random variables.

Another aspect that makes these distributions suitable for modelling is the fact that they are parametric. Indeed they are fully described by four parame-

ters. Since their discovery by Paul Levy in 1925, a great amount of knowledge has been accumulated about the theoretical properties of these probability distributions. On the other hand, they have been found to provide useful models for various application fields, especially phenomena with large fluctuations and high variability that are not compatible with the Gaussian models.

Except the Gaussian, the Cauchy and the Levy distributions which are special cases of the stable class, there is no exact expression of the probability density function of an $\alpha-$stable distribution. However we can approximate it through its characteristic function which is given by:

$$\Phi(\theta) = \begin{cases} \exp\{-\sigma^\alpha |\theta|^\alpha (1 - i\beta \text{sign}(\theta) \tan\frac{\pi\alpha}{2}) + i\mu\theta\} & \text{if } \alpha \neq 1 \\ \exp\{-\sigma|\theta|(1 + i\beta\frac{2}{\pi}\text{sign}(\theta)\ln|\theta|) + i\mu\theta\} & \text{if } \alpha = 1 \end{cases} \tag{1.1}$$

where

$$\text{sign}(\theta) = \begin{cases} 1 & \text{if} \quad \theta > 0 \\ 0 & \text{if} \quad \theta = 0 \\ -1 & \text{if} \quad \theta < 0 \end{cases} \tag{1.2}$$

α, σ, β and μ are the four parameters characterizing the stable distribution[1].

- α is called the characteristic exponent ($0 < \alpha \leq 2$) : it measures the thickness of the tail of the distribution. Thus larger is the value of α, less likely it is to observe values which are far from the central location.
- μ is the location parameter ($-\infty < \mu < \infty$) : for instance, in an observed sample most of the observations are concentrated about its value. It corresponds to the mean for $1 < \alpha \leq 2$ and to the median for $0 < \alpha \leq 1$
- σ is the dispersion parameter ($\sigma > 0$) : it is like the standard error in the case of a Gaussian distribution.
- β is the index of symmetry ($-1 \leq \beta \leq 1$) which characterizes the dissymmetry of the density function about its central location. When $\beta = 1$ we say that the distribution is totally skewed to the right; it is symmetric if $\beta = 0$.

[1]There exist several ways to define the characteristic function of a stable distribution. For instance the definition of parameter σ can be different. We recommend to be careful on the definition you use, especially when you share programs or use already implemented toolboxes.

Figure 1.1 presents the density function obtained for different values of the parameters α and β and illustrates their effect on the behaviour and the form of an α-stable distribution.

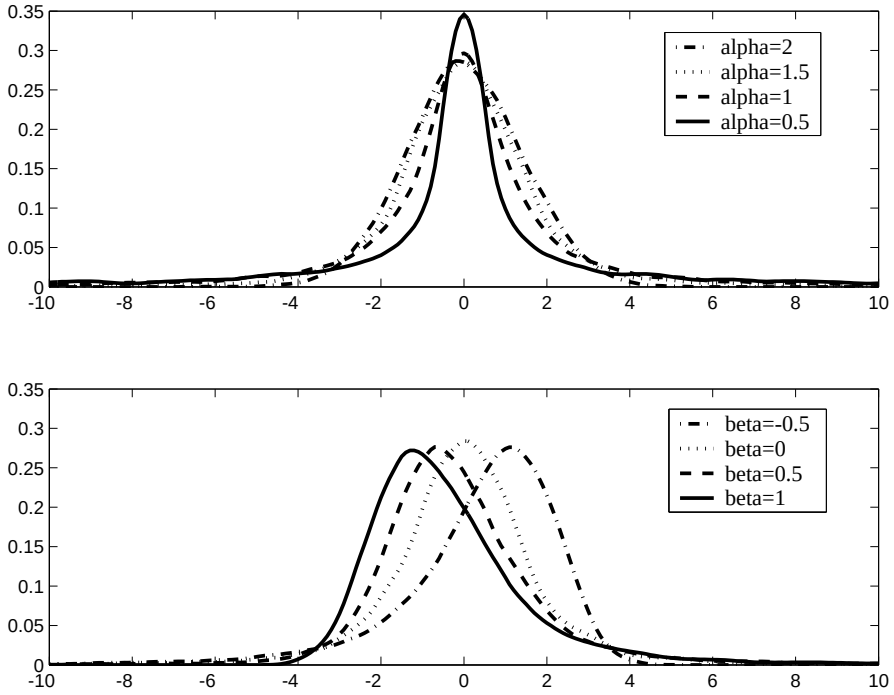

Figure 1.1: the probability density function of a stable distribution with $\mu = 0$, $\sigma = 1$ and different values of α and β

Figure 1.2 gives one example of symmetric α stable distribution. Stable laws with heavier tail are better suited for rare events modelling.

1.2.2 Parameter estimation

Due to the lack of analytical expression for most of the densities of α-stables variables, it is difficult to provide a simple estimator of its parameters. However in practical situations, it is very important to estimate these parameters from an observed sample, especially the index α and the scale parameter σ. Several methods have been proposed in literature, the most known are: Maximum likelihood techniques, the quantiles methods and the characteristic function based method.

- **Maximum likelihood method**: DuMouchel [29] was the first to obtain a Maximum Likelihood (ML) estimate of α and σ (assuming $\mu = 0$). Under some additional assumptions on $\hat{\alpha}$ and the likelihood function which

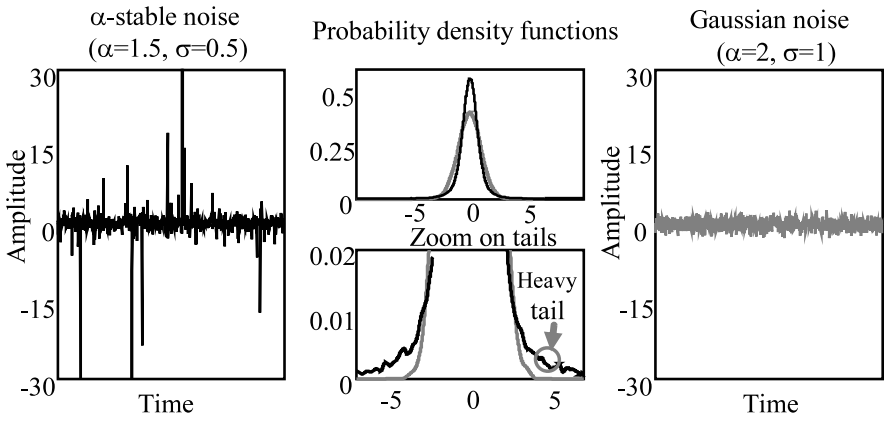

Figure 1.2: Comparison of probability density function for symmetric α stable distribution (α=1.5) and the Gaussian case (α=2)

was approximated by multinomial's, DuMouchel has shown the obtained estimates to be consistent and asymptotically normal. Another direct ML estimation was introduced by Brorsen and Yang [12]. It should be noted that ML techniques are asymptotically efficient but difficult to compute.

- **Quantiles method**: Fama and Roll [31] provided estimates for parameters of symmetric ($\beta = 0, \mu = 0$) stable laws with $1 < \alpha \leq 2$. Firstly, they have given an approximation of the parameter σ by using the properties of sample quantiles of a symmetric α-stable variable. Secondly, the parameter α is estimated by using the tail property of an α-stable distribution. Fama and Roll's method is simple but suffers from a small asymptotic bias in $\hat{\alpha}$ and $\hat{\sigma}$ and theoretical restrictions on α and β. In order to overcome this problem, McCulloch [54] generalized and improved this method. He provided a consistent estimator of all the four parameters, when $0.6 \leq \alpha \leq 2$, while retaining the computational simplicity of Fama and Roll's method.

- **Regression-type method**: Koutrouvelis [49] presented a regression-type method to estimate the four parameters. It is based on the following observations concerning the characteristic function $\phi(t)$ given in (1.1). First, from (1.1), it is easily seen that:

$$\log(\log|\phi(t)|^2) = \log(2\sigma^\alpha) + \alpha\log(|t|)$$

This last equation depends only on α and σ. We can then estimate these parameters by regressing $y_k = \log(\log|\phi(t_k)|^2)$ on $w_k = log(|t_k|)$ in the model:

$$y_k = m + \alpha w_k, \text{ and } k = 1, 2, ..., K$$

where $t_k = \frac{\pi k}{25}$, $m = \log(2\sigma^\alpha)$ and K is an appropriate integer chosen between 9 and 134. On the other hand, from (1.1) we can derive the following equation:

$$\arctan\left(\frac{Im(\phi(t))}{Re(\phi(t))}\right) = \mu.t + \beta\sigma^\alpha \text{sign}(\theta)\tan(\frac{\pi\alpha}{2})|t|^\alpha.$$

Then we can estimate β and μ by regressing $z_l = \arctan\left(\frac{Im(\phi(u_l))}{Re(\phi(u_l))}\right)$ on u_l and $\text{sign}(u_l)|u_l|^\alpha$ in the model:

$$z_l = \mu.u_l + \beta\sigma^\alpha.\text{sign}(u_l)\tan\frac{\pi\alpha}{2})|u_l|^\alpha, \text{ and } l = 1, ..., L$$

where $u_l = \frac{\pi l}{50}$ and L is an appropriate integer ranging between 9 and 70. For further details about these techniques see [49].

Many works have dealt with the performance of these three estimation techniques [76, 9]. It was shown that the regression-type method is a little better than both quantile methods (Fama-Roll's and McCulloch's) when α is close to 2. This can be explained by the small size of the tail when the population distribution approaches the Gaussian; quantile methods, especially McCulloch's, are slightly better for $0.6 \leq \alpha \leq 1.0$. However it cannot be used to estimate α when it is below 0.6. Finally, the characteristic function based method is easy to compute and appears to be more accurate if no parameter is *a priori* known. Besides, in contrast to the other techniques, it does not suppose any condition on the theoretical values of the parameters. However, when α is less than 1, the estimation looses accuracy.

1.2.3 Generation

Chambers, Mallows and Stuck [19] proposed an accurate and inexpensive algorithm for simulating stable random variables for any α, $(0 < \alpha \leq 2)$ and β, $(-1 \leq \beta \leq 1)$. It is based on a non-linear transformation of two independent uniform random variables into on stable random variable.

Consider that we want to generate a random sample X from the standard (α, β) stable distribution, with $0 < \alpha \leq 2$ and $-1 \leq \beta \leq 1$. Define:

$$\beta_A = \beta, \qquad \gamma_A = \pi/2 \tag{1.3}$$

And, if $\alpha \neq 1$, define:

$$k(\alpha) = 1 - |1 - \alpha| \tag{1.4}$$

$$\beta_A = 2 * \arctan\left(\beta / \cot\left(\pi\alpha/2\right)\right) / \left(\pi k\left(\alpha\right)\right) \tag{1.5}$$

$$\gamma_B = \cos\left(\pi\beta_A k\left(\alpha\right)/2\right) \tag{1.6}$$

$$\Phi_0 = -0.5\pi\beta_A\left(k\left(\alpha\right)/\alpha\right) \tag{1.7}$$

Furthermore, define:

$$\beta' = \begin{cases} -\tan\left(0.5\pi\left(1-\alpha\right)\right)\tan\left(\alpha\Phi_0\right) & \alpha \neq 1 \\ \beta_A & \alpha = 1 \end{cases} \tag{1.8}$$

Then, $Y = X/\gamma_B^{\frac{1}{\alpha}}$ has the following characteristic function:

$$\phi_Y\left(t\right) = \begin{cases} \exp\left(-|t|^\alpha - jt\left(1-|t|^{\alpha-1}\right)\beta'\tan\left(0.5\alpha\pi\right)\right) & \alpha \neq 1 \\ \exp\left(-|t|\left(1+\frac{2}{\pi}j\beta'\log|t|\,\mathrm{sign}\left(t\right)\right)\right) & \alpha = 1 \end{cases} \tag{1.9}$$

We can now generate the random variable Y as follows: we first generate two independent samples Φ and W, where Φ is uniform on $(-\frac{\pi}{2}, \frac{\pi}{2})$ and W is exponentially distributed with unit mean. We then calculate the following quantities:

$$\epsilon = 1 - \alpha \tag{1.10}$$

$$\tau = -\epsilon\tan\left(\alpha\Phi_0\right) \tag{1.11}$$

$$a = \tan\left(0.5\Phi\right) \tag{1.12}$$

$$B = \frac{\tan\left(0.5\epsilon\Phi\right)}{0.5\epsilon\Phi} \tag{1.13}$$

$$b = \tan\left(0.5\epsilon\Phi\right) \tag{1.14}$$

$$z = \frac{\cos\left(\epsilon\Phi\right) - \tan\left(\alpha\Phi_0\right)\sin\left(\epsilon\Phi\right)}{W\cos\left(\Phi\right)} \tag{1.15}$$

$$d = \frac{z^{\frac{\epsilon}{\alpha}} - 1}{\epsilon}. \tag{1.16}$$

Then,

$$Y = \frac{2\left(a-b\right)\left(1+ab\right) - \Phi\tau B\left(b\left(1-a^2\right)-2a\right)}{\left(\left(1-a^2\right)\left(1+b^2\right)\right)}\left(1+\epsilon d\right) + \tau d. \tag{1.17}$$

1.3 Demonstration of the stable model for MAI

We consider the characteristic function:

$$\phi_Y\left(\omega\right) = \mathbb{E}\left[e^{jwY}\right], \tag{1.18}$$

where Y is the interference term, which can be in a very general way written as

$$Y = \sum_{i=1}^{\kappa} \gamma_i \psi_i. \tag{1.19}$$

κ is the number of interferers, γ_i is the channel attenuation and ψ_i depends on the system characteristics and can be defined differently to represent several physical layers. In the following calculations, we consider the simple channel $\gamma_i = d^a$ but it can be extended to other more complex channels (see for instance [78]).

We use the demonstration proposed by Sousa [71]. We define a circle C of radius R and denote by κ the number of interferers present in C. We compute the characteristic function of Y but we first restrict the sum in (1.19) to the users included in C. We then make R tends towards infinity. We suppose that the number of active interferers follow a Poisson field process, which means that the probability of the number of active interferers in C is given by:

$$P\left(\kappa = k\right) = \frac{e^{-\lambda\pi R^2}\left(\lambda\pi R^2\right)^k}{k!} \tag{1.20}$$

λ is the expected number of interferer per unit area which is linked to the density of the network.

We can then write:

$$\begin{aligned}\phi_Y(\omega) &= \mathbb{E}\left[e^{j\omega\left(\sum_{i=1}^{\kappa}\gamma_i\psi_i\right)}\right] \\ &= \lim_{R\to+\infty}\sum_{k=0}^{+\infty} P(\kappa=k)\,\mathbb{E}\left[e^{j\omega\gamma\psi}\right]^k \\ &= \lim_{R\to+\infty}\sum_{k=0}^{+\infty}\frac{e^{-\lambda\pi R^2}\left(\lambda\pi R^2\right)^k}{k!}\mathbb{E}\left[e^{j\omega\gamma\psi}\right]^k \\ &= \lim_{R\to+\infty} e^{-\lambda\pi R^2}\sum_{k=0}^{+\infty}\frac{\left(\lambda\pi R^2\mathbb{E}\left[e^{j\omega\gamma\psi}\right]\right)^k}{k!} \\ &= \lim_{R\to+\infty} e^{-\lambda\pi R^2}e^{\lambda\pi R^2\mathbb{E}\left[e^{j\omega\gamma\psi}\right]}.\end{aligned} \tag{1.21}$$

We take the logarithm of ϕ_Y:

$$\begin{aligned}\varphi_Y(\omega) &= \ln(\phi_Y) \\ &= \lim_{R\to+\infty}\lambda\pi R^2\left(\mathbb{E}\left[e^{j\omega\gamma\psi}\right]-1\right).\end{aligned} \tag{1.22}$$

The expectation is taken over the two random variables γ and ψ. In a first step we will calculate the expectation over γ for a given R. The distribution of γ is derived in appendix A.

$$\begin{aligned}\mathbb{E}\left[e^{j\omega\gamma\psi}\right] &= \int_{R^{-\frac{a}{2}}}^{+\infty}\mathbb{E}\left[e^{j\omega\gamma\psi}\,|\gamma=x\right]f_\gamma(x)\mathrm{d}x \\ &= \int_{R^{-\frac{a}{2}}}^{+\infty}\phi_\psi(\omega x)\,\frac{4x^{-\frac{4}{a}-1}}{aR^2}\mathrm{d}x.\end{aligned} \tag{1.23}$$

Integrating (1.23) by parts we obtain:

$$\begin{aligned}\mathbb{E}\left[e^{j\omega\gamma\psi}\right] &= \left[-\frac{1}{R^2}x^{-\frac{4}{a}}\phi_\psi(\omega x)\right]_{R^{-\frac{a}{2}}}^{+\infty}+\frac{1}{R^2}\int_{R^{-\frac{a}{2}}}^{+\infty}\omega\frac{\mathrm{d}\phi_\psi}{\mathrm{d}x}(\omega x)\,x^{-\frac{4}{a}}\mathrm{d}x \\ &= \phi_\psi\left(\omega R^{-\frac{a}{2}}\right)+\frac{1}{R^2}\int_{\omega R^{-\frac{a}{2}}}^{+\infty}\frac{\mathrm{d}\phi_\psi}{\mathrm{d}u}(u)\left(\frac{u}{\omega}\right)^{-\frac{4}{a}}\mathrm{d}u.\end{aligned} \tag{1.24}$$

We can then use (1.24) in (1.22):

$$\begin{aligned}\varphi_Y(\omega) &= \lim_{R\to+\infty} \lambda\pi R^2 \left(\phi_\psi\left(\omega R^{-\frac{a}{2}}\right) + \frac{1}{R^2}\int_{\omega R^{-\frac{a}{2}}}^{+\infty} \frac{\mathrm{d}\phi_\psi}{\mathrm{d}u}(u)\left(\frac{u}{\omega}\right)^{-\frac{4}{a}}\mathrm{d}u - 1\right) \\ &= \lim_{R\to+\infty} \lambda\pi R^2\left(\phi_\psi\left(\omega R^{-\frac{a}{2}}\right) - 1\right) \\ &\qquad + \lim_{R\to+\infty}\left(\lambda\pi\omega^{\frac{4}{a}}\int_{\omega R^{-\frac{a}{2}}}^{+\infty}\frac{\mathrm{d}\phi_\psi}{\mathrm{d}u}(u)\,u^{-\frac{4}{a}}\mathrm{d}u\right) \\ &= \lim_{R\to+\infty} \lambda\pi R^2\left(\phi_\psi\left(\omega R^{-\frac{a}{2}}\right) - 1\right) + \lambda\pi\omega^{\frac{4}{a}}\int_0^{+\infty}\frac{\mathrm{d}\phi_\psi}{\mathrm{d}u}(u)\,u^{-\frac{4}{a}}\mathrm{d}u.\end{aligned} \tag{1.25}$$

We show in appendix B that $\lim_{R\to+\infty}\lambda\pi R^2\left(\phi_\psi\left(\omega R^{-\frac{a}{2}}\right)-1\right)=0$. As a consequence, only the second term remains. We show its existence in appendix C. If ψ has a spherically symmetric probability density function, we can then write $\phi_\psi(\omega)$ as $\phi_{\psi_0}(\|\omega\|)$, where $\|.\|$ is the Euclidean norm. Finally we can write:

$$\varphi_Y(\omega) = \lambda\pi\|\omega\|^{\frac{4}{a}}\int_0^{+\infty}\frac{\mathrm{d}.\phi_{\psi_0}}{\mathrm{d}u}(u)\,u^{-\frac{4}{a}}\mathrm{d}u \tag{1.26}$$

In (1.26), the integral does not depend on ω and we can finally write:

$$\varphi_Y(\omega) = -\sigma\|\omega\|^{\frac{4}{a}}. \tag{1.27}$$

With

$$\sigma = -\lambda\pi\int_0^{+\infty}\frac{\mathrm{d}\phi_{\psi_0}}{du}(u)\,u^{-\frac{4}{a}}\mathrm{d}u, \tag{1.28}$$

equation (1.27) is the log-characteristic function for the spherically symmetric stable distribution of exponent $\alpha=\frac{4}{a}$. A similar result is obtained in different channel contexts and for other systems [60, 77, 71].

1.4 Power solution for heavy-tailed process

1.4.1 Strength of stable variables

To evaluate the performance of communication equipment, we usually illustrate bit error rate (BER) in terms of signal-to-noise ratio (SNR). However, in the case of stable laws with $\alpha<2$, the usual arithmetic power, which is a second order

moment, is infinite. We then have to find alternative solutions to represent the interference strength and the ratio between useful signal and noise strengths.

Knowing that in the Gaussian noise model, the inverse of the dispersion ($1/\gamma$) is proportional to the SNR, Souryal [70] used $1/\gamma$ to compare the decoding performance. Chitre [21] employed $N_0 = 4\gamma^{2/\alpha}$ in order to indicate the dependence of α. All these methods are to avoid infinity of second-order power resulting from the heavy tailed distribution. Two other proposed solutions are based on the Fractional Lower Order Moments (FLOMs) [58, 68] and the zero-order statistics [40].

Let X be an α-stable random variable (RV) with zero location parameter and dispersion γ. We want to evaluate the strength of X.

With FLOMs solution

The FLOM of order p ($0 < p < \alpha$) is given by $\mathbb{E}\left[|X|^p\right]$. For an α-stable RV, we have:

$$\mathbb{E}\left[|X_\alpha|^p\right] = C\left(p, \alpha\right) \gamma^{\left(\frac{p}{\alpha}\right)}, \tag{1.29}$$

where

$$C\left(p, \alpha\right) = \frac{2^{p+1}\Gamma\left(\frac{p+1}{2}\right)\Gamma\left(-\frac{p}{\alpha}\right)}{\alpha\sqrt{\pi}\Gamma\left(-\frac{p}{2}\right)}, \tag{1.30}$$

depends only on α and p, not on X_α. $\Gamma(.)$ is the gamma function defined as

$$\Gamma(x) = \int_0^\infty t^{x-1}e^{-t}\mathrm{d}t.$$

With geometric power defined in zero-order statistics

We can define the geometric power as:

$$S(X) = \exp\left(\mathbb{E}\left[\log|X|\right]\right). \tag{1.31}$$

For an α-stable random process, the geometric power can be expressed as

$$S(X) = \frac{\left(C_g\gamma\right)^{1/\alpha}}{C_g}, \tag{1.32}$$

where $C_g \approx 1.78$ is the exponential of the Euler constant. This expression presents the advantage that it exits for whatever the value of α. It has also the properties of a scale parameter and can be used as an indicator of the power strength.

We have the following properties:

- Scale parameter:
  1. $S(X) \geq 0$
  2. $S(cX) = |c|\, S(X)$
- Strength indicator:
  1. $S(c) = |c|$,
  2. $0 \leq c_1 < |X| < c_2$ implies $c_1 < S(X) < c_2$,
  3. $S(X) = 0$ if and only if $\mathbb{P}(|X| < \epsilon) > 0$ for all $\epsilon > 0$.
- Multiplicativity: For any pair of logarithmic-order random variables X and Y and any real constant c,
  1. $S(XY) = S(X)S(Y)$,
  2. $S(X/Y) = S(X)/S(Y)$,
  3. $S(X^c) = S(X)^c$.
- Absolute value inequality: For any pair of logarithmic-order random variables X and Y and any real constant c,
  1. $S(|X| + |Y|) \geq S(X) + S(Y)$.

It is rather easy to estimate the geometric power. If $x_1, x_2, \ldots, x_N$ is a sequence of independent samples generated from a distribution with geometric power S, by taking into account that S exists and is finite, the estimation of geometric power results from

$$\hat{S}(X) = \exp\left(\frac{1}{N}\sum_{i=1}^{N} \log|x_i|\right), \tag{1.33}$$

which is a consistent estimator of $S(X)$.

One difficulty with the geometric power is however that it is not linear. The power of a sum is not the sum of powers which makes things a bit unusual. The

problem of non linearity also exists with FLOMs and we replace the correlation with the co-variation, which is a classical tool for stable distributions [58].

The geometric signal-to-noise ratio (GSNR) can be defined accordingly in the stable context as:

$$\text{GSNR} = \frac{1}{2C_g}\left(\frac{A}{S(X)}\right)^2, \tag{1.34}$$

where A is the signal amplitude. The geometric definitions ensure that in the Gaussian case ($\alpha = 2$), the GSNR corresponds to the standard SNR.

1.4.2 Strength illustrations for stable variables

We provide some illustrations for stable RVs strength representation. In Figure 1.3, the signal strength (in dB) of stable RVs are compared between the FLOMs solution and geometric power framework, as a function of stable dispersion γ. We notice that the signal strength using FLOMs raises less rapidly than that using geometric power definition. Some stable signals generated using different α and γ combinations are shown in Figure 1.3 as well. We can see that the value of α controls the impulsiveness of the stable signal while γ reflects rather the signal strength.

As a result, we have the following comparison. We try to generate stable RVs under the same power each defined in FLOMs and geometric manner respectively, by changing the value of α (the impulsiveness of interference). Hence the dispersion parameter γ has to be changed according to (1.29) and (1.32). The results are illustrated in Figure 1.4 and 1.5.

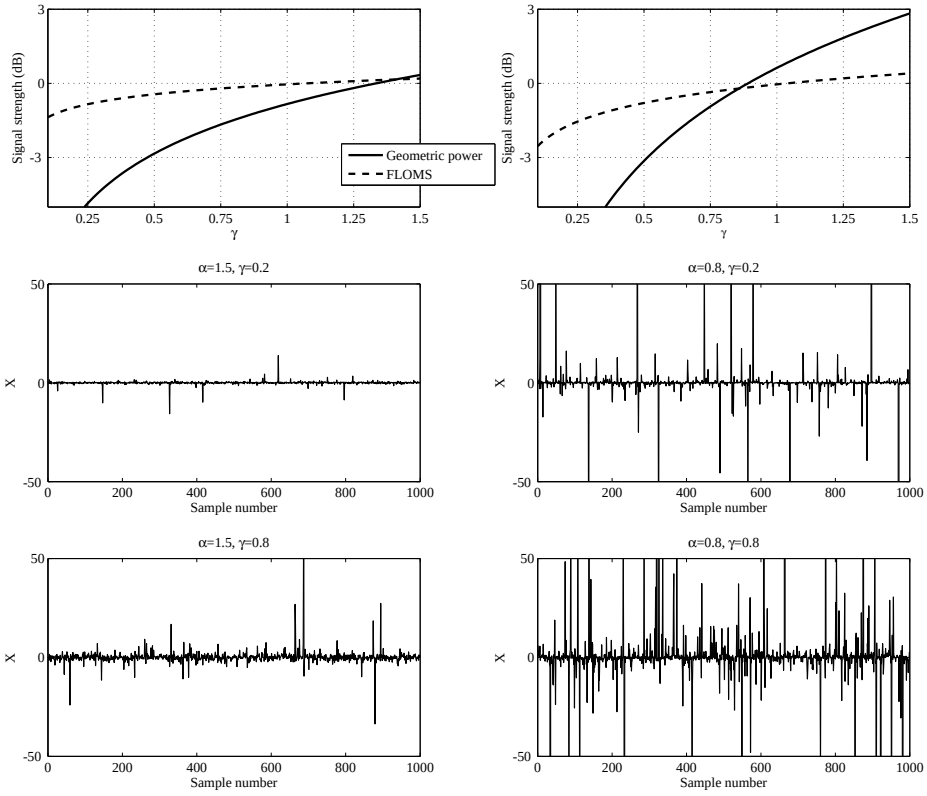

Figure 1.3: Stable RV strength comparison using FLOMs and geometric power as a function of stable dispersion γ, and some illustrations of stable RVs for different α and γ combinations.

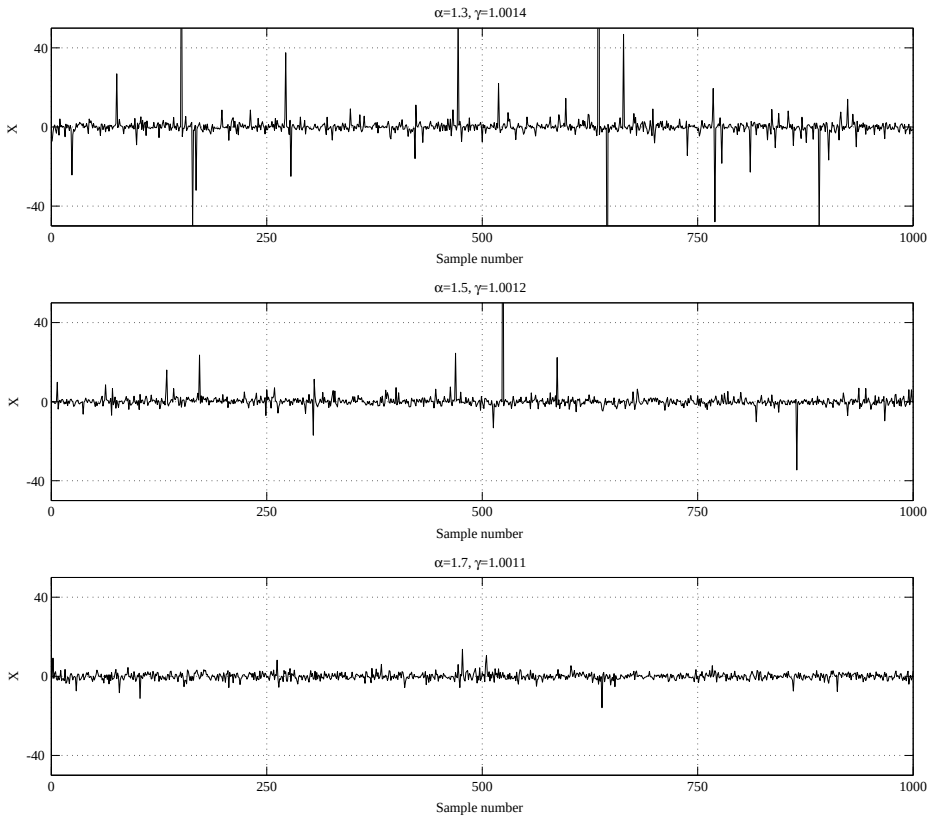

Figure 1.4: Illustration of stable RVs with the same power for 1000 samples using FLOMs.

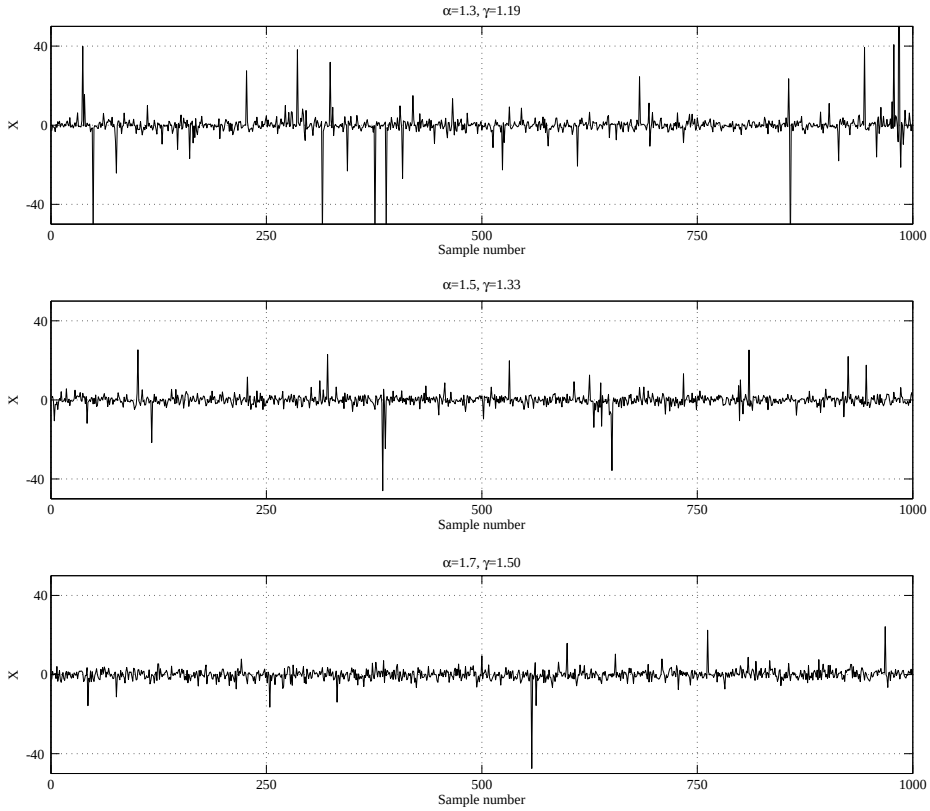

Figure 1.5: Illustration of stable RVs with the same power for 1000 samples using geometric power.

We observe that the signal are more similar when we use geometric power than FLOMs (same power for different α). Though this is not our main concern in this work, we will choose geometric power framework for the representation of SNR.

1.5 Illustration of the model validity

We consider an IR-UWB system and an *ad hoc* configuration to illustrate the validity of stable model. The receiver output Z_d is:

$$Z_d = \int_0^{N_S T_S} \sum_{k=0}^{N} \left(S^{(k)}(t) * h^{(k)}(t) + n(t) \right) m(t) \mathrm{d}t, \tag{1.35}$$

where $*$ stands for convolution, $h^{(k)}$ is the channel impulse response and $n(t)$ is the thermal noise, circularly symmetric white and Gaussian, N_s is the number of times a bit is repeated to form a symbol, T_s is the frame duration (one pulse per frame), N is the number of interferences, $m(t)$ is the reference template at the receiver that forms the correlator. Links are short and line-of-sight (LOS) so that we consider to receive a strong LOS path. Consequently, we only consider single path channels. This of course is not very realistic but it allows to check the validity of the theoretical parameters we derived in [38].

Channel attenuation is based on hypothesis from section 1.1: $\gamma_i \propto d^{-a/2}$ and we take $N_S = 1$. A summary of parameters used in simulation is presented in table 1.1.

Parameter	Value
Frame duration T_s	10ns
Pulse duration T_m	0.3ns
PPM delay ϵ	0.3ns
d_u	1m

Table 1.1: Impulse radio system parameters used in simulation.

Neglecting the near field for reasons explained in section 1.1, we can show (see section 1.3) that the log-characteristic function can be written as:

$$\begin{aligned} \varphi_Z(\omega) &= \frac{\bar{N}q}{R^2}|\omega|^{\frac{4}{a}} \int_0^{+\infty} \frac{\mathrm{d}\phi_\psi}{\mathrm{d}u}(u)\, u^{-\frac{4}{a}} \mathrm{d}u \\ &= \frac{\bar{N}q}{R^2}|\omega|^{\frac{4}{a}} F, \end{aligned} \tag{1.36}$$

where $\phi_\psi(\omega)$ is the characteristic function of $\psi(\omega)$ (defined in (1.23)). The value F is independent of ω so that Z is a symmetric α-stable random variable with parameters $\alpha = 4/a$ and $\sigma = -\left(\bar{N}q/R^2\right) F$ (the two remaining parameters are zero). Since ψ has finite moments, the integral to calculate F exists when a is larger than 2, which is the case in most of the situations.

To evaluate σ, we need to calculate F in (1.36). It can be analytically obtained when $\omega_p(t)$ is a rectangular pulse that is why the comparison between simulations and theory is made with this pulse shape (although it is not a practical one). The characteristic function of ψ is $\phi_\psi(\omega) = \frac{\sin(\omega)}{\omega}$. Then F is given by:

$$F = \frac{2^{-1-\frac{4}{a}}\sqrt{\pi}\,\Gamma\left(\frac{-2}{a}\right)}{\Gamma\left(\frac{1}{2}+\frac{2}{a}\right)} - \frac{2^{-2-\frac{4}{a}}\sqrt{\pi}\,\Gamma\left(\frac{-2}{a}\right)}{\Gamma\left(\frac{3}{2}+\frac{2}{a}\right)} \tag{1.37}$$

Finally, in (1.38), P_e is calculated using numerical integration:

$$P_e = \int_{-\infty}^{+\infty} \mathbb{P}\left(Z < -x \left| a_0^{(0)} = 0, Z_n \right.\right) f_X(x) \mathrm{d}x \tag{1.38}$$

Because Z is an α-stable random variable, we do not have an expression of its probability density function. To solve this difficulty and obtain $\mathbb{P}\left(Z < -x \left| a_0^{(0)} = 0, Z_n \right.\right)$, we simulate the random variable Z and use a non parametric estimate of its probability density function. In Figure 1.6 we represent several situations (different values of the attenuation coefficient a, the mean number of users per unit area λ and the size of the considered zone R). We show a good fit between the semi-

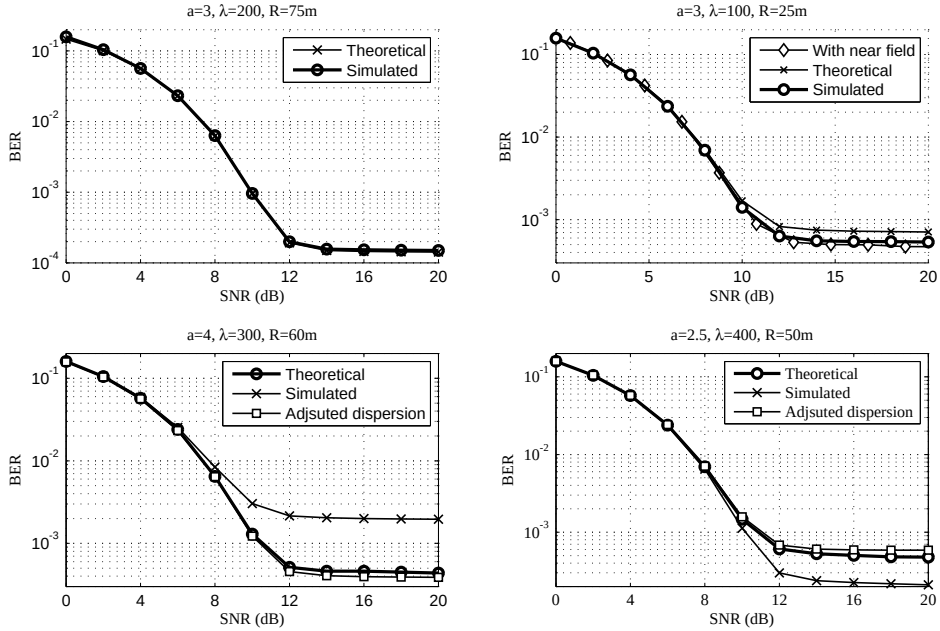

Figure 1.6: Comparison between semi-analytical and simulated BER in different situations with a rectangular pulse. The signal to noise ratio is the ratio between the useful signal power and the thermal noise power at the receiver, not including the multiple access noise.

analytical BER and the simulated system for the rectangular pulse. However, this fit is not always perfect and some errors can sometimes be noticed. In such cases we adjust the dispersion of the distribution and obtain an accurate fit between the curves. Similar behaviour are obtained with other pulse shapes but the dispersion has to be estimated because we do not have an analytical expression for

F.

For a rectangular shape, the parameters of MAI distribution are analytically derived and the good fit validates the theoretical study. Similar results are obtained if we increase the number of repetitions. The impact of strong interferers, which generate a heavy tailed distribution, is well captured by the α-stable distributions when other distributions with finite second order moments generally fail to do so. For instance, Generalized Gaussian distributions are well fitted for time hopping [33] but does not represent as well the *ad hoc* configuration [39].

The simulated BER with a near field assumption of 10 cm is also depicted in Figure 1.6 (top-right scheme). This value is much larger than the true near field area if a 60 GHz transmission is considered but the impact remains very small although the useful link is only ten times longer. In some cases (bottom schemes is Figure 1.6) the Monte Carlo simulations and the theoretical curves do not fit so well but a slight modification of the dispersion parameter can correct the misadjustment.

1.6 Some receiver strategies

1.6.1 Problem formulation

The mathematical model is the following hypothesis testing problem:

$$\begin{cases} H_0 : x(k)=s_0(k) + n_g(k) + n_\alpha(k), k = 1, 2, \ldots, N \\ H_1 : x(k)=s_1(k) + n_g(k) + n_\alpha(k), k = 1, 2, \ldots, N \end{cases} \tag{1.39}$$

where $s_i(.)$, $i = 0, 1$, is one of the two possible transmitted signals, $n_\alpha(.)$ is a realization of a sequence of N i.i.d. zero-mean symmetric α-stable (SαS) random variables of characteristic exponent α ($0 < \alpha \leq 2$) and dispersion γ, and $n_g(.)$ is a realization of a sequence of N i.i.d. zero-mean Gaussian random variables with variance σ^2. Furthermore, the Gaussian and the impulsive noises are independent of each other and of the signal. The SαS random variable with zero-mean is defined through its characteristics function

$$\phi_{n_\alpha}(\omega) = \exp(-\gamma \left|\omega\right|^\alpha) \tag{1.40}$$

The characteristic function of the total additive noise is:

$$\phi_X(\omega) = \exp(-\gamma \left|\omega\right|^\alpha - \frac{\sigma^2}{2}\omega^2) \tag{1.41}$$

The density function is given by the inverse-Fourier transform of the characteristic function:

$$f_X(x) = \frac{1}{\pi} \int_0^{+\infty} \phi_X(\omega) \cos(xt)\, \mathrm{d}t. \tag{1.42}$$

A numerical integration can be used to evaluate $f_X(x)$.

1.6.2 Optimum receiver

To decide between the two hypothesis H_0 and H_1, the optimum (in the maximum likelihood sense) receiver computes the test statistic:

$$\Lambda = \sum_{k=1}^{N} \log \left\{ \frac{f_X(x(k) - s_1(k))}{f_X(x(k) - s_0(k))} \right\}, \tag{1.43}$$

and compares it to a present threshold η. When $\Lambda \geq \eta$, the receiver decides that $s_1(.)$ was sent, otherwise that $s_0(.)$ was sent.

For large N, from the central limit theorem, the authors in [73, 1] assume that Λ has a Gaussian distribution and for equiprobable signalling, the probability of error is given by:

$$P_e = \text{erfc}\left(\frac{\mu_0}{\sqrt{2\sigma_0^2}} \right), \tag{1.44}$$

where erfc$(.)$ is the complementary error function, μ_0 the mean and σ_0^2 the variance of Λ given that s_0 was sent. We have:

$$\mu_0 = \sum_{k=1}^{N} \int_{-\infty}^{+\infty} f_X\left(\xi - s_0(k)\right) \log \left\{ \frac{f_X\left(\xi - s_1(k)\right)}{f_X\left(\xi - s_0(k)\right)} \right\} \mathrm{d}\xi, \tag{1.45}$$

$$\sigma_0^2 = \sum_{k=1}^{N} \int_{-\infty}^{+\infty} f_X\left(\xi - s_0(k)\right) \log^2 \left\{ \frac{f_X\left(\xi - s_1(k)\right)}{f_X\left(\xi - s_0(k)\right)} \right\} \mathrm{d}\xi - \frac{\mu_0^2}{N}, \tag{1.46}$$

As explained in [73], the expression for the probability of error is only asymptotically valid, i.e. they hold true only when the length N of the data sequence is large enough for the true distribution of the test statistic to be well approximated by a Gaussian distribution. However, it is not guaranteed that for a high number N of data samples, the asymptotic expressions for the probability of error will

always be valid because of sensitivity of the probability of error to the far tails of the pdf of the test statistic for which the Gaussian pdf provides only a poor approximation. A better estimate of the probability of error of the receiver can be obtained by performing extensive Monte Carlo simulations.

It is rather straightforward to draw samples from a stable law [86, 58]. However, the fact that rare events have a major impact on the performance results, a large numbers of samples have to be simulated. It is out of the scope of the thesis but strategies to fasten the procedure would be welcome.

1.6.3 Optimal performance evaluation

To test the normality assumption, we apply the Kolmogorov-Smirnov test at the 5% significance level for 10000 samples drawn from the log-likelihood ratio Λ for different values of the signal to noise ratio and the repetition parameter N. A sample of our results for $\alpha = 1.5$ and $\gamma = 0.3$ are shown in Figure 1.7 to 1.10. We see, as the SNR grows that the number of samples N necessary for the Gaussian approximation to be accepted gets larger. The same pattern holds for different values of the parameters α and γ.

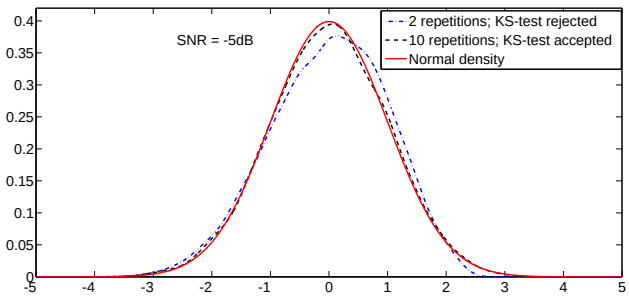

Figure 1.7: Kolmogorov-Smirnov tests for Gaussianity $\alpha = 1.5$ and $\gamma = 0.3$, SNR$=-5$ dB.

The Kolmogorov-Smirnov goodness of fit test statistic D_n is drawn in Figure 1.11 and is given by $D_n = \sup_{x\in} |F_n(x) - F(x)|$, where $F_n(x)$ is the empirical cumulative distribution function of the log-likelihood ratio Λ and $F(x)$ is the cumulative Gaussian distribution function. Whenever D_n is greater than the critical value of the test, the Null hypothesis that Λ has a normal distribution is rejected.

We confirm in Figure 1.11 that the number N necessary for the Gaussian hypothesis to be valid gets larger when the Gaussian noise becomes weaker. At classical SNR levels (5 to 10 dB), we see that N has to be very large, which will not necessary be true. However we can further wonder if, although not

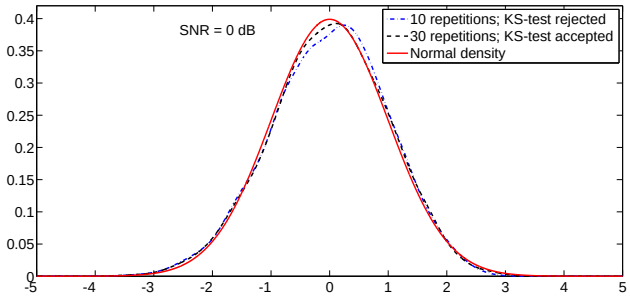

Figure 1.8: Kolmogorov-Smirnov tests for Gaussianity $\alpha = 1.5$ and $\gamma = 0.3$, SNR=0 dB.

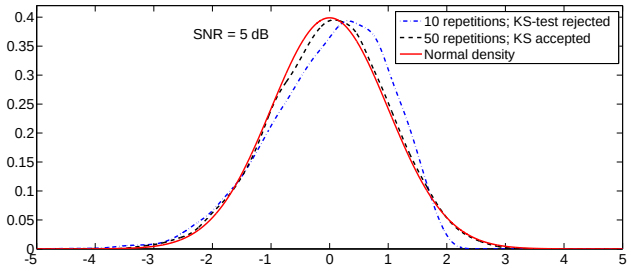

Figure 1.9: Kolmogorov-Smirnov tests for Gaussianity $\alpha = 1.5$ and $\gamma = 0.3$, SNR=5 dB.

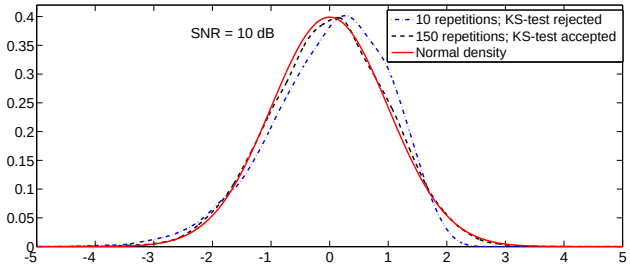

Figure 1.10: Kolmogorov-Smirnov tests for Gaussianity $\alpha = 1.5$ and $\gamma = 0.3$, SNR=10 dB.

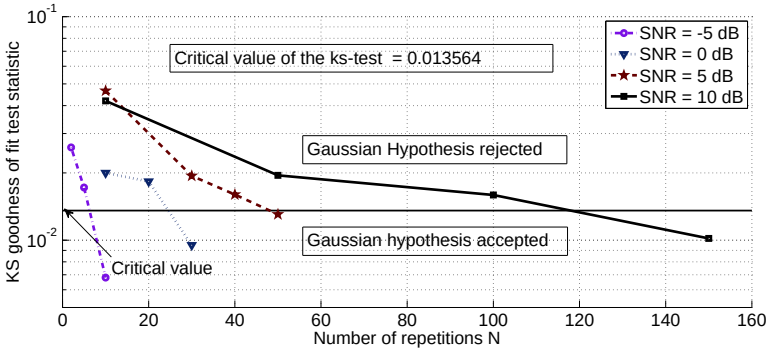

Figure 1.11: Kolmogorov-Smirnov goodness of fit test statistic D_n for $\alpha = 1.5$ and $\gamma = 0.3$.

validated by KS test, the Gaussian approximation will not give a sufficiently accurate result for the error probability estimation. As a consequence we compute the probability of error of our optimal receiver in two ways, by using the Normality assumption and by extensive Monte Carlo simulations. The simulations are done with a number of samples large enough to ensure 1000 errors per data samples. In the implementation the data are generated from the α-stable generator proposed by [19]. Next, because of the lack of a closed form expression for the general $S\alpha S$ density, we use an extensive numerical integration to compute the density function from the characteristic function based on Fourier transform. The results confirm in another way that the Normality assumption is far from being a reasonable approximation of the log-likelihood ratio Λ. We present in Figure 1.12 to 1.15 the probabilities of error for $\alpha = 1.5$ and $\gamma = 0.05, 0.3, 0.5$.

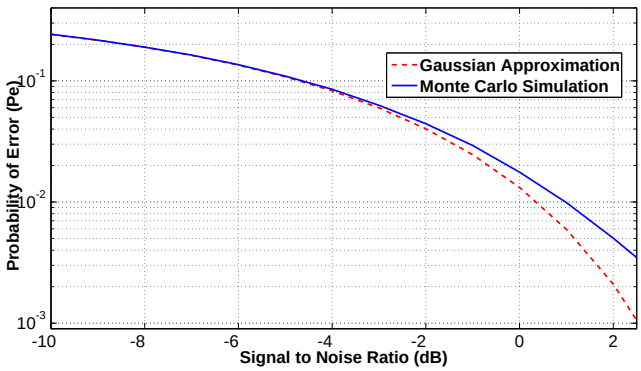

Figure 1.12: Error probability for $\alpha = 1.5$ and $\gamma = 0.05$, 5 repetitions.

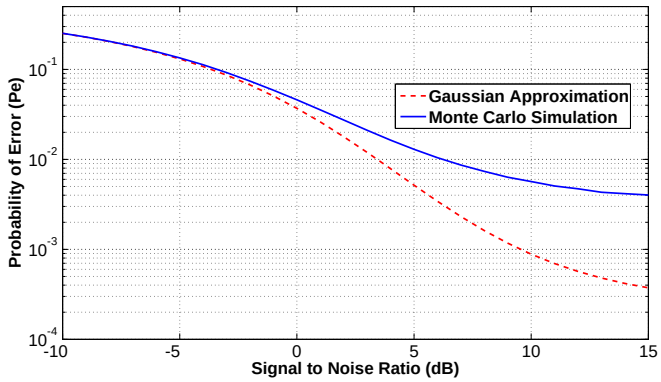

Figure 1.13: Error probability for $\alpha = 1.5$ and $\gamma = 0.3$, 5 repetitions.

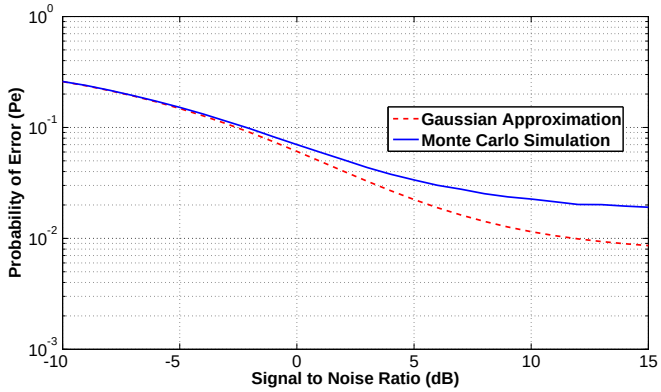

Figure 1.14: Error probability for $\alpha = 1.5$ and $\gamma = 0.5$, 5 repetitions.

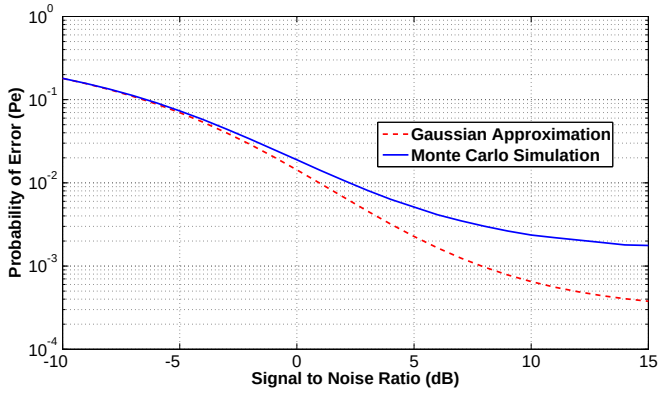

Figure 1.15: Error probability for $\alpha = 1.5$ and $\gamma = 0.5$, 10 repetitions.

1.6.4 Suboptimal strategies

Classical receivers consider that the received signal is mixed with a Gaussian noise and are not optimal in our situation. In IR-UWB system, Fiorina [33] models the MAI with a generalized Gaussian distribution to derive the maximum likelihood matched filter. Beaulieu [4] assumes that the signal is immersed in a mixture of Laplacian and Gaussian noise. It outperforms the receiver based on the Gaussian assumption. Considering the impulsive nature of the MAI, Erseghe [30] has suggested Gaussian mixtures for the interference to derive the optimal receiver. Performance improves when compared to the Gaussian receiver and the cost of implementation remains weak. This approach is also found for detection when the additive noise is α-stable [50]. Tsihrintzis and Nikias in [73] studied the performance of optimal and suboptimal (including the Cauchy) receivers in such a noise. Those receivers are non linear solutions and a linear solution is proposed in [46]. A non parametric rank-based solution is studied in [13] and suboptimal parametric solutions are presented in [87]. Ambike *et al.* [1] have also tested a hole puncher and a soft limiter receivers in a mixture of Gaussian and α-stable noises. All proposed approaches are compromises between performance and complexity and an overview can be found in [6].

We have chosen to test the non linear Cauchy receiver, meaning the receiver obtained when we consider that a Cauchy noise is added to the information bearing signal. This receiver was found to perform closely to the optimum receiver for a wide range of characteristic exponent α [73]. It was also shown by Friedmann *et al.* in [36] that the maximum likelihood estimator of a deterministic signal derived for a Cauchy noise achieves good performance when the noise is symmetric α-stable, even when α is not equal to one. The definition of the optimal receiver is however a difficult task and is not included in the scope of this thesis. Indeed, the noise is not an α-stable noise but a mixture of three different noises: the α-stable multiple access interference, the Gaussian thermal noise and the multipath interference. The resulting noise distribution is then very difficult to obtain.

Let $a_0^{(0)}$ be the source bit from the desired user. We consider that the correlation function ψ_0 in (1.26) is equal to 1 if $\Delta_0 = 0$ (meaning a perfect synchronization and $a_0^{(0)} = 0$) and to -1 if $\Delta_0 = \epsilon$ (meaning a perfect synchronization and $a_0^{(0)} = 1$). For the desired user, the received samples are then, after the correlation receiver: $x_0^{(0)}(j) = d_u^{-\frac{a}{2}}(-1)^{a_0^{(0)}} + n_\alpha(j)$ where index j indicates the repetitions ($j = 1, \ldots, N_S$). Sequence $\{n_\alpha(j)\}_{j=1,\ldots,N_S}$ is a realization of N_S independent, identically distributed symmetric α-stable random variables. Distance d_u is the useful link length. The optimum (in the maximum likelihood sense)

test statistic Λ is:

$$\Lambda = \sum_{j=1}^{N_S} \log \left\{ \frac{f_\alpha \left[x_0^{(0)}(j) - d_u^{-\frac{a}{2}} \right]}{f_\alpha \left[x_0^{(0)}(j) + d_u^{-\frac{a}{2}} \right]} \right\}, \tag{1.47}$$

where $f_\alpha(u)$ is the probability density function of n_α and the sign of Λ gives the estimated signal. As already mentioned, the main difficulty is that $f_\alpha(u)$ has not an explicit form for most of α values. Fortunately, f_α is known for $\alpha = 2$, the Gaussian case, and $\alpha = 1$ where n_α is a Cauchy random variable ($f_\alpha(u) = \sigma / (\pi [u^2 + \sigma^2])$). Our objective is to propose a receiver able to cope with impulsive noise. The Cauchy receiver, resulting from our analysis on the MAI, is then the first solution that comes to mind. By Cauchy receiver, we mean the receiver that employs Λ derived from (1.47) under the assumption that $\alpha = 1$. The Gaussian receiver uses the assumption that $\alpha = 2$.

We have also implemented receivers based on the metric induced by the covariation norm $\|.\|_\alpha$ (see for instance [64, p. 95]). From a practical point of view, this norm is linked to the L^p norm, with $p < \alpha$, by the equality:

$$\|X\|_\alpha = C_\alpha(p)(E|X|^p)^{\frac{1}{p}}; \tag{1.48}$$

the constant $C_\alpha(p)$ depends only on α and p and is given by (see for instance [58, p. 32]):

$$C_\alpha(p) = \left(\frac{\alpha\sqrt{\pi}\Gamma(-\frac{p}{2})}{2^{p+1}\Gamma(\frac{1+p}{2})\Gamma(-\frac{p}{\alpha})} \right)^{\frac{1}{p}}. \tag{1.49}$$

This suggests an empirical estimation of this metric by:

$$\|X - Y\|_\alpha = C_\alpha(p) \left(\frac{1}{N_S} \sum_{j=1}^{N_S} |x_j - y_j|^p \right)^{\frac{1}{p}}, \tag{1.50}$$

where $p < \alpha$. Two ideas lie behind this metric. First, if Euclidean distance is a logical estimation of standard deviation when Gaussian noise is considered, the proposed solution is adapted to SαS distributions since it estimates its scale parameter. Choosing an adapted distance seems then rather logical. The second aspect is that we do not want to give too much weight for the decision to large values because they are mixed with an important noise sample. The Euclidean distance is poorly adapted in that sense and we prefer using the co-

variation norm. Beaulieu *et al.* proposed a similar solution in [5] that is an optimal solution for generalized Gaussian interference. We however did not use their estimation procedure for p which is not consistent with our approach. It is based on second and higher order moments which are not defined for stable distributions.

Finally, to get an idea of an optimal solution, we have implemented a genie-aided receiver: in the simulation we extract the exact noise samples and use a kernel type non parametric estimation of the noise distribution (a Gaussian kernel is considered). We then use this distribution to calculate the log-likelihood function. This distribution is calculated on each packet that we have taken rather short (50 source bits repeated 4 times) to avoid too much computation complexity.

1.6.5 Simulation results

We have considered two scenarios. The first one uses a Gaussian channel so that only Gaussian noise and multiple access interference play a role. The second one includes an important multipath impact. Figure 1.16 presents the BER as a function of the mean number of users λ. On the left graph, with no multipath,

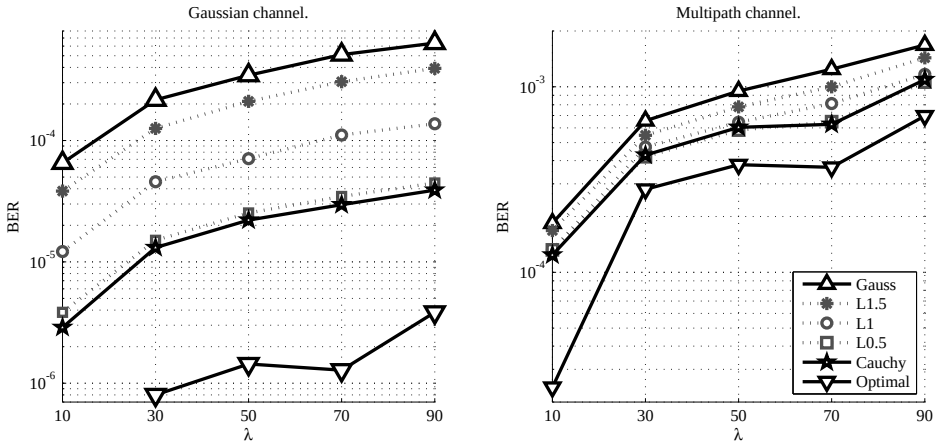

Figure 1.16: BER as a function of the mean number of users for different receivers and two different scenarios. The SNR per pulse after the correlation receiver is 10dB. The radius of the area is $R = 30m$.

we clearly see the improvement brought by the Cauchy receiver, the number of errors being reduced by a factor 10. The proposed metric is also an attractive solution when p takes small values. For $p = 0.5$, the proposed metric gives similar results to the Cauchy receiver. The genie-aided receiver exhibits of course better performance. It is not clear how close to this optimal curve we can get.

We have also simulated an *ad hoc* network situation but with a multipath channel. We have chosen the residential model proposed by the IEEE 802.15.4a [55, 56]. The useful link is in Line Of Sight (LOS) while the interfering links can be either LOS or non LOS with probability 0.5. The global power attenuation is d^{-a} and an additional shadowing factor of 0.5 is used for non LOS users. Each object uses the same transmit power. The improvement due to the Cauchy receiver is reduced but still significant. The conclusion on the use of the proposed metric are similar to the previous case. The optimal solution offers a further gain but the much more difficult transmission conditions make the benefit smaller.

An appropriate solution for an indoor *ad hoc* networks, eventually at 60 GHz, would be to use directive antennas and links with a LOS path. The resulting conditions would then be in between the two considered scenarios, the importance of multipath depending on the antenna directivity and the environment. The benefits resulting from the proposed metric or the Cauchy receiver would then be significant. Taking the impulsive nature of the interference into account is important and the stable model can certainly bring an accurate general mathematical framework [78].

1.7 Conclusion

In this chapter, we investigated multiple-access-interference occurred in sensor networks. Due to its impulsive behaviour, the conventional Gaussian model is no longer valid. Stable distributions were introduced and proved as an accurate model to represent impulsive interference like MAI. The parameters of stable distributions were introduced with estimation approaches, and one of their generation methods was provided. Then a demonstration was offered to show how the stable distribution applies for MAI. One difficulty for the stable distribution is the fact that the second-order moments of stable variables are infinite, thus alternative methods such as FLOMs and geometric power framework were introduced and compared, in order to estimate the strength of stable random variables. Then geometric signal-to-noise ratio was proposed accordingly. An example of an IR-UWB system with an *ad hoc* configuration was utilised to illustrate the validity of stable model. Another difficulty lies in the non-existence of probability density function for stable distributions, which brings some novel challenges in the receiver design. We took some optimal and suboptimal receiver strategies, for example, to show how to carry out the receiver strategies with the stable model. More solutions of addressing stable-modelled interference in different communication works can be found in the following chapters.

Chapter 2

Channel coding study in direct link

We firstly investigate the robustness in sensors networks in the context of point-to-point communications by the means of channel coding. Turbo codes are employed for their strong error correcting performance and wide use in the practical communication systems. As a type of error correcting code, turbo codes were firstly presented in the *International Conference on Communications* at Geneva in Switzerland in 1993, based on the work of Claude Berrou, Alain Glavieux and Punya Thitimajshima [8, 7]. The error correcting performance of turbo codes can be close to the theoretical limit predicted by Shannon with acceptable decoding complexity. The codes are typically built from two *recursive systematic convolutional* (RSC) encoders linked together by an interleaver. Generally, the same RSC encoder is used to generate two constituent parity codes, and we use this general model in this thesis.

2.1 Turbo code principle

2.1.1 Turbo encoder

A conventional turbo encoder consists of two RSC encoders, which are connected with a random interleaver. If necessary, a puncture block is linked at the output of encoders to increase the code rate. The turbo encoder structure is shown in Figure 2.1:

Each RSC encoder generates a systematic code and a convolutional code with code rate $R_c = 1/2$. As the two encoders export the same systematic code as the input sequence $\mathbf{m}$, the overall turbo code is composed of one systematic and two coded sequences as $\mathbf{c} = (\mathbf{m}, \mathbf{c_1}, \mathbf{c_2})$, giving a code rate $R_c = 1/3$. In

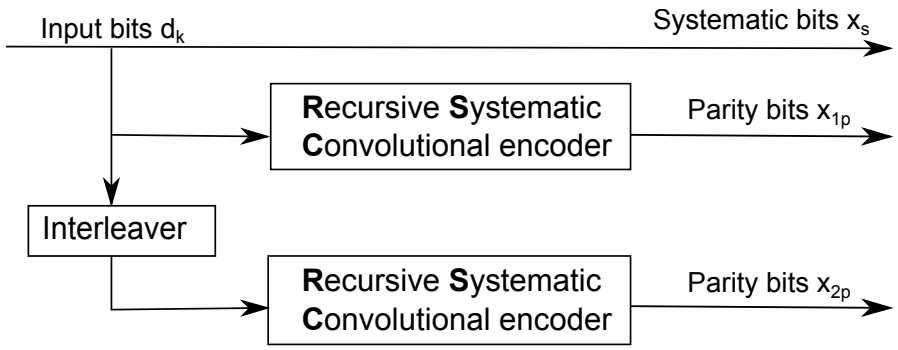

Figure 2.1: Turbo encoder structure

order to improve the code rate, the puncturing technique is sometimes used by eliminating alternatively parity bit from two encoders, which reduces the code redundancy but at the price of a loss in Bit Error Rate (BER) performance [15].

2.1.2 Turbo decoder

Turbo decoder involves iterative exchange of information between two constituent decoders. For this reason, these codes get their name "turbo". The decoder structure is shown in Figure 2.2. Each decoder accepts in turns signals from the

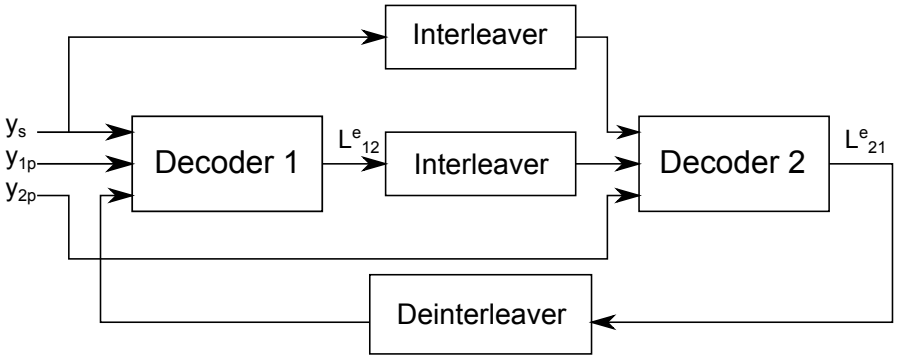

Figure 2.2: Turbo decoder structure

channel, which corresponds to the systematic and parity codes, as well as the extrinsic information from the other constituent decoder, which is regarded as *a priori* information about the decoded bit. The *a priori* information is a kind of soft output which measures the probability that each decoding bit should be one predefined bit value. In a bipolar signal processing system, if we use the log-likelihood ratio (LLR) form to express the output, it is more convenient to have a soft decision. The sign of the output indicates the decoded bit "0" or "1", and the

magnitude provides the probability that this bit is a "0" or an "1". The BCJR MAP algorithm involves this soft output form and we use it as our decoding algorithm.

2.2 The BCJR MAP algorithm for decoding of turbo codes

2.2.1 The BCJR MAP decoding algorithm

The BCJR MAP algorithm was firstly proposed by Bahl, Cocke, Jelinek and Raviv [2], for estimating the *a posteriori* probabilities of the states and transitions of a Markov source observed in memoryless noise. Despite of its complexity compared with the Viterbi decoding algorithm, the BCJR MAP algorithm shows more efficient error-correcting performance when it is involved in an iterative decoding scheme [57]. Unlike the Viterbi decoding method, the BCJR MAP algorithm provides simultaneously the estimated sequence and the probability of decision for each decoded bit. In the following, the decoding procedure is described in terms of LLR. The utilization of LLR allows the cancellation of constant terms on both the numerator and the denominator, thus a simple implementation can be performed.

Given a received sequence $\mathbf{y}$ and the transmitted bit ($d_k = \pm 1$), the BCJR MAP algorithm calculates *a posteriori* probabilities for each time instant k, composing two possible probability products into a ratio form:

$$L(d_k|\mathbf{y}) = \ln\left[\frac{P(d_k = +1|\mathbf{y})}{P(d_k = -1|\mathbf{y})}\right]. \tag{2.1}$$

For equal-probability inputs, (2.1) can be reformed by introducing the Bayes' rule as shown in appendix D:

$$L(d_k|\mathbf{y}) = \ln\left[\frac{P(d_k = +1, \mathbf{y})}{P(d_k = -1, \mathbf{y})}\right]. \tag{2.2}$$

It is more convenient to transmit the signal in bipolar form in the channel. If the source symbol is "0" and "1", we can make the correspondence for that -1 in the channel represents 0 in the source and $+1$ in the channel represents 1 in the source. The LLR provides both a hard decision for each decoded bit by its sign ($+$ for $+1$ and $-$ for -1) and a soft "likelihood" by its magnitude, which indicates the reliability of this decision.

2.2.2 LLR decoding structure

Generally, the signal estimation for turbo codes is done over the transitions of trellis with which the input bit is associated. At time instant k, the input d_k is the bit that gave rise to the transition from the previous state $S_{k-1} = s'$ to the present one $S_k = s$ in the decoding trellis. Then the LLR (2.2) can be expressed as:

$$L(d_k|\mathbf{y}) = \ln \left[\frac{\sum_{\substack{(s',s)\Rightarrow \\ d_k=+1}} P(S_{k-1} = s', S_k = s, \mathbf{y})}{\sum_{\substack{(s',s)\Rightarrow \\ d_k=-1}} P(S_{k-1} = s', S_k = s, \mathbf{y})} \right]. \tag{2.3}$$

The transition $(s', s) \Rightarrow d_k = +1$ represents all the transitions which are caused by the input bit $d_k = +1$, the same correspondence is true for the input bit $d_k = -1$.

We can decompose the probability $P(S_{k-1} = s', S_k = s, \mathbf{y})$ (for brevity purpose, $S_{k-1} = s'$ and $S_k = s$ is represented as s' and s respectively in the following description) into the product of three terms:

$$P(s', s, \mathbf{y}) = P(\{y_k, s\}|s')P(s', \mathbf{y}_{j<k})P(\mathbf{y}_{j>k}|s). \tag{2.4}$$

These three terms are denoted as:

$$\gamma_k(s', s) = P(\{y_k, s\}|s'), \tag{2.5}$$

$$\alpha_{k-1}(s') = P(s', \mathbf{y}_{j<k}), \tag{2.6}$$

$$\beta_k(s) = P(\mathbf{y}_{j>k}|s) \tag{2.7}$$

where the term $\gamma_k(s', s) = P(\{y_k, s\}|s')$ is the branch transition probability, which indicates the probability that knowing the previous state s', the received message is y_k at the present state s.

The state decomposition can be illustrated in the decoding trellis as

Once the values of $\gamma_k(s', s)$ are known, the remaining coefficients $\alpha_{k-1}(s')$ and $\beta_k(s)$ can be calculated over the decoding trellis by iteration as a function of $\gamma_k(s', s)$, using forward and backward recursions respectively.

For $k = 0, 1, 2, \ldots, n$, the definition of $\alpha_{k-1}(s')$ allows to calculate $\alpha_k(s)$ as:

$$\alpha_k(s) = P(s, \mathbf{y}_{j<k+1}) = P(s, \mathbf{y}_{j<k}, y_k). \tag{2.8}$$

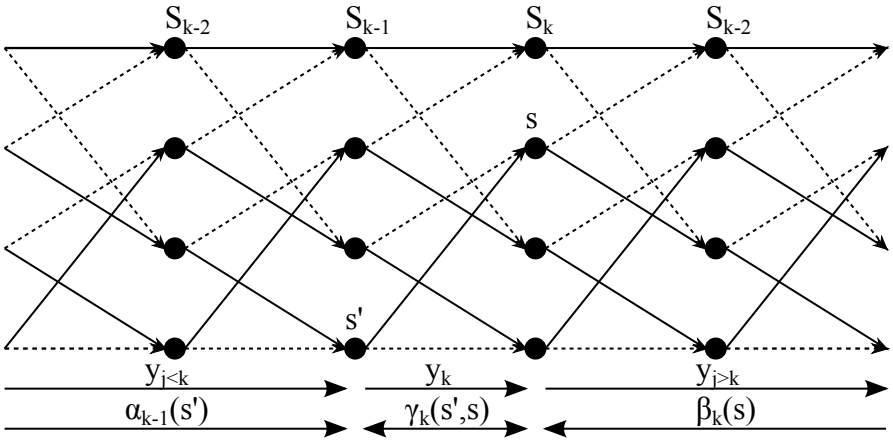

Figure 2.3: Turbo decoding trellis with 3 bit constraint length

Then from State 0 to State $S-1$ in the instant k, we have

$$\begin{aligned}\alpha_k(s) &= \sum_{s'=0}^{S-1} P(s', s, \mathbf{y}_{j<k}, y_k) \\ &= \sum_{s'=0}^{S-1} P(s', \mathbf{y}_{j<k}) P(\{s, y_k\} | \{s', \mathbf{y}_{j<k}\}) \\ &= \sum_{s'=0}^{S-1} P(s', \mathbf{y}_{j<k}) P(\{s, y_k\} | s') \\ &= \sum_{s'=0}^{S-1} \alpha_{k-1}(s') \gamma_k(s', s).\end{aligned} \tag{2.9}$$

The initial conditions for $k = 0$ are defined as $\alpha_0(0) = 1$ and $\alpha_0(s) = 0, s \neq 0$.

In an inverse way for $k = 1, 2, \ldots, n$, the definition of $\beta_k(s)$ allows to calculate

$\beta_{k-1}(s')$ as:

$$\begin{aligned}\beta_{k-1}(s') &= \sum_{s=0}^{S-1} P(\{s, \mathbf{y}_{j>k-1}\}|s') \\ &= \sum_{s=0}^{S-1} P(\{s, y_k, \mathbf{y}_{j>k}\}|s') \\ &= \sum_{s=0}^{S-1} P(\{s, y_k\}|s') P(\mathbf{y}_{j>k}|\{s', s, y_k\}) \\ &= \sum_{s=0}^{S-1} \gamma_k(s', s)\beta_k(s).\end{aligned} \tag{2.10}$$

The termination conditions for $k = n$ are defined as

- $\beta_n(0) = 1$ and $\beta_n(s) = 0, s \neq 0$, if the trellis is terminated (the trellis starts and ends in zero state);
- $\beta_n(s) = 1, \forall s$, if the trellis is not terminated.

For the calculation of $\gamma_k(s', s)$, we sum up over the input alphabet A_x:

$$\begin{aligned}\gamma_k(s', s) &= \sum_{A_x} P(\{X = x_k, y_k, s\}|s') \\ &= \sum_{A_x} P(X = x_k|\{y_k, s', s\}) P(\{y_k, s\}|s') \\ &= \sum_{A_x} P(X = x_k|\{s', s\}) P(s|s') P(y_k|\{s', s\}) \\ &= \sum_{A_x} p_k(X|\{s', s\}) q_k(s|s') P(y_k|x_k).\end{aligned} \tag{2.11}$$

The detailed calculation of term $\gamma_k(s', s)$ will be provided in Section 2.2.3.

Finally, the MAP LLR can be obtained by combining these probability terms:

$$L(d_k|\mathbf{y}) = \ln \left[\frac{\sum_{\substack{(s',s)\Rightarrow \\ d_k=+1}} \gamma_k(s', s)\alpha_{k-1}(s')\beta_k(s)}{\sum_{\substack{(s',s)\Rightarrow \\ d_k=-1}} \gamma_k(s', s)\alpha_{k-1}(s')\beta_k(s)} \right]. \tag{2.12}$$

2.2.3 LLR calculation

As shown in (2.9) and (2.10), $\alpha_{k-1}(s')$ and $\beta_k(s)$ terms are determined as functions of $\gamma_k(s', s)$. Hence the branch transition probability $\gamma_k(s', s) = P(\{y_k, s\}|s')$ is the pivotal one and should be calculated first. It can be written using the Bayes' rule as shown in appendix D as:

$$\begin{aligned}\gamma_k(s', s) &= P(\{y_k, s\}|s') \\ &= P(y_k|\{s', s\})P(s'|s) \\ &= P(y_k|\{s', s\})P(d_k).\end{aligned} \tag{2.13}$$

where d_k is the input bit which cause the transition from state s' to state s, and $P(d_k)$ is the *a priori* probability of this bit.

The LLR for bit d_k is firstly established to help later calculation. It is the natural logarithm of the quotient between the probabilities that the bit is "+1" and "-1":

$$L(d_k) = \ln\left[\frac{P(d_k = +1)}{P(d_k = -1)}\right]. \tag{2.14}$$

As $P(d_k = +1) = 1 - P(d_k = -1)$, then

$$\exp\left(L(d_k)\right) = \frac{P(d_k = +1)}{1 - P(d_k = +1)}. \tag{2.15}$$

Hence

$$P(d_k = +1) = \frac{\exp\left(L(d_k)\right)}{1 + \exp\left(L(d_k)\right)} = \frac{1}{1 + \exp\left(-L(d_k)\right)} \tag{2.16}$$

$$P(d_k = -1) = \frac{\exp\left(-L(d_k)\right)}{1 + \exp\left(-L(d_k)\right)} = \frac{1}{1 + \exp\left(L(d_k)\right)}. \tag{2.17}$$

In a summarized form, equations (2.16) and (2.17) become:

$$\begin{aligned}P(d_k = \pm 1) &= \frac{\exp\left(-L(d_k)/2\right)}{1 + \exp\left(-L(d_k)\right)} \exp\left(\pm[L(d_k)/2]\right) \\ &= \frac{\exp\left(-L(d_k)/2\right)}{1 + \exp\left(-L(d_k)\right)} \exp\left(d_k[L(d_k)/2]\right)\end{aligned} \tag{2.18}$$

We notice that the common factor

$$\frac{\exp\left(-L(d_k)/2\right)}{1+\exp\left(-L(d_k)\right)}$$

appears at both the numerator and the denominator so that it can be removed for further calculation.

In order to calculate the probability term $P(y_k|\{s',s\})$, the equivalent probability $P(y_k|x_k)$ is used, since x_k is the transmitted codeword associated with the transition from the state s' to s. This term represents thus the probability that given the transmitted signal x_k, the received signal is y_k. In a memoryless channel, the conditional probability $P(y_k/x_k)$ can be expressed as the product of the n sub-conditional probabilities:

$$P(y_k|x_k) = \prod_{i=1}^{n} P(y_{ki}|x_{ki}), \tag{2.19}$$

where n is the length of the code word y_k or x_k, y_{ki} and x_{ki} are the ith received and transmitted bit from y_k and x_k respectively.

A memoryless Additive White Gaussian Noise (AWGN) channel is taken for instance to explain the whole turbo decoding procedure, as this kind of channel is regarded in literature as a general example model. Consequently the probability term $P(y_k|x_k)$ can be written by introducing the Gaussian probability density as:

$$\begin{aligned} P(y_k|x_k) &= \prod_{i=1}^{n} P(y_{ki}|x_{ki}) \\ &= \prod_{i=1}^{n} \frac{1}{\sqrt{2\pi}\sigma} \exp\left[-\frac{E_b(y_{ki}-x_{ki})^2}{2\sigma^2}\right] \\ &= \frac{1}{(\sqrt{2\pi}\sigma)^n} \exp\left[-\frac{E_b}{2\sigma^2}\sum_{i=1}^{n}(y_{ki}-x_{ki})^2\right], \end{aligned} \tag{2.20}$$

where the first factor $1/(\sqrt{2\pi}\sigma)^n$ is a constant, leaving only the second term

$$\exp\left[-\frac{E_b}{2\sigma^2}\sum_{i=1}^{n}(y_{ki}-x_{ki})^2\right]$$

to be useful in the MAP LLR expression.

Hence the whole branch transition probability can be written in the memoryless AWGN channel as:

$$\begin{aligned}\gamma_k(s', s) &= P(y_k|\{s', s\})P(d_k) \\ &= C\exp\left(d_k[L(d_k)/2]\right)\exp\left[-\frac{E_b}{2\sigma^2}\sum_{i=1}^{n}(y_{ki}-x_{ki})^2\right],\end{aligned} \tag{2.21}$$

where C represents all the constants discussed above.

The coefficient $L(d_k)$ in (2.21) is obtained from the output of another constituent decoder as extrinsic information, which is calculated in the previous iteration. The channel reliability information $L_c = 2E_b/\sigma^2$ is employed, which depends only on the signal-to-noise ratio (SNR). If a general $1/n$ code rate RSC encoder is considered as the constituent turbo encoder, the first bit of output is the systematic bit (original input bit) and the others should be the redundant bits (coded bits). In this case, only one input bit is associated to each trellis transition. Hence in $\gamma_k(s', s)$ expression the systematic bit and the redundant bits can be distinguished as

$$\begin{aligned}\gamma_k(s', s) &= P(y_k|\{s', s\})P(d_k) \\ &= C\exp\left(d_k[L(d_k)/2]\right)\exp\left[-\frac{E_b}{2\sigma^2}\sum_{i=1}^{n}(y_{ki}-x_{ki})^2\right] \\ &= C\exp\left(d_k[L(d_k)/2]\right)\exp\left[-\frac{L_c}{4}(y_{k1}-x_{k1})^2-\frac{L_c}{4}\sum_{i=2}^{n}(y_{ki}-x_{ki})^2\right] \\ &= C\exp\left(d_k[L(d_k)/2]\right)\exp\left[-\frac{L_c}{4}(y_{k1}-d_k)^2\right]\exp\left[-\frac{L_c}{4}\sum_{i=2}^{n}(y_{ki}-x_{ki})^2\right].\end{aligned} \tag{2.22}$$

The original input bit $x_{k1} = d_k$ and its received version y_{k1} locate at the first place of the received signal for a time instant k. Applying the above expression in the

whole MAP LLR (2.12):

$$
\begin{aligned}
L(d_k|\mathbf{y}) &= \ln\left[\frac{\sum_{\substack{(s',s)\Rightarrow \\ d_k=+1}} \gamma_k(s',s)\alpha_{k-1}(s')\beta_k(s)}{\sum_{\substack{(s',s)\Rightarrow \\ d_k=-1}} \gamma_k(s',s)\alpha_{k-1}(s')\beta_k(s)}\right] \\
&= \ln\left\{\frac{\sum_{\substack{(s',s)\Rightarrow \\ d_k=+1}} \exp\left(+[L(d_k)/2]\right)\exp\left[-\frac{L_c}{4}(y_{k1}-d_k)^2\right]\exp\left[-\frac{L_c}{4}\sum_{i=2}^{n}(y_{ki}-x_{ki})^2\right]\alpha_{k-1}(s')\beta_k(s)}{\sum_{\substack{(s',s)\Rightarrow \\ d_k=-1}} \exp\left(-[L(d_k)/2]\right)\exp\left[-\frac{L_c}{4}(y_{k1}-d_k)^2\right]\exp\left[-\frac{L_c}{4}\sum_{i=2}^{n}(y_{ki}-x_{ki})^2\right]\alpha_{k-1}(s')\beta_k(s)}\right\} \\
&= \ln\left\{\frac{\sum_{\substack{(s',s)\Rightarrow \\ d_k=+1}} \exp\left(+[L(d_k)/2]\right)\exp\left[-\frac{L_c}{4}(y_{k1}-1)^2\right]\gamma_k^{ext}(s',s)\alpha_{k-1}(s')\beta_k(s)}{\sum_{\substack{(s',s)\Rightarrow \\ d_k=-1}} \exp\left(-[L(d_k)/2]\right)\exp\left[-\frac{L_c}{4}(y_{k1}+1)^2\right]\gamma_k^{ext}(s',s)\alpha_{k-1}(s')\beta_k(s)}\right\} \\
&= L(d_k) + \frac{L_c}{4}[(y_{k1}+1)^2-(y_{k1}-1)^2] + L^{ext}(d_k),
\end{aligned}
\tag{2.23}
$$

where

$$
\gamma_k^{ext}(s',s) = \exp\left[-\frac{L_c}{4}\sum_{i=2}^{n}(y_{ki}-x_{ki})^2\right] \tag{2.24}
$$

and

$$
L^{ext}(d_k) = \ln\left[\frac{\sum_{\substack{(s',s)\Rightarrow \\ d_k=+1}} \gamma_k^{ext}(s',s)\alpha_{k-1}(s')\beta_k(s)}{\sum_{\substack{(s',s)\Rightarrow \\ d_k=-1}} \gamma_k^{ext}(s',s)\alpha_{k-1}(s')\beta_k(s)}\right] \tag{2.25}
$$

are extrinsic $\gamma_k(s',s)$ and LLR respectively. Equation (2.25) is the soft output of each turbo decoder, which is communicated in each decoding iteration from one constituent decoder to another. The extrinsic LLR contains the information provided by other bits related to d_k that are different for each decoder, due to the fact that the bit d_k was interleaved and encoded in different manners by two constituent encoders [57].

According to (2.23), the extrinsic LLR is obtained as

$$
L^{ext}(d_k) = L(d_k|\mathbf{y}) - L(d_k) - \frac{L_c}{4}[(y_{k1}+1)^2-(y_{k1}-1)^2]. \tag{2.26}
$$

Thus all these coefficients can be calculated from the decoding procedure, which allows the probability term $\gamma_k(s',s) = P(y_k|\{s',s\})P(d_k)$ to be determined for all the trellis transitions.

Once $\gamma_k(s',s)$ is known, we can calculate $\alpha_k(s)$ for the current state through

forward recursions over the trellis when the signals are receiving, as $\alpha_k(s)$ depends on the value of $\gamma_k(s', s)$ and its previous state version: $\alpha_{k-1}(s')$. The term $\beta_{k-1}(s')$ for the previous state is determined after the whole signal has been received, using backward recursions, which depends on the value of $\gamma_k(s', s)$ and the current state version: $\beta_k(s)$. Then, the MAP LLR $L(d_k|\mathbf{y})$ can be calculated immediately $\alpha_{k-1}(s')$, $\beta_k(s)$ and $\gamma_k(s', s)$ are determined.

Finally in each decoding iteration, one decoder provides the result of MAP LLR, in the mean time, it communicates to another constituent decoder with its $L^{ext}(d_k)$, which is considered in another decoder as $L(d_k)$.

To sum up, the BCJR MAP algorithm for the decoding of turbo codes can be outlined as follows [62]:

1. Set the initial conditions $\alpha_0(0) = 1$ and $\alpha_0(s) = 0, s \neq 0$, and the termination conditions $\beta_n(0) = 1$ and $\beta_n(s) = 0, s \neq 0$ for $s = 0, 1, 2, \ldots, S-1$;

2. Given priori probabilities of d_k (usually assumed equiprobable to be 0 or 1), the channel reliability L_c and the received sequence y_k, the decoder calculates $\gamma_k(s', s)$ with equation (2.11);

3. Calculate $\alpha_k(s)$ with equation (2.9) using forward recursion. The determined values are stored for every time instant k and state s;

4. After receiving the whole sequence $\mathbf{y}$, the decoder computes $\beta_{k-1}(s')$ recursively using (2.10);

5. Once all the $\beta_k(s)$ values are obtained, the product of $\alpha_{k-1}(s')$, $\beta_k(s)$ and $\gamma_k(s', s)$ terms makes the decoding decision LLR (2.12) accomplished.

2.3 Applying turbo codes in the MAI environment

Now we consider the problem of applying the turbo codes in the non-Gaussian environment discussed in Chapter 1. The noise environment is composed by the convolution between an independent SαS distributed network interference and a Gaussian distributed thermal noise, the result of which is not stable distributed. There is no explicit pdf for neither a general SαS distribution nor a mixture of the Gaussian and SαS distributions.

The lack of PDF for the noise distribution causes a problem when calculating LLR in the decoding algorithm, in which the probability density is needed to determine $\gamma_k(s', s)$, $\alpha_{k-1}(s')$ and $\beta_k(s)$ terms.

One method used in [24] is the Huber metric, first proposed by Huber in robust statistics for the work on M-estimation [44]. As a hybrid metric which

combines the L_1 norm and the Euclidean distance, Huber function handled well the task in the soft-decision decoding of convolutional codes [23] and turbo codes [24], when only the SαS interference is present.

Another method carried out in [67] is the numerical-based SαS pdf computation for the MAP decoder of turbo codes. In this solution, the pdf of the SαS is derived using numerical inverse Fourier transformation, limiting the integral over a finite interval. In spite of the proximity to the real SαS pdf value, the numerical computation costs too much computer resource and time, and the estimation of noise parameters (α, σ, and γ) used in the computation remains a difficult task.

Our proposal is based on the theory of SαS norm and the definition of SαS variable distance. Within a general combination of SαS interference and Gaussian noise, the p-norm expression can be easily derived, with its parameter p according to the SαS interference exponent value α, or a very rough estimation of noise environment is sufficient.

The methods discussed above will be detailed in the following sections. A comparison among these solutions will be shown through simulations.

2.3.1 Huber metric in MAP LLR

Huber function

It is noticed that equation (2.20) measures the Euclidean distance between the received and the transmitted code word. This is obtained when the transmission is interfered by only the Gaussian thermal noise. This metric is referred to as an estimator of the least squares (LS) type [24]. In some statistics literatures [47, 73], it is noted that the performance of the LS estimator will be seriously degraded in non-Gaussian environment, especially when impulsive but rare-appeared noise is present in the signal. This is due to the quadratic type signal processing scheme used in the LS estimator.

In order to still profit the formulated framework under the Gaussian assumption in Section 2.2.3, a hybrid-metric method was investigated which led to a still good performance with the Gaussian model and meanwhile performed satisfactorily on deviations from the Gaussian assumption [24].

The soft metric in terms of a penalty function ρ is first introduced. Take the

equation (2.20) for example:

$$\begin{aligned} P(y_k|x_k) &= \frac{1}{(\sqrt{2\pi}\sigma)^n} \exp\left[-\frac{E_b}{2\sigma^2}\sum_{i=1}^{n}(y_{ki}-x_{ki})^2\right] \\ &= \frac{1}{(\sqrt{2\pi}\sigma)^n} \exp\left[-\frac{L_c}{2}\sum_{i=1}^{n}\rho_{LS}(y_{ki}-x_{ki})\right], \end{aligned} \tag{2.27}$$

where the LS penalty function ρ_{LS} is

$$\rho_{LS}(x) = \frac{1}{2}x^2. \tag{2.28}$$

It is noticed that the LS estimator performs a quadratic calculation for all the entry amplitudes without a selection. The impulsive values will distort heavily the estimator output with the quadratic process. Thus an alternative form in the sense of slowing down the quadratic expanding is needed. This means that the penalty function ρ_{LS} should fulfil both the Gaussian-like and impulsive heavy-tailed noise.

The Huber function is of such a type, proposed firstly by Huber on M-estimation work [44]. As a robust metric, the Huber function combines the conventional LS penalty function and L_1 norm:

$$\rho_H(x) = \begin{cases} \frac{1}{2}x^2, & \text{for } |x| \leqslant h \\ h|x| - \frac{1}{2}h^2, & \text{for } |x| > h \end{cases} \tag{2.29}$$

where $h > 0$ is the Huber threshold to divide the conventional LS and L_1 norm. From the Huber function, we notice that the input value smaller than h is treated as least squares type. In this case, if the input is the received code word minus transmitted code word, their difference is measured by Euclidean distance, which is in fact the L_2 norm. Then for the input value greater than h, the Huber function penalises the value with L_1 norm.

Huber metric based MAP LLR

Based on the Huber function, a Huber metric base MAP LLR can be stated by replacing the conventional LS penalty function with the Huber penalty function.

Firstly, the branch transition probability (2.13) is redefined with the Huber

metric:

$$\gamma_k^H(s', s) = P^H(y_k|x_k)P^H(d_k), \tag{2.30}$$

where

$$P^H(y_k|x_k) = \frac{1}{(\sqrt{2\pi}\sigma)^n} \exp\left[-\frac{L_c}{2}\sum_{i=1}^{n}\rho_H(y_{ki} - x_{ki})\right], \tag{2.31}$$

and $P^H(d_k)$ will be define after.

Hence the Huber metric based term for $\alpha_k(s)$ and $\beta_{k-1}(s')$ can be calculated recursively as a function of the new definition of $\gamma_k(s', s)$:

$$\alpha_k^H(s) = \sum_{s'=0}^{S-1}\alpha_{k-1}^H(s')\gamma_k^H(s', s), \tag{2.32}$$

$$\beta_{k-1}^H(s') = \sum_{s=0}^{S-1}\gamma_k^H(s', s)\beta_k^H(s). \tag{2.33}$$

Then the Huber metric based MAP LLR expression turns out as

$$L^H(d_k|\mathbf{y}) = \ln\left[\frac{\sum_{\substack{(s',s)\Rightarrow \\ d_k=+1}}\gamma_k^H(s', s)\alpha_{k-1}^H(s')\beta_k^H(s)}{\sum_{\substack{(s',s)\Rightarrow \\ d_k=-1}}\gamma_k^H(s', s)\alpha_{k-1}^H(s')\beta_k^H(s)}\right]. \tag{2.34}$$

In order to obtain the Huber metric based *a priori* probability for the input bit d_k, we have

$$\begin{aligned}
L^H(d_k|\mathbf{y}) &= \ln\left[\frac{\sum_{\substack{(s',s)\Rightarrow \\ d_k=+1}}\gamma_k^H(s', s)\alpha_{k-1}^H(s')\beta_k^H(s)}{\sum_{\substack{(s',s)\Rightarrow \\ d_k=-1}}\gamma_k^H(s', s)\alpha_{k-1}^H(s')\beta_k^H(s)}\right] \\
&= \ln\left\{\frac{\sum_{\substack{(s',s)\Rightarrow \\ d_k=+1}}\exp\left(+[L(d_k)/2]\right)\exp\left[-\frac{L_c}{2}\rho_H(y_{k1}-1)\right]\gamma_k^{ext,H}(s', s)\alpha_{k-1}^H(s')\beta_k^H(s)}{\sum_{\substack{(s',s)\Rightarrow \\ d_k=-1}}\exp\left(-[L(d_k)/2]\right)\exp\left[-\frac{L_c}{2}\rho_H(y_{k1}+1)\right]\gamma_k^{ext,H}(s', s)\alpha_{k-1}^H(s')\beta_k^H(s)}\right\} \\
&= L(d_k) + \frac{L_c}{2}[\rho_H(y_{k1}+1) - \rho_H(y_{k1}-1)] + L^{ext,H}(d_k).
\end{aligned} \tag{2.35}$$

Thus the extrinsic LLR for d_k based on the Huber metric is

$$L^{ext,H}(d_k) = L^H(d_k|\mathbf{y}) - L^H(d_k) - \frac{L_c}{2}[\rho_H(y_{k1}+1) - \rho_H(y_{k1}-1)]. \quad (2.36)$$

In each decoding iteration of the turbo codes, one constituent decoder communicates to the other constituent decoder the Huber metric based extrinsic LLR of d_k. To the other decoder, this extrinsic LLR $L^{ext,H}(d_k)$ is used as $L(d_k)$ to produce another $L^{ext,H}(d_k)$. Once the communication of $L^{ext,H}(d_k)$ between two constituent decoders starts, the initial $L(d_k)$ is updated and noted as $L^H(d_k)$. Then the Huber metric based $P^H(d_k)$ can be obtained as

$$P^H(d_k = \pm 1) = \frac{\exp\left(-L^H(d_k)/2\right)}{1+\exp\left(-L^H(d_k)\right)} \exp\left(d_k[L^H(d_k)/2]\right) \quad (2.37)$$

With the help of $P^H(y_k|x_k)$ and $P^H(d_k)$, the calculation of $\gamma_k^H(s',s)$ is accomplished, then the MAP LLR based on the Huber metric (2.34) can be resolved.

2.3.2 Numerical-based PDF calculation

It is clear that the main problem for calculating the MAP LLR in decoding procedure is the lack of closed-form PDF expression for either the SαS or the mixture of the SαS and Gaussian distributions. Based on the fact that the characteristic functions for both the above distributions are closed, and that the characteristic function is the Fourier transform of the PDF, a direct solution is given by the numerical calculation of the inverse Fourier transform.

In our case, the characteristic function of the SαS distribution has its form:

$$\phi(\omega) = \exp(-\gamma|\omega|^\alpha), -\infty < \omega < \infty. \quad (2.38)$$

By employing the inverse Fourier transform on the characteristic function, the general SαS PDF can be evaluated as

$$f_\alpha(x) = \frac{1}{2\pi}\int_{-\infty}^{\infty} \exp(-\gamma|\omega|^\alpha) e^{-j\omega x} \mathrm{d}\omega, \quad (2.39)$$

where the subscript α indicates the characteristic exponent in the SαS distribution.

With some acceptable tolerance, the PDF of the SαS distribution was approx-

imated in [67] by an integral over a finite interval:

$$f_\alpha(x) \approx \frac{1}{2\pi}\int_{-\pi L}^{\pi L} \exp(-\gamma|\omega|^\alpha)e^{-j\omega x}\mathrm{d}\omega. \tag{2.40}$$

The obtained numerical PDF $f_\alpha(x)$ can be applied on the term $\gamma_k(s', s)$ of the MAP LLR equation. The term $P(y_k|\{s', s\})$ in (2.13) needs the probability density $f_\alpha(x)$. In a general α-stable noise environment, (2.13) can be expressed as:

$$\begin{aligned}\gamma_k(s', s) &= P(y_k|\{s', s\})P(d_k) \\ &= C' \exp\left(d_k[L(d_k)/2]\right) \prod_{i=1}^{n} f_\alpha(y_{ki} - x_{ki}),\end{aligned} \tag{2.41}$$

where i denotes the i^{th} bit in a code word at instant k.

For the numerical calculation, the finite interval $[-\pi L, \pi L]$ was divided into N subintervals of length $2\pi L/N$ and the partition points were chosen as $\omega_m = 2\pi mL/N$ for $m = -(N/2), -(N/2-1), \ldots, -1, 0, 1, \ldots, (N/2-2), (N/2-1)$. By discrete inverse Fourier transform, $f_\alpha(x)$ can be calculated as

$$\begin{aligned}f_\alpha(x) &\approx \frac{1}{2\pi}\sum_{m=-(N/2)}^{N/2-1} \exp\left(-\gamma\left|\frac{2\pi mL}{N}\right|^\alpha\right) e^{-2\pi jmLx/N}\left(\frac{2\pi L}{N}\right) \\ &= \frac{L}{N}\sum_{m=-(N/2)}^{N/2-1} \exp\left(-\gamma\left|\frac{2\pi mL}{N}\right|^\alpha\right) e^{-2\pi jmLx/N}.\end{aligned} \tag{2.42}$$

If $f_\alpha(x)$ is still sampled at intervals of $1/L$ at sampling points $n = 0, \pm 1, \pm 2, \ldots$, equation (2.42) can be written as:

$$f_\alpha\left(\frac{n}{L}\right) \approx \frac{L}{N}\sum_{m=-(N/2)}^{N/2-1} \exp\left(-\gamma\left|\frac{2\pi mL}{N}\right|^\alpha\right) e^{-2\pi jmn/N}. \tag{2.43}$$

In [67], the tolerance $N \geqslant 8L \times M$ was selected, where M is the largest value of $|y_{ki} - x_{ki}|$ in (2.41) and L was chosen large enough such that the area under the characteristic function beyond the range $[-\pi L, \pi L]$ is small and can be neglected. In practical work, the value N turned out to be 256 for the case of [67]. The $f_\alpha(x)$ was calculated in advance for a desired range and the result was stored in a lookup table in [67].

However, what we considered is the convolution of Gaussian and stable noises,

the characteristic function of which is $\phi(\omega) = \exp(-\gamma|\omega|^\alpha - \frac{\sigma^2}{2}\omega^2), -\infty < \omega < \infty$. Besides, we have tested that the value $N = 256$ is only sufficient for $\gamma = 1$. A period $N = 5000$ was used in our simulation in order to ensure the accuracy of the PDF calculation.

2.3.3 *p*-norm metric

It is seen in the MAP LLR expression (2.12) and the decoding outline for turbo codes, the term $\gamma_k(s', s)$ is calculated first, then the remaining terms $\alpha_{k-1}(s')$ and $\beta_k(s)$ can be determined as a function of $\gamma_k(s', s)$. Inside the term $\gamma_k(s', s)$, only $P(y_k|\{s', s\})$ is unknown without the knowledge of noise probability density according to the calculation procedure of (2.13). The value of $P(y_k|\{s', s\})$ in the memoryless AWGN channel in the example of section 2.2.3 is finally acquired by estimating the Euclidean distance between the received and transmitted code words, as shown in (2.21). Thus a distance measurement corresponding to the SαS distribution should replace the Euclidean distance.

In spite of the non-existence for the second-order moment of a SαS random variable with $0 < \alpha < 2$, all moments of order less than α exist with the name fractional lower order moments (FLOMs) [58]. Based on the dispersion γ and characteristic exponent α of a SαS random variable, the FLOMs can be defined as:

$$E(|x|^p) = C(\alpha, p)\gamma^{\frac{p}{\alpha}} \quad 0 < p < \alpha, \tag{2.44}$$

where

$$C(\alpha, p) = \frac{2^{p+1}\Gamma((p+1)/2)\Gamma(-p/\alpha)}{\alpha\sqrt{\pi}\Gamma(-p/2)}$$

is a constant depending only on α and p, and $\Gamma(.)$ is the usual gamma function defined as

$$\Gamma(x) = \int_0^\infty t^{x-1}e^{-t}\mathrm{d}t.$$

Then, combining (2.44) with the definition of the stable variable norm [58]

$$||X||_\alpha = \begin{cases} \gamma^{\frac{1}{\alpha}} & 1 \leqslant \alpha \leqslant 2 \\ \gamma & 0 < \alpha < 1, \end{cases} \tag{2.45}$$

the distance between two SαS variables can be then expressed for $0 < p < \alpha$ as

$$||X - Y||_\alpha = \begin{cases} [E|X - Y|^p / C(\alpha, p)]^{1/p} & 1 \leqslant \alpha \leqslant 2 \\ [E|X - Y|^p / C(\alpha, p)]^{\alpha/p} & 0 < \alpha < 1. \end{cases} \tag{2.46}$$

where the equation measures the p^{th}-order moment of the difference between these two random variables, or we can say the distance measures the difference between them under the p-norm.

Inspired by such a distance metric for SαS random variables, and the advantage that this measurement does not depend on any estimation of distribution parameters (at most a rough estimation to fulfil the condition $0 < p < \alpha$ is sufficient), we shall employ the expression given in (2.47) as a distance metric in the term $P(y_k|\{s', s\})$ for the MAP decoding, choosing p as $0 < p < \alpha$:

$$\hat{d}(y_k, x_k) = \sum_{i=1}^{n} |y_{ki} - x_{ki}|^p. \tag{2.47}$$

When $p = 2$, the p-norm metric becomes the conventional Euclidean distance.

2.4 Simulation results

In this section, performance of different turbo decoder proposals for the MAI environment are presented. Simulations were carried out under Matlab environment. The performance are evaluated through the BER versus geometric SNR.

The turbo encoder is configured using two $(1, 5/7)$ RSC codes, in which the forward generator polynomial is $\mathbf{g}_1 = 1 + D^2$ and the backward generator polynomial is $\mathbf{g}_2 = 1 + D + D^2$. Then given the n-length input sequence $\mathbf{d} = \{d_1, d_2, \ldots, d_n\}$, the encoded bipolar sequence without puncturing is represented as $\mathbf{x} = \{x_1, x_2, \ldots, x_{3n}\}$, thus with a code rate $1/3$. A 1024-length random interleaver is employed between two constituent RSC encoders.

The performance of turbo codes improves by increasing the number of iterations. We show in Figure 2.4 the influence of iteration numbers in the decoding algorithm. As an example, only SαS modelled network interference is presented in the channel with $\alpha = 1.5$. The p-norm is used as the decoding metric with $p = 1.3$. As this is a SαS adapted metric, the p-norm decoder can reduce the BER with increasing of iteration number. As seen in Figure 2.4, the BER decreases more and more with the increase of iteration number. But the performance improvement becomes limited after the 4^{th} iteration under our simulation con-

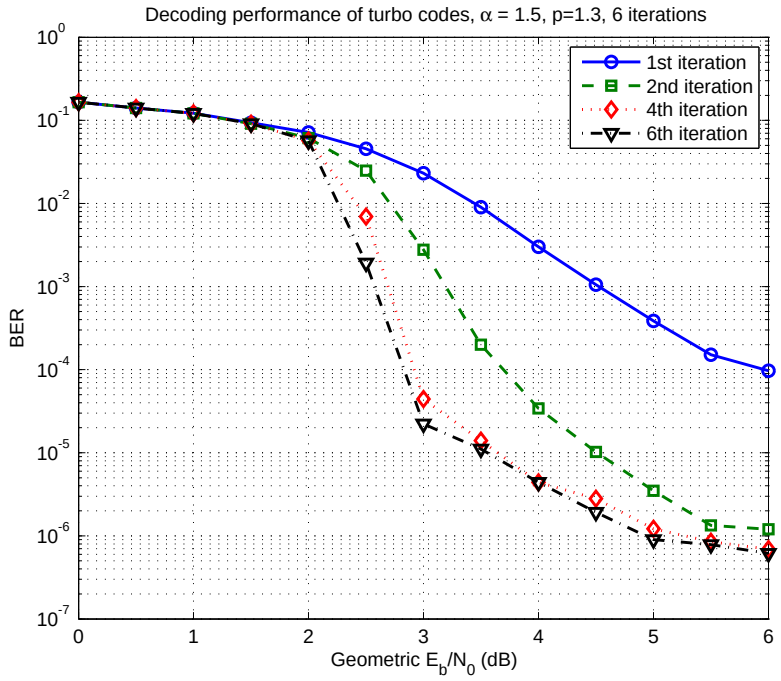

Figure 2.4: Improvement of performance by increasing the iteration number in the decoding of turbo codes.

figuration. Thus we choose the 6^{th} iteration as the maximum iteration in all the simulations, since the performance of this iteration number distinguishes already greatly from the 1^{st} iteration, and keeps a reasonable cost of time and computation. For each figure presented below, only the 1^{st} and the 6^{th} iteration results are left, in order to make the comparison clear but without loss of validity.

For the decoder metric comparison, the noise environment is divided into two categories to better investigate each method:

- only SαS modelled impulsive interference is present, thus $\mathbf{y} = \mathbf{x} + \mathbf{I}$;
- SαS interference and Gaussian noise are both present, thus $\mathbf{y} = \mathbf{x} + \mathbf{N} + \mathbf{I}$.

2.4.1 Stable interference only

In this section, the decoding performance of turbo codes is evaluated in the SαS modelled noise environment. As a replacement of Euclidean distance in the decoding LLR criterion, the p-norm metric is compared first of all with the conventional Euclidean distance. In the second time, the decoding performance of the p-norm metric is compared with the Huber function metric, with many different noise parameters. At last, the performance is evaluated as a function of the value p, to investigate the influence of p in the p-norm metric.

Comparison between the p-norm and Euclidean distance

In order to present performance improvement by a SαS adapted metric from the conventional Euclidean distance metric, the p-norm with several p values is tested in $\alpha = 1.5$ and $\alpha = 1.0$ SαS interference in Figure 2.5 and 2.6. It is shown in both the impulsive ($\alpha = 1.0$) and less impulsive environments ($\alpha = 1.5$) that the conventional Euclidean distance cannot have an acceptable performance. The BER obtained by the Euclidean distance ($p = 2.0$) metric are always above the level of 10^{-3} even with a geometric E_b/N_0 up to 10 dB in $\alpha = 1.5$ case. The performance becomes worse when the noise becomes more impulsive ($\alpha = 1.0$), where the BER are greater than the level of 10^{-2}. It proves that the conventional metric in the decoding structure cannot deal with the impulsive environment.

When using the p-norm metric ($p < \alpha$), a considerable improvement is acquired compared with the use of the Euclidean distance ($p = 2.0$). Although the BER is not small enough for the 1^{st} iteration, it descends quickly with the growth of iterative number, and the performance gain is obvious at the 6^{th} iteration. For example, in the case when $\alpha = 1.5$, a gain of about 3.5 dB is obtained in terms of geometric E_b/N_0 at 10^{-3} BER by using $p = 1.3$ for p-norm, compared with the Euclidean distance. In a more impulsive case, it is seen from Figure 2.6, the

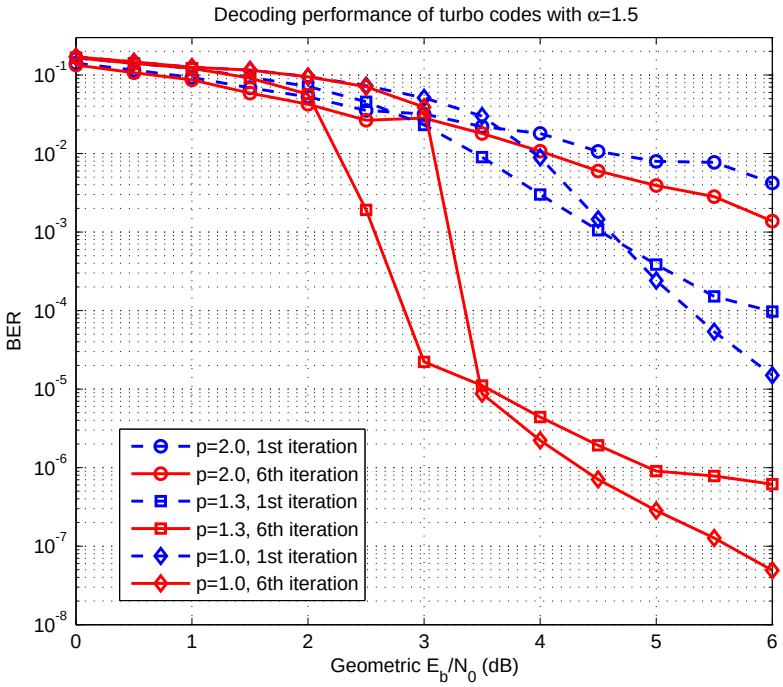

Figure 2.5: Turbo decoder performance using p-norm and Euclidean distance in SαS noise ($\alpha = 1.5$).

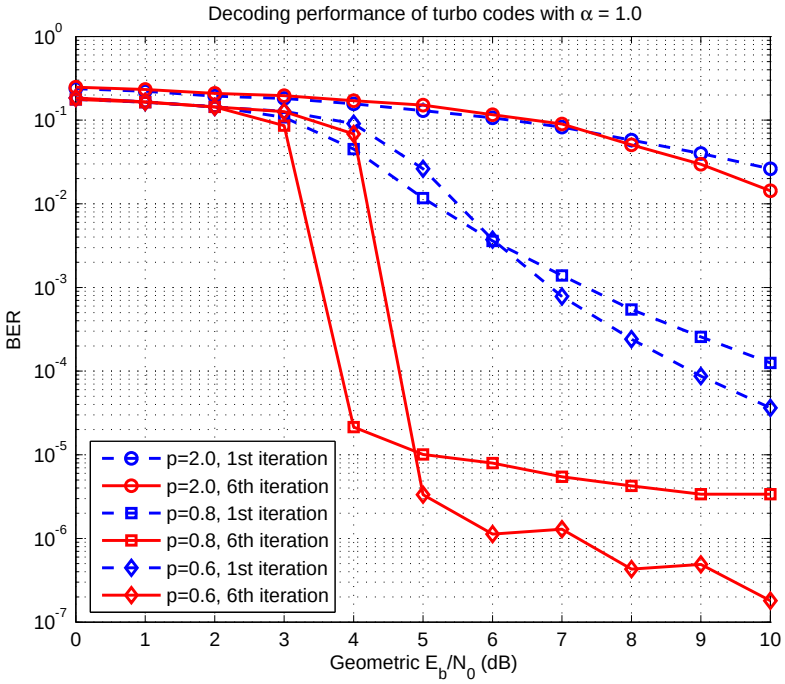

Figure 2.6: Turbo decoder performance using p-norm and Euclidean distance in SαS noise ($\alpha = 1.0$).

p-norm can still obtain a small BER, and may even reach the level of 10^{-7} at a high SNR.

Comparison between the p-norm and Huber function

Since the Huber function has been proved useful in dealing with the impulsive interference for the decoding of convolutional codes [23] or turbo codes [24, 67], we compare this metric with the p-norm in the following simulations. We have simulated the SαS noise environments with $\alpha = \{1.6, 1.4, 1.0, 0.8\}$, four different situations. The SαS was set to be more and more impulsive and in each condition, both the p-norm metric and the Huber function metric were tested. The threshold for the Huber function (2.29) is set as 3γ as proposed and tested in [23].

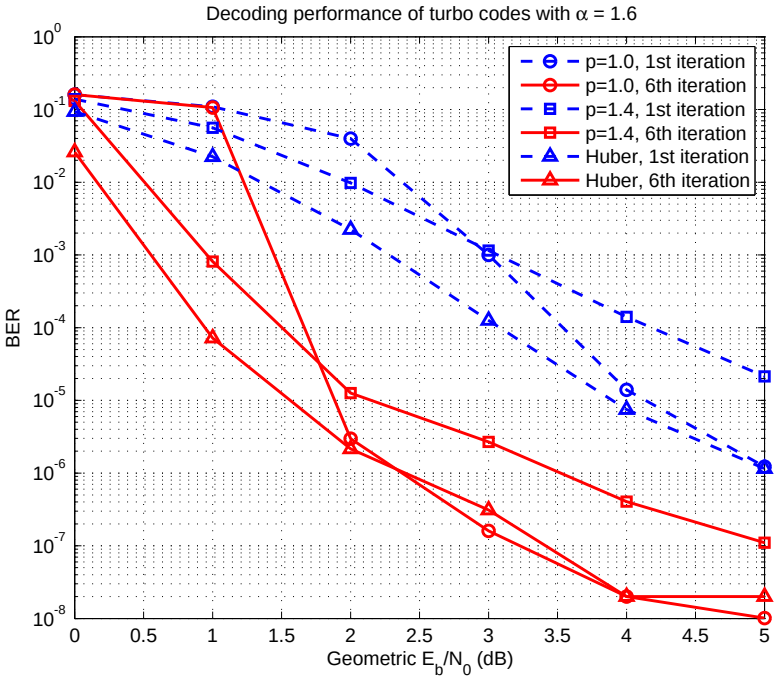

Figure 2.7: Turbo decoder performance using p-norm and Huber function in SαS noise ($\alpha = 1.6$).

We can observe from Figure 2.7 to 2.10, that both the p-norm and Huber function perform well. Their BERs can reach a low level, except in $\alpha = 0.8$ case, Huber metric cannot bring down the BER below the level of 10^{-3}. For the less impulsive cases (α close to 2, thus the cases with $\alpha = 1.6$ and $\alpha = 1.4$), the Huber metric is comparable with the p-norm metric, as their curves are close to each

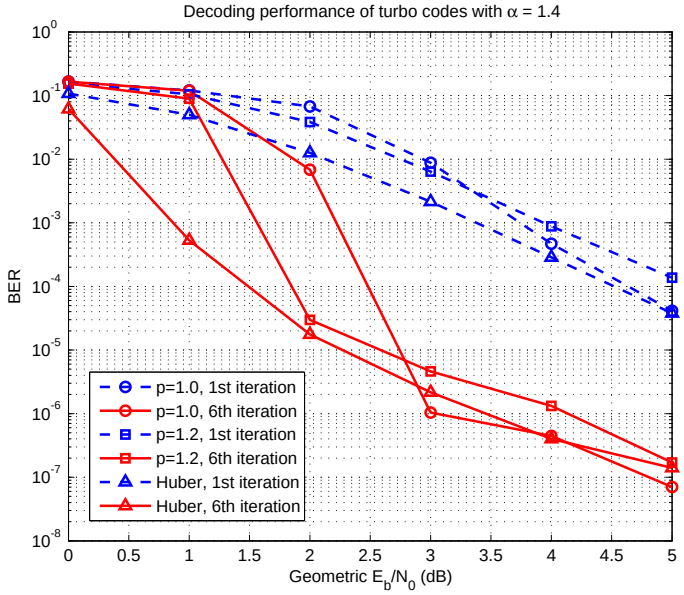

Figure 2.8: Turbo decoder performance using p-norm and Huber function in SαS noise ($\alpha = 1.4$).

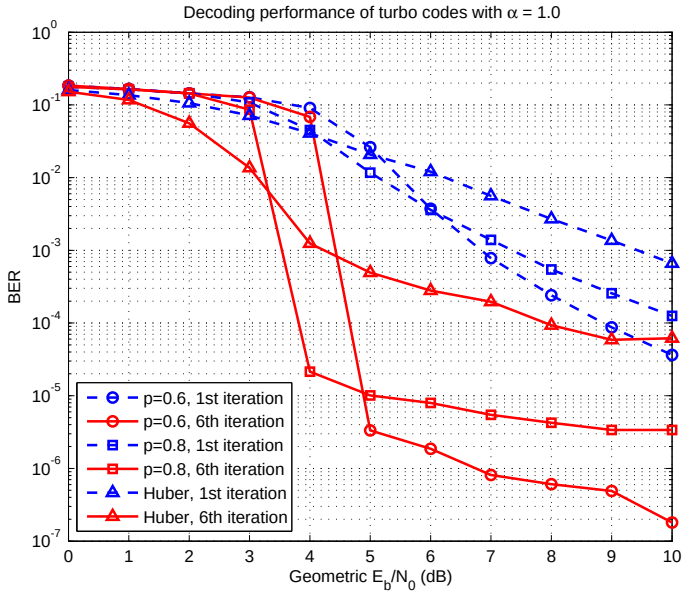

Figure 2.9: Turbo decoder performance using p-norm and Huber function in SαS noise ($\alpha = 1.0$).

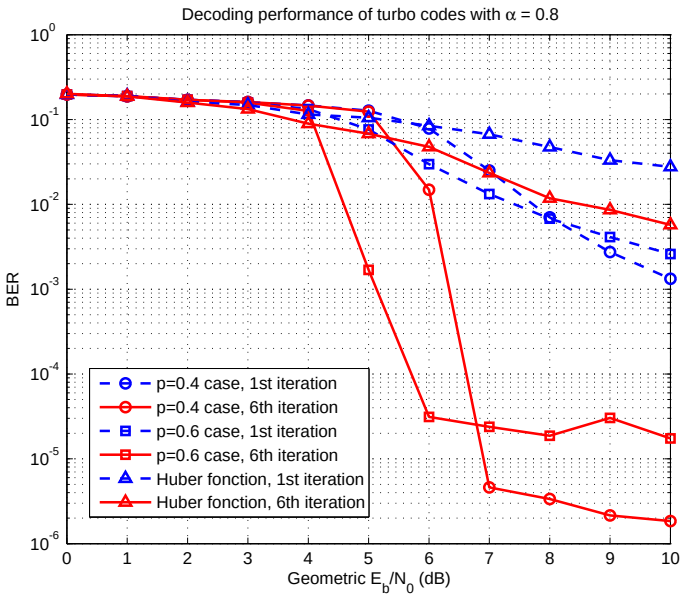

Figure 2.10: Turbo decoder performance using p-norm and Huber function in SαS noise ($\alpha = 0.8$).

other. However, when the noise becomes more impulsive (the cases with $\alpha = 1.0$ and $\alpha = 0.8$), only the p-norm metric can reach a low BER with the increase of geometric SNR. The Huber metric can have a descending trend, but not as fast as the p-norm. Especially in the most impulsive case that we tested ($\alpha = 0.8$), the 6^{th} iteration result of the Huber metric performed even worse than the 1^{st} iteration results of the p-norm.

The comparison showed that the Huber function can be used as a good decoding metric in impulsive noise environment, but the impulsiveness should be limited to a certain level. The p-norm is more robust and can face any impulsive noise environment, if the condition $p < \alpha$ is fulfilled. Hence the p-norm can be a good candidate for the decoding metric of turbo codes. It depends only on one noise parameter α, and a rough estimation of α may be sufficient.

Investigation of p values for the p-norm metric

In order to investigate the influence of the value of p in the p-norm, we launched another series of tests to compare different p values. We choose a less impulsive environment with $\alpha = 1.5$ and a more impulsive one with $\alpha = 1.0$. The p values are chosen to be $p = \{1.0, 1.3, 1.4\}$ for $\alpha = 1.5$ case and $p = \{0.4, 0.6, 0.8\}$ for $\alpha = 1.0$ case.

From Figure 2.11 to 2.12, we can find that the curves representing different

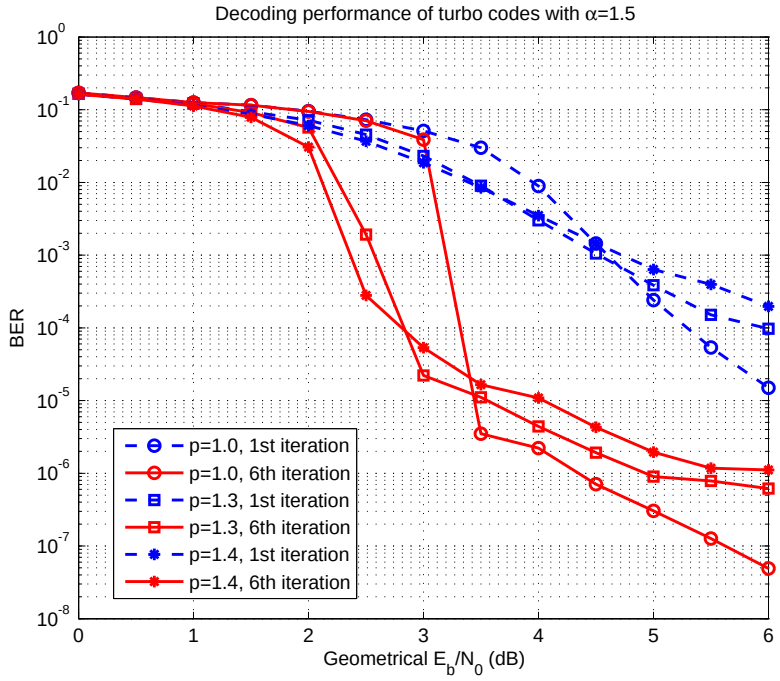

Figure 2.11: Turbo decoder performance using p-norm in SαS noise ($\alpha = 1.5$).

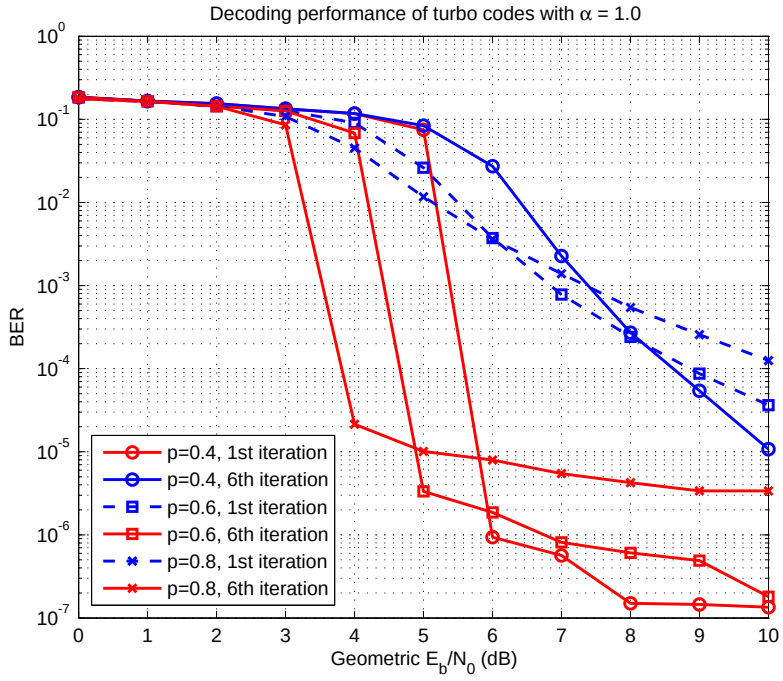

Figure 2.12: Turbo decoder performance using p-norm in SαS noise ($\alpha = 1.0$).

values of p are not far from each other. They turn out to descend very sharply from a given SNR and then tend to converge to a certain level. One can see that the greater the value of p, the earlier the curve descends but the higher level the BER converges to. It is clearer in the case $\alpha = 1.0$. With increasing of p value by 0.2, a gap about 1 dB is gained in terms of geometric E_b/N_0 for the descending zones. However, a 0.2 smaller value of p allows to reduce the BER by a factor 2 to 3.

The results showed that the value of p is not so sensitive to the whole decoding performance, but slightly modifies the BER curves. This leaves some flexibility in the decoding design but without any loss of robustness.

A further study is necessary to better assess the choice of p. A fixed value can probably cope with most of the possible situations in a given context. However our work only relies on simulations and a faster way to obtain the efficiency of a given p is necessary.

2.4.2 Stable interference plus Gaussian noise

In this section, we evaluate the different turbo decoders in the impulsive noise environments modelled by SαS interference plus Gaussian noise. The SNR of Gaussian noise is set to 10 dB for all the following simulations. We vary the dispersion of SαS interference and represent the error probability as a function of the geometric energy-to-interference ratio E_b/I (in the environment where both the Gaussian noise and SαS interference are present, we use letter I to stand for the SαS noise instead of N in the SNR expression, more details about the geometric power theory can be found in Chapter 1):

$$(E_b/I)_{\text{geo}} = \frac{C_g}{4r}\left(\frac{A}{(C_g\gamma)^{1/\alpha}}\right)^2, \tag{2.48}$$

where r is the code rate, A is the signal amplitude and $C_g \approx 1.78$ is the exponential of the Euler constant.

As a benchmark, we provide the optimal turbo decoder as well (marked in figures as "pdf"), in which the probability density in the MAP LLR expression was calculated through numerical approach, using the discrete Fourier transform of the characteristic function with 5000 intervals. The metric using the Huber function was tested in this environment and is presented as well. As a combination of 1-norm and 2-norm, we chose the threshold 3γ in the Huber function as proposed in [23]. We illustrate in the following figures the decoding BER from the first and the sixth decoding iteration.

Comparison of different decoder metrics

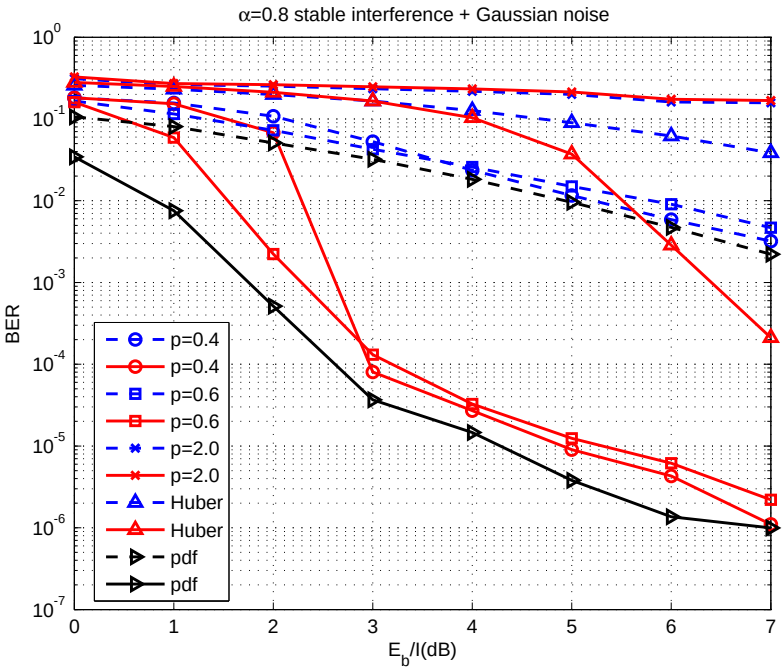

Figure 2.13: BER versus geometric (E_b/I) in $\alpha = 0.8$ interference + Gaussian noise (SNR = 10 dB).

Once again, from Figure 2.13 to 2.16, we notice first of all that the Euclidean distance ($p = 2.0$) cannot deal with any decoding task in all these environments. The error rate given by this conventional metric show to be between 0.1% and 10%, which is unacceptable in communication transmissions. The Huber function improves the error correction performance if $\alpha > 1$ and (E_b/I) is high. In very impulsive environments (small values of α), only the p-norm can reach a relatively low BER. For example when $\alpha = 0.8$, the p-norm with $p = 0.4$ can still have a BER of 10^{-5} at 4 dB (E_b/I).

We can also observe that the p-norm gives performance close to the optimal decoder which is based on the numerically calculated pdf. In our test, the smaller the value of p we choose, the better BER is obtained, but the later the BER curve falls. Similarly as observed in Section 2.4.1, the choice of p is shown not to be very sensitive (we show the difference between $p = \alpha - 0.2$ and $p = \alpha - 0.4$) as long as $p < \alpha$. This result reveals again some flexibility for the decoding metric when the estimated value of α is not available (or only a rough estimate of α exists).

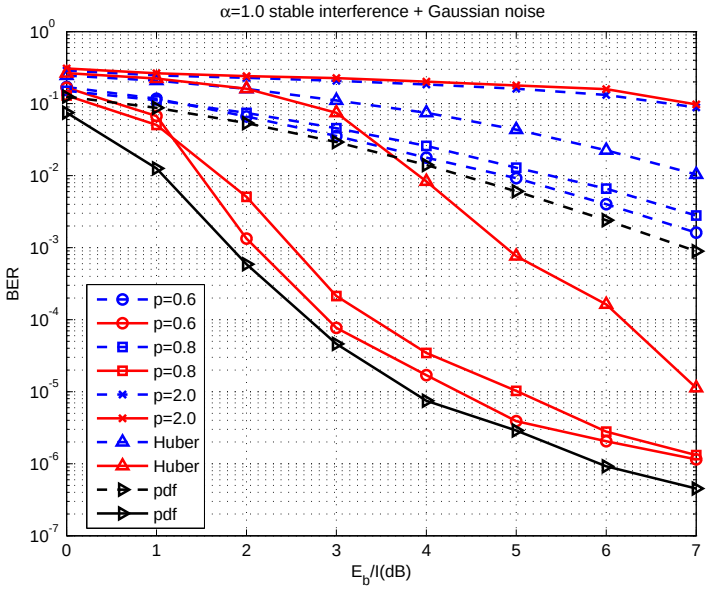

Figure 2.14: BER versus geometric (E_b/I) in $\alpha = 1.0$ interference + Gaussian noise (SNR = 10 dB).

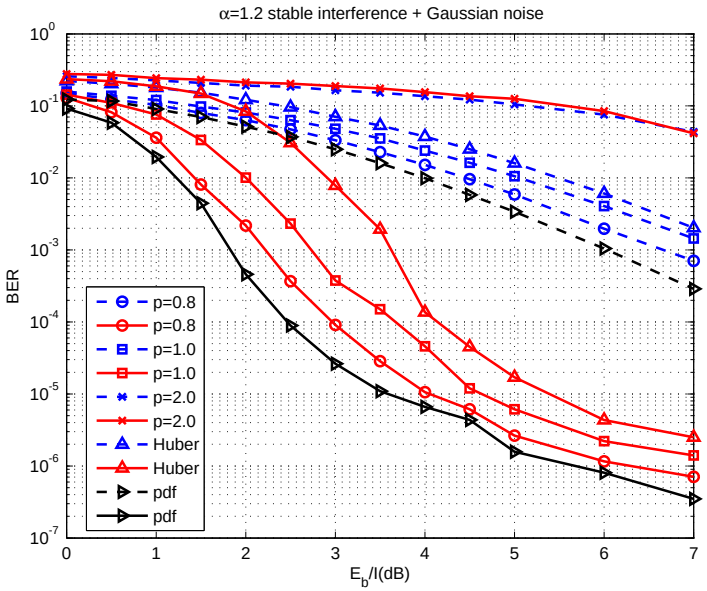

Figure 2.15: BER versus geometric (E_b/I) in $\alpha = 1.2$ interference + Gaussian noise (SNR = 10 dB).

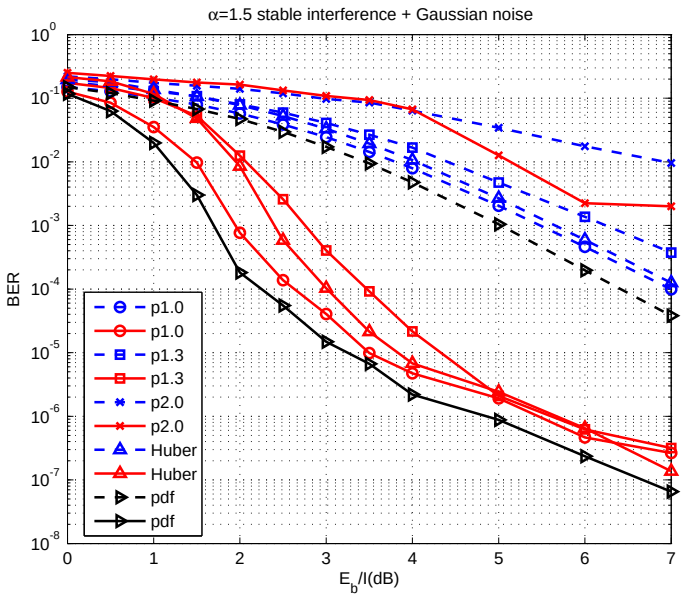

Figure 2.16: BER versus geometric (E_b/I) in $\alpha = 1.5$ interference + Gaussian noise (SNR = 10 dB).

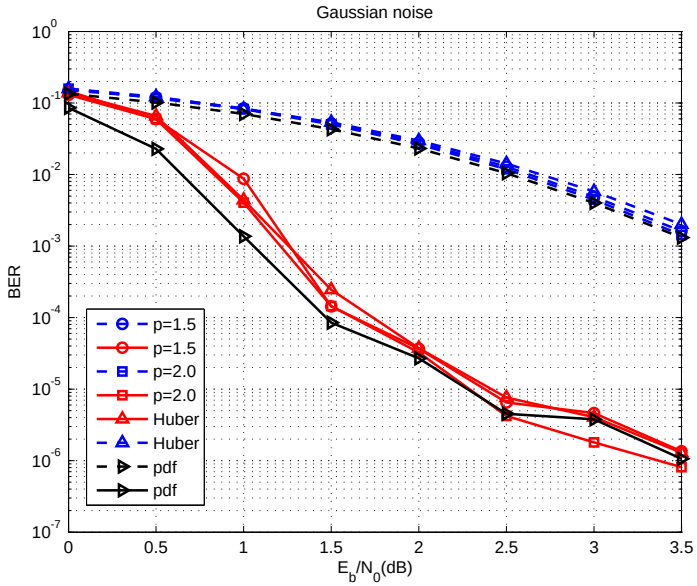

Figure 2.17: BER versus (E_b/N_0) in Gaussian noise (SNR = 10 dB).

Through another test with only Gaussian noise present, we can see from Figure 2.17 that the Huber function and the p-norm have similar performance, and offer almost the equivalent results as the optimal decoder obtained with the Euclidean distance i.e. $p = 2.0$. This proves that all the decoders investigated are suitable for decoding signals embedded in a Gaussian noise.

LLR comparison of different decoders

In order to further investigate the effect of the different proposed metrics and try to understand why they so significantly improve performance, the LLR of the p-norm and the Huber function are established, comparing with the LLR obtained from the numerically computed probability density for the mixture of the SαS interference and Gaussian noise. We assume that one bit x_{kl} from the code word x_k is either $+1$ or -1. Then the LLR is defined as:

$$L(y_{kl}|x_{kl}) = \ln \frac{P(y_{kl}|x_{kl} = +1)}{P(y_{kl}|x_{kl} = -1)} = \ln \frac{f(y_{kl} - 1)}{f(y_{kl} + 1)}, \tag{2.49}$$

$f(.)$ stands for the PDF. The sign of $L(y_{kl}|x_{kl})$ implies the transmitted bit x_{kl} sign ($+1$ or -1) and the magnitude indicates how likely the sign is. The utilization of only one bit of the code word is to simplify the calculation and be able to represent the LLR curves.

For the p-norm, the corresponding LLR is derived through the similar procedure of (2.20), but with a replacement of Euclidean distance with the p-norm metric. If the channel reliability L_c is known and is employed again, the LLR for the p-norm becomes:

$$\begin{aligned} L_p(y_{kl}|x_{kl}) &= \ln \frac{\exp\left(-\frac{L_c}{4}|y_{kl} - 1|^p\right)}{\exp\left(-\frac{L_c}{4}|y_{kl} + 1|^p\right)} \\ &= \frac{L_c}{4}\left[|y_{kl} + 1|^p - |y_{kl} - 1|^p\right]. \end{aligned} \tag{2.50}$$

For the Huber metric, we have also the similar procedure as (2.31) to deduce the LLR:

$$\begin{aligned} L_H(y_{kl}|x_{kl}) &= \ln \frac{\exp\left(-\frac{L_c}{2}\rho_H(y_{kl} - 1)\right)}{\exp\left(-\frac{L_c}{2}\rho_H(y_{kl} + 1)\right)} \\ &= \frac{L_c}{2}\left[\rho_H(y_{kl} + 1) - \rho_H(y_{kl} - 1)\right]. \end{aligned} \tag{2.51}$$

For the LLR obtained from numerical computation, PDF values for SαS plus

Gaussian distributions are directly used as:

$$L(y_{kl}|x_{kl}) = \ln \frac{f_{s+g}(y_{kl}-1)}{f_{s+g}(y_{kl}+1)}, \tag{2.52}$$

where $f_{s+g}(.)$ stands for the PDF of SαS plus Gaussian distributions. The PDF calculation was realized from discrete inverse Fourier transform (DIFT), using a similar approach as section 2.3.2. The integration period for the DIFT was set to $N = 5000$ to ensure the accuracy of the calculation.

We compare these decoding metrics or methods through a simulation with $\alpha = 0.8$ SαS interference plus 10 dB SNR Gaussian noise. The bound of received bit y_{kl} was chosen between -12 and $+12$ with 0.01 step. Each value of y_{kl} yields a corresponding LLR result. The result is shown in Figure 2.18. As a benchmark,

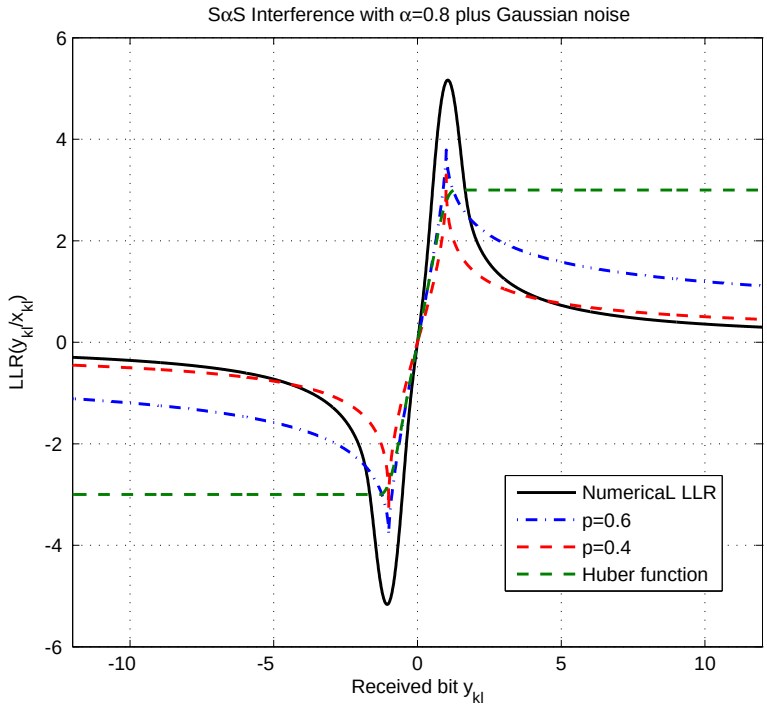

Figure 2.18: LLR of $(y_k|x_k)$ for different decoders.

the solid line represents the LLR from the numerical PDF calculation method, which results in optimal BER curve. The curve which matches the most the numerical LLR should be a good choice for the decoding metric.

It is obvious that the p-norm curves agree well with the numerical LLR. The choice of p only concerns essentially the tail behaviour but will not significantly

change the shape which is similar to the optimal curve. The Huber function touches the numerical LLR for only a small range of y_{kl} (when the absolute value of y_{kl} is small), but leaves a large part as a limiter. This explains why the Huber metric cannot deal with the very impulsive situations when the received signal takes large amplitudes more often.

2.5 Conclusion

In this chapter, we studied the decoding metric of turbo codes when both the SαS modelled network interference and Gaussian modelled thermal noise are present in the channel. In order to adapt to this model, we proposed the p-norm as a distance metric based on the definition of FLOMs and stable norm. We tested decoding performance of turbo codes in direct link using this new metric and compared it with the Euclidean distance, the Huber function and the optimal decoder. The results showed that the classical metric cannot cope with the impulsive environment and the Huber function has difficulties in dealing with very impulsive cases (especially when $\alpha \leq 1$). The LLR comparison of these decoding metrics explained their difference with anther point of view. We conclude that the use of the p-norm can allow to significantly improve performance and approach the optimal decoder, whatever the value of α, and with a limited impact of the parameter estimation.

Chapter 3

Robustness in cooperative communications

In this chapter, we will develop our work in a wireless network with sufficient channel knowledge. Due to random variations in space, time and frequency in wireless network context, communications will be influenced by wireless propagation effects, including path loss, shadowing and multi-path fading, as well as the network interference and equipment thermal noise [78].

In practical system, multiple-input multiple-output (MIMO) antenna deployment strategy [79, 35, 22] has proved successful in improving spatial diversity gains. In some context like sensor networks, it is however impractical to install multiple antennas on each communication device due to the size and cost issues [42]. Such technical bottleneck has brought a distributed antenna strategy, realized by the cooperation of network nodes, referred to as cooperative communications, with the helping nodes served as relays.

As described in [42], most cooperative communications involve two phases of transmission: a coordination phase (i.e., Phase I) and a cooperation phase (i/e., Phase II). In Phase I, the source broadcasts its data to both the relay and the destination, and in Phase II, the relay forwards the source's information. Depending on the relative transmitter location or channel conditions, different cooperative relaying strategies exist such as decode-and-forward (DF), amplify-and-forward (AF) and compress-and-forward (CF) etc.

We will employ a conventional DF scheme supposing that the relay decodes correctly the information in Phase I and forwards the same source message to the destination.

3.1 System scenario

For simplification purpose and without loss of generality, we propose the network scenario in a two-hop decode-and-forward (DF) relaying communication. The two-hop network is firstly investigated consisting of one source, N possible relays and one destination.

For the signal detection problem in a cooperative communication with the help of relays, we take into account the wireless propagation effects, network interference and thermal noise, according to [78]. We suppose

- a slow-fading channel, for which the channel coefficients $\mathbf{h}$ are constant for each time slot and change independently from one time to another;
- a symmetric α-stable (SαS) distributions to model the network interference, which is the accumulation of undesired signals from other nodes;
- a Gaussian distribution to model the thermal noise caused by network equipments, which is additional to and independent from the network interference.

A set of K relays is selected among N possibilities and these select relays are the ones with the strongest relay-to-destination channel coefficient h_{rd}. Furthermore, we assume that the received signal at relays are decoded without error before forwarding to the destination. The relay-to-destination transmissions are made on orthogonal channels, and the synchronization is perfect with corrected phase.

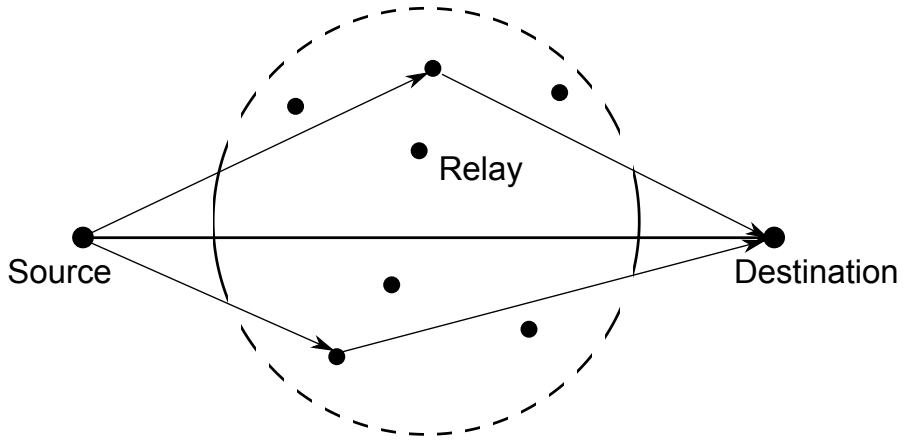

Figure 3.1: K relays are selected among N possible ones

Thus the received signal at the destination from the relays and directly from the source at time t can be given by

$$y_{(l),t} = h_{(l)}x + i_{(l)} + n_{(l)}, \tag{3.1}$$

where $l \in \{0, 1, ..., K\}$, index 0 donates the direct link from the source to the destination and index 1 to K represent K selected relays. The received signal $y_{(l),t}$ is composed of the transmitted binary symbol x through the channel $h_{(l)}$, and two independent additive noise components, where

- $h_{(l)}$ follows the Rayleigh distribution with the power expectation $\mathbb{E}[|h_{(l)}|^2] = 1$,
- $i_{(l)} \sim S(\mu_s, \gamma)$ represents the $S\alpha S$ network interference,
- $n_{(l)} \sim \mathcal{N}(\mu_n, \sigma^2)$ denotes the Gaussian thermal noise.

Moreover, we suppose that the noise parameters don't vary within each relay during one transmission, and these parameters have been estimated *a priori*.

3.2 Detection problem

Knowing the received signal $\mathbf{y}$ and the channel realization $\mathbf{h}$, the Maximum *a posteriori* (MAP) receiver can be established in the sense of finding a decoded version of signal x, which has the maximum likelihood probability at each time slot t:

$$\hat{x}_{\text{MAP},t} = \arg\max \Pr(x_t|\mathbf{y}_t, \mathbf{h}). \tag{3.2}$$

This is reasonable and practical in communications receiver design, as the probability reflects the statistic situation of the possible transmitted signals leading to such a reception, when only the received signals are available at the destination terminal.

We can have the following transformation using the Bayes rule:

$$\Pr(x_t|\mathbf{y}_t, \mathbf{h}) = \frac{\Pr(\mathbf{y}_t|x_t, \mathbf{h}) \Pr(x_t)}{\Pr(\mathbf{y}_t)}. \tag{3.3}$$

If the signal is sent and received with equal probability, and the signal x_t has, for example, two possible choice $x \in \{s_0, s_1\}$, the Bayes receiver can be employed

which involves the likelihood ratio as its decision criteria:

$$\Lambda = \frac{\Pr(\mathbf{y}_t|s_1,\mathbf{h})}{\Pr(\mathbf{y}_t|s_0,\mathbf{h})} = \prod_{l=1}^{K} \frac{p(y_{(l),t}|s_1,\mathbf{h})}{p(y_{(l),t}|s_0,\mathbf{h})} \underset{s_0}{\overset{s_1}{\gtrless}} 0, \tag{3.4}$$

where the probability terms in both the numerator and denominator require the corresponding noise probability densities, which are intractable for convolved $S\alpha S$ interference plus Gaussian noise distributions.

3.3 Receiver strategies

3.3.1 Optimal receiver

Optimal receiver criterion

The detection problem for a binary source (i.e. $x \in \{s_0, s_1\}$) in the presence of stable network interference plus independent Gaussian thermal noise can be formally specified through a statement of a hypothesis test as

$$\begin{cases} H_0 : \mathbf{y} = \mathbf{h}s_0 + \mathbf{i} + \mathbf{n} \\ H_1 : \mathbf{y} = \mathbf{h}s_1 + \mathbf{i} + \mathbf{n}. \end{cases} \tag{3.5}$$

Given the transmitted binary symbols s_1 and s_0 and the observed received signal y, we define $\mathbb{P}_{i+n}(y|s_1)$ and $\mathbb{P}_{i+n}(y|s_0)$, where $\mathbb{P}_{i+n}(.)$ represents the intractable probability distribution function obtained from the convolution between the stable network interference plus independent Gaussian thermal noise.

We want to define an optimal receiver model is the sense of minimizing the bit error rate (BER). The error happens when the signal of s_1 is sent, the received signal y drops into the observation space of s_0 or the s_0 is sent, y drops into the space of s_1. As these events are equiprobable, the average error probability of the receiver can be calculated as

$$P_e = P(s_1) \times \int_{s_0} f_{i+n}(y|s_1)\mathrm{d}y + P(s_0) \times \int_{s_1} f_{i+n}(y|s_0)\mathrm{d}y, \tag{3.6}$$

where $P(s_1)$ and $P(s_0)$ are the *a priori* probabilities of the source signal, $f_{i+n}(.)$ is the probability density function (PDF) of the stable network interference plus Gaussian thermal noise.

If the transmitted signal from the source is assumed to be s_1, we have

$$\int_{s_0} f_{i+n}(y|s_1)\mathrm{d}u = \int_{s} f_{i+n}(y|s_1)\mathrm{d}u - \int_{s_1} f_{i+n}(y|s_1)\mathrm{d}u = 1 - \int_{s_1} f_{i+n}(y|s_1)\mathrm{d}u. \quad (3.7)$$

By substituting (3.7) for (3.6), P_e becomes

$$P_e = P(s_1) + \int_{s_1} [P(s_0)f_{i+n}(y|s_0) - P(s_1)f_{i+n}(y|s_1)]\mathrm{d}y. \quad (3.8)$$

In order to minimize P_e, we should have

$$P(s_0)f_{i+n}(y|s_0) - P(s_1)f_{i+n}(y|s_1) < 0, \quad (3.9)$$

thus

$$P(s_0)f_{i+n}(y|s_0) < P(s_1)f_{i+n}(y|s_1)$$

or

$$\frac{f_{i+n}(y|s_1)}{f_{i+n}(y|s_0)} > \frac{P(s_0)}{P(s_1)}. \quad (3.10)$$

This is the Bayes criterion in the case the decision is made for s_1.

Accordingly, we can have the Bayes optimal receiver in the form of the log-likelihood ratio (LLR) as

$$\begin{aligned} \Lambda &= \log \frac{P_{i+n}(\mathbf{y}|s_1)}{P_{i+n}(\mathbf{y}|s_0)} \\ &= \log \frac{\prod_k f_{i+n}(y_k|s_1)}{\prod_k f_{i+n}(y_k|s_0)} \\ &= \sum_k \log \frac{f_{i+n}(y_k|s_1)}{f_{i+n}(y_k|s_0)} \underset{H_0}{\overset{H_1}{\gtrless}} \eta. \end{aligned} \quad (3.11)$$

The decision between two hypothesis is made by comparing the LLR to a threshold η.

In our proposed scenario, if the binary symbols sent from the source are with equal probability ($\eta = 0$), and the transmitted signals and channel coefficients

are known, we have the *a priori* decision statistic as

$$\Lambda = \sum_{k=1}^{K} \log \frac{f_{i+n}(y_k|h_k s_1)}{f_{i+n}(y_k|h_k s_0)} \underset{H_0}{\overset{H_1}{\gtrless}} 0, \tag{3.12}$$

where k indicates the k^{th} relay-to-destination channel.

It is noted in [73] that for a very large K, the asymptotic distribution for the statistic Λ is Gaussian with finite mean and variance. However, as described in 1.6.3, the error included by this assumption can be quite large when K is not big enough. We then prefer to implement the optimum receiver even if it is not practically reasonable.

The Bayes detector demanded above requires the exact knowledge of the noise density. As previously mentioned, there is no explicit PDF expressions for α-stable distributions, yet no closed-form for the convolved network interference plus Gaussian thermal noise.

The first idea could be the numerical integration, since the PDF is the inverse Fourier transform of the characteristic function:

$$f_{i+n}(x) = \frac{1}{\pi} \int_0^{+\infty} \phi_{i+n}(t) \cos(xt) \mathrm{d}t, \tag{3.13}$$

where $\phi_{i+n}(t) = \exp(-\gamma|t|^\alpha - \sigma^2 t^2/2)$ is the characteristic function for the convolution of network interference plus Gaussian thermal noise.

However, the difficulty lies in fixing the discrete integral step and truncation, which highly depend on the interference and noise parameters (α, γ and δ). What's more, a heavy computation cost is inevitable for each channel realization in our case. The Monte-Carlo simulation could be another method. Since the network interference is a strong but rare event, a large number of samples are needed for the simulation. We use the idea from the importance sampling method to implement the Monte-Carlo simulation.

Introduction of Importance Sampling method

The importance sampling (IS) method was introduced in [10] as an efficient technique in the reduction of variance in random sampling, in respect that the method concentrates on the sample points where the value of the function is large. We can take advantage of IS for the simulation of rare random events, and for the generation of samples under a distribution which is difficult to generate directly [26].

In order to show the difference between the IS and the conventional MC method, an example model is presented below. If the probability to estimate is

$$p = P(X(t) \leq C)$$

and let

$$S = \{t : X(t) \leq C\}$$

be the sampling space, we can estimate p as

$$p = \int_S I(t) f(t) \mathrm{d}t = \mathrm{E}[I(t \in S)], \tag{3.14}$$

where $I(t)$ is the indicator function in which $I(t) = 1$ if $t \in S,$ otherwise $I(t) = 0$, and $f(t)$ is the PDF of X.

For a conventional MC simulation, the procedure is to generate K i.i.d. random samples under the PDF $f(.)$ and estimate the integral by

$$\hat{p} = \frac{1}{K} \sum_{k=1}^{K} I(t_k). \tag{3.15}$$

While in IS method, the idea is to change $f(.)$ so as to allow a more frequent occurring for the estimation event, thus the number of testing samples can be less for a given estimator variance. We choose another PDF $g(.)$, referred to as a biasing density, under which the sampling is made. We get p by

$$p = \int_S I(t) \frac{f(t)}{g(t)} g(t) \mathrm{d}t = \mathrm{E}\left[I(t \in S) \frac{f(t \in S)}{g(t \in S)} \right], \tag{3.16}$$

where $f(.)/g(.) \equiv W(.)$ is the weighting function.

In the simulation, the value $\hat{p}$ can be acquired in the same way from the average of K trials. The i.i.d. samples are weighted by $W(.)$, which allows the PDF $g(.)$ to generate the sample instead of $f(.)$:

$$\hat{p} = \frac{1}{K} \sum_{k=1}^{K} I(t_k) W(t_k). \tag{3.17}$$

Hence the IS estimator is said to be unbiased thanks to the weighting function.

Implementation of IS on optimal receiver

The decision of the optimal receiver is made on the criterion function (3.12), in which the calculation for each $f_{i+n}(.)$ is directly intractable. We can make use of IS method to calculate each $f_{i+n}(.)$, choosing a biasing probability function under which the sampling is much easier.

We noticed that the generation of α-stable random variables is trivial, hence we can sample the network interference component $\mathbf{i_k}$ for each received signal $y_k = h_k x + i_k + n_k$. That is, for every channel realization, y_k can be considered as under a normal distribution with the mean $h_k x + i_k$ and with the variance of n_k (σ^2), which can be calculated as:

$$f_{i+n}(y_k|h_k x) = \int_I I(t) f_n(t) f_i(t) \mathrm{d}t, \tag{3.18}$$

where I represents the network interference sampling space, $f_n(.)$ is the normal distribution PDF.

In the simulation, if a number of N i.i.d. network interference samples $\mathbf{i}_k$ are generated under $f_i(.)$, and the weighting function is defined as $\mathcal{N}(h_k x + i_k, \sigma^2)$, we have

$$\hat{f}_{i+n}(y_k|h_k x) = \frac{1}{N} \sum_{n=1}^{N} I_{k_n} \mathcal{N}(h_k x + i_{k_n}, \sigma^2). \tag{3.19}$$

Once the probability term $f_{i+n}(.)$ is calculated, the decision of the optimal receiver can be made.

Determination of sampling number

In order to reduce the computation cost but without losing the reliability of probability density calculation by the IS method, we made some tests in hopes of finding an appropriate sampling number for the network interference term. Based on the same cooperative network scheme as introduced in 3.1, we chose the two strongest relay-to-destination channels among 5 for instance. A 1000-bit-length signal is generated as source information. We use the optimal receiver described in 3.3.1 for detection. According to the error number counted in terms of amount of samples used, we have the following result:

In Figure 3.2, we observe a convergence of the number of errors when the number of interference samples increases. We picked in all our following simulations the sampling number as 10^6 with which the probability calculation is sufficiently accurate to our context.

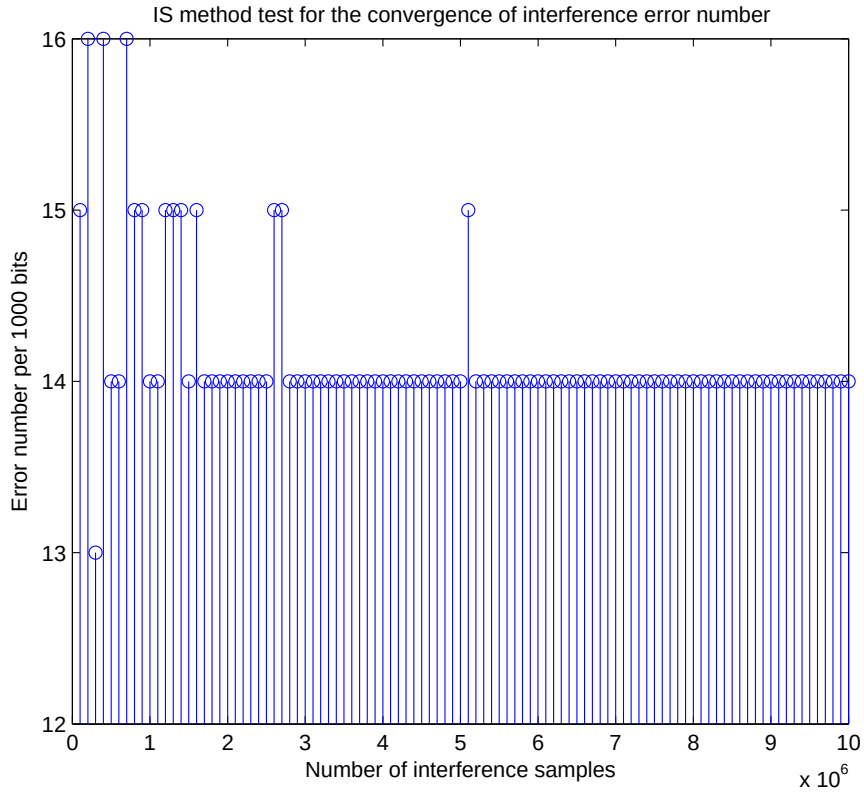

Figure 3.2: Detected error numbers in terms of sampling numbers

3.4 Suboptimal receiver

3.4.1 Linear receiver

The linear receiver is realized by assuming that the PDF used in the decision statistic (3.12) is the Gaussian one (stable PDF when $\alpha = 2$). The linear receiver is also known as the Gaussian receiver. It is optimal when the interference is Gaussian distributed. The corresponding decision statistic is

$$\begin{aligned}\Lambda_{\text{linear}} &= \sum_{k=1}^{K} \log \frac{f_2(y_k|h_k s_1)}{f_2(y_k|h_k s_0)} \\ &= \sum_{k=1}^{K} \log \frac{\exp[-(y_k - s_1)^2/2\sigma^2]}{\exp[-(y_k - s_0)^2/2\sigma^2]} \\ &= \frac{1}{\sigma^2} \sum_{k=1}^{K} y_k(s_1 - s_0) \underset{H_0}{\overset{H_1}{\gtrless}} 0,\end{aligned} \tag{3.20}$$

where σ is the standard deviation of the Gaussian distribution. We will test such a receiver in the environment of stable ($\alpha < 2$) interference plus Gaussian noise. We primarily consider this choice for its simple implementation structure, though we predict that it will perform poorly when $\alpha \ll 2$.

3.4.2 Linear combiner

An alternative linear solution is developed by considering the maximal ratio combiner (MRC), which is also simple to implement as a suboptimal receiver. The MRC has its original output form given by

$$\Lambda_{\text{MRC}} = \sum_{k=1}^{K} w_k y_k = \hat{\mathbf{s}} + \hat{\mathbf{n}}, \tag{3.21}$$

where $\mathbf{w} = \{w_k\}_{k=1}^{K} \in \mathbb{R}^K$ are the combiner weights, $\hat{\mathbf{s}}$ and $\hat{\mathbf{n}}$ are the weighted signal components and noise components.

The conventional MRC is optimal for independent Gaussian channels, which obtains the optimal weights when $w_k = h_k^*$, where * represent the complex conjugate.

However, for detection in a stable interference plus Gaussian noise environment, the combiner has to take into account the interference parameters [32].

An adapted optimal MRC is proposed in [46, 59], which provides the corresponding weights when only the SαS interference is present:

$$\begin{cases} w_k^* = \text{sign}(s_k)|s_k|^{1/(\alpha-1)}, & 1 < \alpha \leq 2 \\ w_j^* = \text{sign}(s_j), w_k^* = 0 \ \forall k \neq j, & 0 < \alpha \leq 1 \end{cases} \tag{3.22}$$

for an arbitrary j in $\mathbf{i} = \arg\{|s_i| = \max\{|s_1|, \ldots, |s_K|\}\}$.

3.4.3 Non-linear receiver

Cauchy receiver

As one special case of SαS distribution, Cauchy distributions ($\alpha = 1$) have their PDF with dispersion γ and median δ:

$$f_1(x) = \frac{\gamma}{\pi[\gamma^2 + (x-\delta)^2]}. \tag{3.23}$$

Cauchy receiver arose originally from the assumption that the tail index $\alpha = 1$ and is optimal for the signal detection under pure Cauchy noise. By replacing $f_{i+n}(.)$ with $f_1(.)$ in (3.11), we have the corresponding decision statistic:

$$\begin{aligned} \Lambda_{\text{Cauchy}} &= \sum_{k=1}^{K} \log \frac{f_1(y_k|h_k s_1)}{f_1(y_k|h_k s_0)} \\ &= \sum_{k=1}^{K} \log \frac{\gamma^2 + (y_k - h_k s_0)^2}{\gamma^2 + (y_k - h_k s_1)^2} \underset{H_0}{\overset{H_1}{\gtrless}} 0. \end{aligned} \tag{3.24}$$

Hole-puncher and Soft-limiter receivers

The implementation of the Cauchy receiver appears to be difficult: we need to determine the parameter γ and the evaluation of (3.24) is complex. A first idea is to add some non-linearity to the Gaussian receiver to limit the impact of large interference samples. As proposed for instance in [58, 1], the hole-puncher and soft-limiter are commonly used non-linear functions. We use in our test these two functions with their forms as:

$$g_{\text{hp}}(x) = \begin{cases} x, & |x| < \kappa \\ 0, & \text{otherwise} \end{cases} \tag{3.25}$$

and

$$g_{\text{sl}}(x) = \begin{cases} -\kappa, & x < -\kappa \\ x, & |x| < \kappa \\ \kappa, & x > \kappa \end{cases}, \tag{3.26}$$

where $g_{\text{hp}}(.)$ and $g_{\text{sl}}(.)$ replace $f_{i+n}(.)$ in (3.11).

p-norm receiver

It is noted that in the decision statistic for the linear receiver (3.20), the metric used in the second step is the Euclidean distance between the received signal and the possible transmitted symbols. The distance between two SαS random variables is defined in [58], which measures the difference between them under the p-norm for $0 < p < \alpha$:

$$||X - Y||_\alpha = \begin{cases} [\mathbb{E}|X - Y|^p / C(\alpha, p)]^{1/p}, & 1 \leq \alpha \leq 2 \\ [\mathbb{E}|X - Y|^p / C(\alpha, p)]^{\alpha/p}, & 0 < \alpha < 1, \end{cases} \tag{3.27}$$

where $C(\alpha, p) = \frac{2^{p+1}\Gamma((p+1)/2)\Gamma(-p/\alpha)}{\alpha\sqrt{\pi}\Gamma(-p/2)}$, and $\Gamma(.)$ is the gamma function.

This expression is of interest as it does not depend on any estimation of distribution parameters and a rough knowledge of α can be sufficient. We employ the p-norm metric in our decision statistic as

$$\Lambda_{p\text{-norm}} = \sum_{k=1}^{K} \left(|y_k - h_k s_0|^p - |y_k - h_k s_1|^p \right) \underset{H_0}{\overset{H_1}{\gtrless}} 0. \tag{3.28}$$

3.4.4 NIG approximation

From the hyper-geometric family of flexible skew-kurtosis models, the Normal Inverse Gaussian (NIG) distributions have analytical expressions for the probability density and first four moments in terms of the model parameters. This family of statistical models includes the Gaussian and Cauchy distributions as special limiting cases [3]. It is therefore of great interest to use this distribution to approximate our intractable PDF in the decision statistic.

The NIG model takes its name from the fact that it represents a Normal variance-mean mixture that occurs as the marginal distribution for a random

variable Y when considering a pair of random variable (Y, Z) when Z is distributed as an inverse Gaussian $Z \sim \mathcal{IG}(\delta, \sqrt{\alpha^2 - \beta^2})$, and Y conditional on Z is $(Y|Z = z) \sim \mathcal{N}(\mu + \beta z, z)$. The resulting density function for the NIG model is given by:

$$f_{\text{NIG}}(y; \alpha, \beta, \mu, \delta) = \frac{\alpha\delta}{\pi} \frac{\exp[g(y)]}{h(y)} K_1[\alpha h(y)], \tag{3.29}$$

where $g(y) = \delta\sqrt{\alpha^2 - \beta^2} + \beta(y - \mu)$ and $h(y) = [(y - \mu)^2 + \delta^2]^{1/2}$, $K_1(.)$ is a modified second kind Bessel function with index 1.

The parameters have the constraints $\mu \in \mathcal{R}, \delta > 0, 0 \leq |\beta| \leq \alpha$. The parameter α is inversely related to the heaviness of the tails, where a small α corresponds to heavy tails that can accommodate outlying observations. The skewness is directly controlled by the parameter β, and $\beta = 0$ is the symmetric model. The location of the distribution is given by the parameter μ and the scale of the distribution is measured by the parameter δ.

We consider in our case a symmetric NIG model, which implies $\beta = 0$. We note the closed-form expressions for the mean, variance, skewness, and kurtosis of the NIG model as:

$$\begin{array}{ll} \mathbb{E}[y_k] = \mu = h_k x; & \mathbb{V}\text{ar}[y_k] = \frac{\delta}{\alpha}; \\ \mathbb{S}\text{kew}[y_k] = 0; & \mathbb{K}\text{urt}[y_k] = \frac{3}{\delta\alpha}. \end{array}$$

In this way, the probability density for each link can be approximated by the estimated closed-form expressions from the observed values.

3.5 Strategy comparison

We present in our simulation three different noise-to-interference ratios ($\sigma^2/2\gamma$) to investigate the described receivers. This ratio reflects different noise dominating environments, and we generated 500 noise samples for illustration in Figure 3.3.

We chose $K = 2$ strongest relay-to-destination channels among $N = 5$ possible ones. The optimal receiver is realized by IS approach as a benchmark, with 10^6 interference samples. The threshold for the hole-puncher receiver is set as $\kappa = 4$ and for the soft-limiter as $\kappa = 1$. An empirical approach based on simulations was used to make choice for those parameters. We set $p = 0.8$ as an example value for all the simulations. Performance is measured by BER in terms of the inverse value of dispersion of SαS interference in logarithm, since the

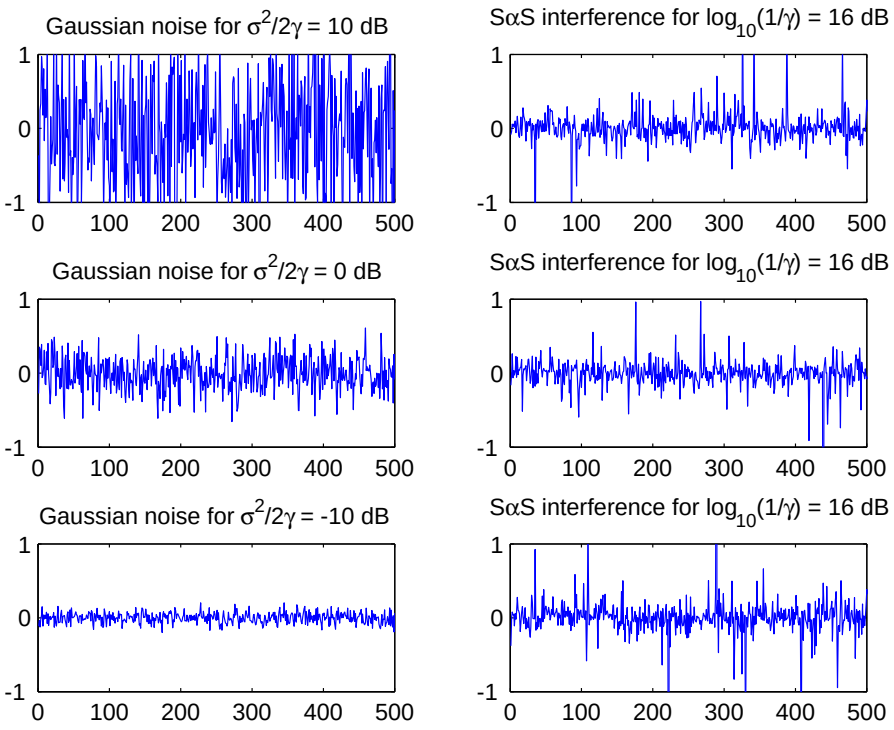

Figure 3.3: Comparison of different noise dominating environments

increasing of the inverse dispersion implies the decreasing of the interference strength.

In Figure 3.4, $\sigma^2/2\gamma$ is set to 10 dB which indicates that the dominant noise is Gaussian. We observe that the Cauchy receiver gives the worst BER, since it is only optimal under Cauchy noise ($\alpha = 1$). The linear receiver and MRC have the same trend and the latter one is better because of its adapted parameters. The NIG approximation shows similar performance as the linear approaches. During the estimation of NIG parameters, the rare SαS interference parts have little influence on the dominant Gaussian noise, hence the obtained NIG density is close to the limiting Gaussian case of this family. The p-norm, hole-puncher and soft-limiter receivers have almost the same performance, which approaches the optimal receiver. In case when the Gaussian noise and the SαS interference are comparable ($\sigma^2/2\gamma = 0$ dB), we can see in Figure 3.5 that the linear receiver and MRC appear less capable to deal with the interference than the others. The Cauchy receiver exhibits a good performance in this condition, even surpassing the hole-puncher and soft-limiter. The p-norm receiver keeps close to the optimal one, and the NIG approximation shows similar ability as the p-norm approach. In Figure 3.6, when the SαS interference dominates the whole noise, the Cauchy receiver provides the best performance, which is very close to the

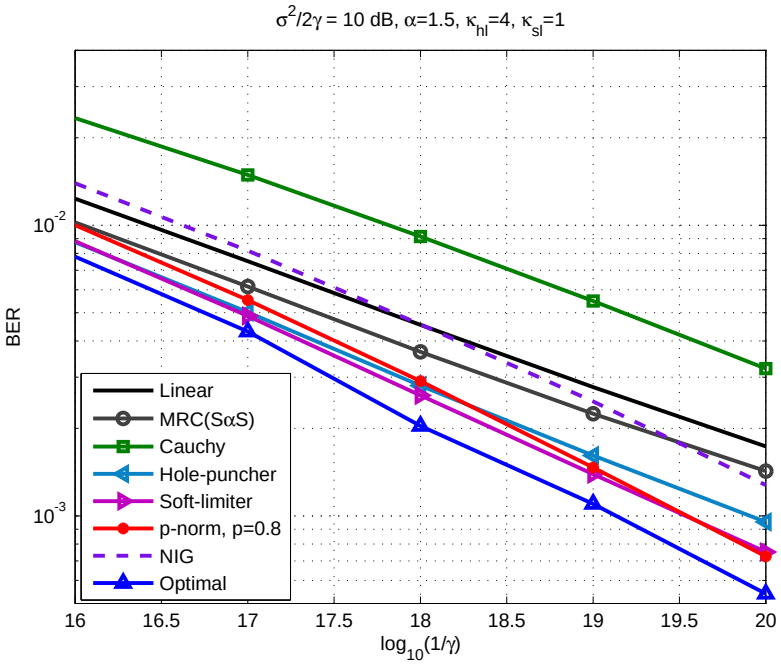

Figure 3.4: Comparison of receivers in Gaussian-noise-dominant environment

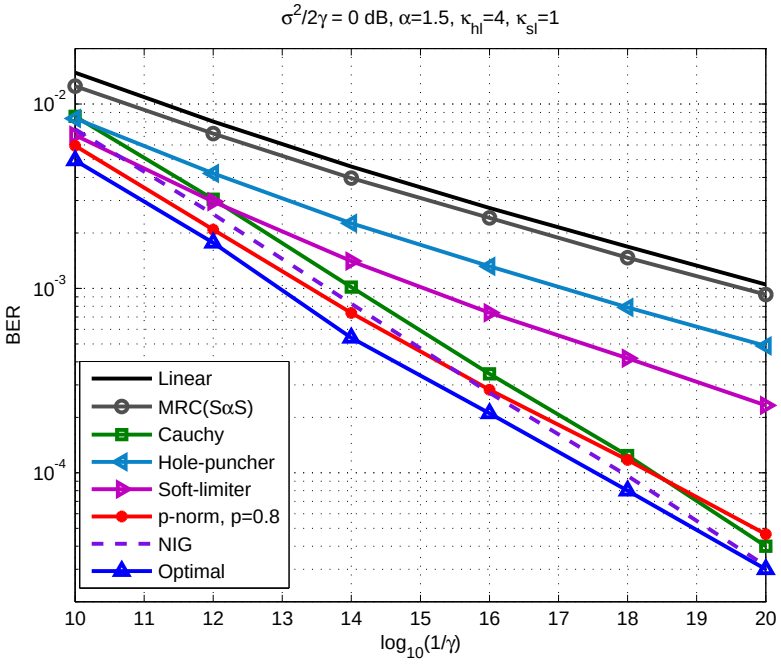

Figure 3.5: Comparison of receivers in Gaussian-stable-comparable environment

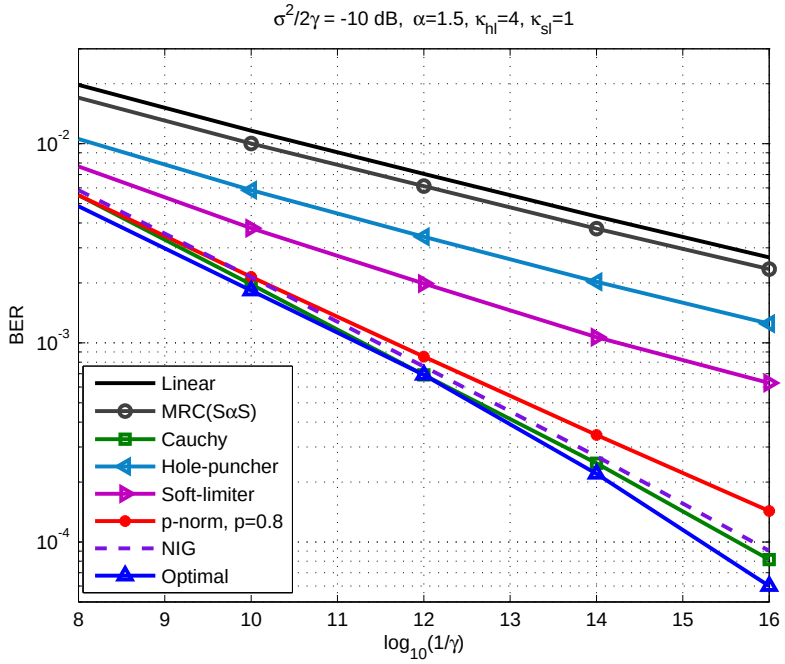

Figure 3.6: Comparison of receivers in stable-interference-dominant environment

optimal receiver. The p-norm and NIG receivers remain close as well, while the other receivers perform poorly.

From the above results, we can draw some conclusions:

- The linear receiver and MRC will have good performance only if the Gaussian noise is dominant.
- The Cauchy receiver performs well except when the Gaussian noise dominates.
- The hole-puncher and soft-limiter are good choices if the thresholds are well configured, but they are still far from optimality when impulsiveness is strong.
- The NIG approximation and the p-norm receiver have very good performance in all environment and approach very closely the optimal receiver when impulsiveness increases. It is noted that the p-norm has the best behaviour when Gaussian noise is dominant and is a non-parametric approach (at most a rough estimation of α is sufficient).

3.6 Conclusion

In this chapter, we have evaluated the performance of several receivers in cooperative communications where both the network interference and the thermal noise are present. The SαS and Gaussian distributions were used to model the network interference and the thermal noise respectively. The chosen relays are the ones having the minimum relay-to-destination channel loss among a set of candidates. We employed an importance sampling approach for the calculation of the optimal decision statistic and listed several suboptimal receiver approaches, in which the p-norm receiver and NIG approximation method were proposed as efficient solutions. The simulation results showed that some parametric designs like the hole-puncher and soft-limiter can have good performance if their thresholds are well configured. The NIG approximation proved to be a very efficient approach. The p-norm exhibited robust performance, no matter which noise was dominant. This approach provides us a simple and feasible receiver strategy, which does not necessitate any noise parameter estimation, and also confirms the study that we made about turbo codes in direct link.

Chapter 4

Distributed channel coding in cooperative communications

In this chapter, we investigate the distributed channel coding technique with the help of relays in the network, establishing cooperative communications to make the signal transmission more reliable and less impacted by interference. Besides, the scheme provided here offers some flexibility, hence making the control of energy consumption possible based on certain error correction level.

In relay networks, the cooperation between the source and relays actually forms a virtual antenna array, therefore intuitively the conventional channel coding schemes can be extended to the relay networks in order to explore the cooperative diversity and coding gain [27]. In addition to the coding advantage, distributed channel coding is based on incremental redundancy and thus allows a more flexible distribution of channel symbols between source and relay nodes, compared to repetition algorithms based on amplify-and-forward relaying protocols [27, 81]. Several kinds of distributed channel coding technologies have been developed, such as distributed space time block coding [28], distributed space time trellis coding [72, 16, 83, 82], distributed space time frequency coding [84, 66]. In order to still improve the decoding performance and meanwhile approach the channel capacity, distributed LDPC coding [18, 43] and distributed turbo coding (DTC) [14, 45, 85, 51, 52] schemes have been proposed and studied in cooperative communication circumstance.

From the idea of channel coding and cooperative communications in this thesis, we built an effective distributed channel coding scheme. Based on a certain level of BER, the energy consumption can be minimized if an appropriate space-time coding topology is chosen. In the following section, we propose a distributed channel coding strategy with the corresponding communication sce-

nario.

4.1 Distributed channel coding strategy

4.1.1 Communication topology and scenario

We assume in the first time a simple relay network topology. This network is composed of one source, one destination and one relay as shown in Figure 4.1. The relay cooperates with the source to send information to the destination but with an interleaved version. We do not consider any synchronization problems in this thesis.

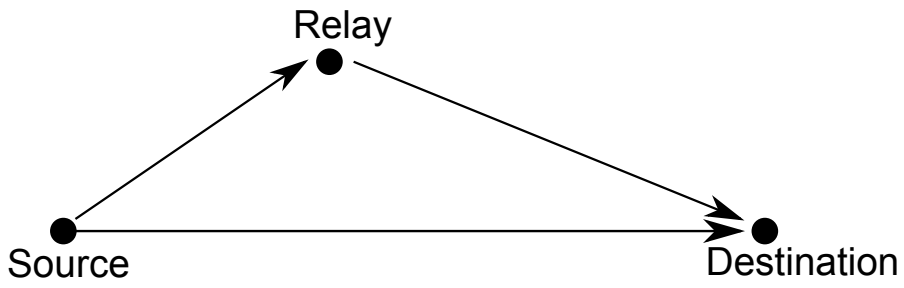

Figure 4.1: Relay network for distributed channel coding

For the network impairments, we consider the wireless propagation effects, network interference and thermal noise. The modelling of the network impairment components are as follows:

- the communications suffer from a slow-fading channel, for which the channel coefficients $\mathbf{h}$ are constant for each time slot and change independently from one time to another;
- the network interference is modelled as a SαS distribution, which is the accumulation of undesired signals from other nodes;
- the network-equipment-caused thermal noise is modelled as a Gaussian distribution, which is additional to and independent from the network interference.

First of all, the source sends the code-word x based on the binary symbols s_0 and s_1 to the relay and destination, and let $\mathbb{E}[x^2] = 1$. The corresponding received signals at time t at the destination and relay with convolved additive

network interference and thermal noise parts are represented as

$$y_{SD,t} = h_{SD,t}\sqrt{P_s}x_t + i_{SD,t} + n_{SD,t}, \tag{4.1a}$$

$$y_{SR,t} = h_{SR,t}\sqrt{P_s}x_t + i_{SR,t} + n_{SR,t}, \tag{4.1b}$$

where $h_{SR,t}$ and $h_{SD,t}$ are the channel coefficients between the source-and-relay (SR) and between the source-and-destination (SD) respectively, which are modelled as Rayleigh random variables. The terms i are channel interference modelled as symmetric α-stable random variables. The thermal noise terms n are modelled as Gaussian random variables ($n_k \sim \mathcal{CN}(0, \sigma_k^2)$). We suppose, for simplification purpose, that the source has unit transmission power ($P_s = 1$).

At the relay, if the signal estimated and forwarded to the destination is marked as $\hat{x}$, the relay-to-destination version of received signal at the destination can be expressed as

$$y_{RD,t} = h_{RD,t}\sqrt{P_r}\hat{x}_t + i_{RD,t} + n_{RD,t}, \tag{4.2}$$

where $h_{RD,t}$ is the channel coefficient between the relay-and-destination (RD). We assume that the relay transmission power $P_r = 1$ in the following investigation.

In order to simplify the evaluation of performance, the received signal at the relay is supposed to be decoded correctly before forwarding to the destination. Hence the decoded signal at the relay is perfectly recovered as $\hat{x}_t = x_t$.

4.1.2 Distributed channel coding scheme

The distributed channel coding works by splitting each code word into two parts, one transmitted by the source and the other by the relay node. The source encodes the information to a RSC code then modulates and broadcasts it omnidirectionally to the network. The relay and destination will receive the signal from the source in some time instant. The destination first demodulates and decodes the received signal.

Depending on the decoding BER, the destination will determine if it still needs redundant information from the relay. If it does, the relay will decode the signal from the source and interleave it before entering to the same RSC decoder as the source. After that the needed information is sent to the destination to ensure the decoding BER at the destination to achieve a certain level.

The system diagram is shown as Figure 4.2. We employ the Viterbi decoder to decode the RSC codes, as Viterbi algorithm [62, 21] is a light weighted method

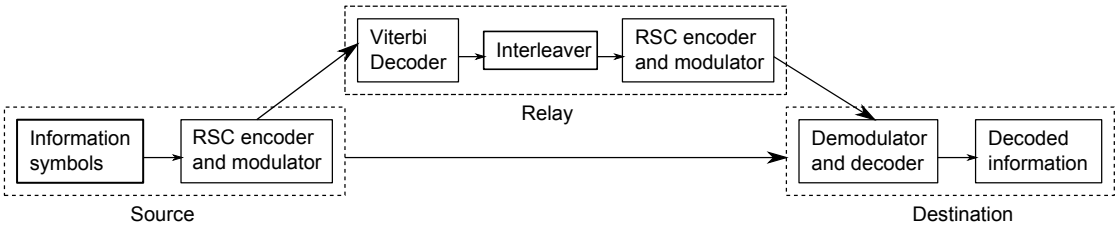

Figure 4.2: Distributed channel coding diagram

compared with BCJR MAP algorithm, and it doesn't need iteration process, hence certain energy consumption can be saved in the implemented system. The turbo codes are still decoded by BCJR MAP algorithm to ensure the performance.

We represent the signal in each communication blocks as in Table 4.1: The systematic and parity bit are respectively denoted using s and p in signal subscripts. The subscript $1p$ indicates the original RSC encoded bit while $2p$ indicates the interleaved version of RSC encoder output. For the distinguish purpose, signals sent from the relay, which are then received at the destination are with a prime $'$ superscript.

signal transmission	signal representation
from source to relay	$\{x_s, x_{1p}\}$
from source to destination	$\{x_s, x_{1p}, x_{2p}\}$
from relay to destination	$\{x'_s, x'_{2p}\}$
received at destination from source	$\{y_s, y_{1p}, y_{2p}\}$
received at destination from relay	$\{y'_s, y'_{2p}\}$

Table 4.1: Signal representation in distributed channel coding network.

Based on the cooperative behaviour of the relay and source, we divide the distributed channel coding scheme into 5 options:

- Option 1: The source firstly broadcasts a RSC code $\{x_s, x_{1p}\}$ to the destination and the relay. The destination decodes the RSC codes $\{y_s, y_{1p}\}$ using Viterbi decoding algorithm. The diagram is shown in Figure 4.3.

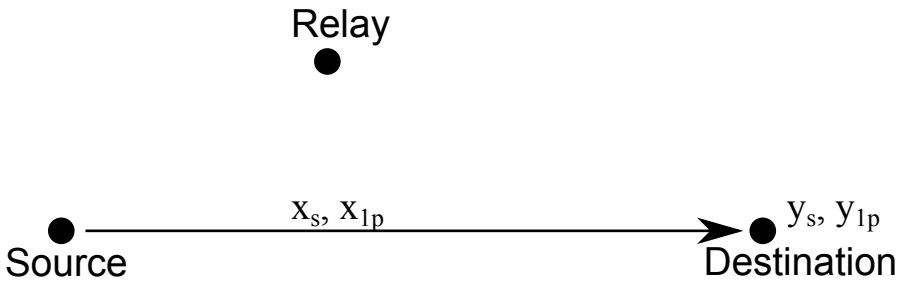

Figure 4.3: Option 1: RSC codes from the source.

- Option 2: The source firstly broadcasts a RSC code $\{x_s, x_{1p}\}$ to the destination and the relay. Then the source sends the interleaved and encoded signal $\{x_{2p}\}$ to the destination. The destination combines the signal $\{y_s, y_{1p}\}$ from the first time and the parity signal y_{2p} from the second time to construct a turbo code $\{y_s, y_{1p}, y_{2p}\}$. Then the BCJR MAP algorithm is employed to decode the turbo code. The diagram is shown in Figure 4.4.

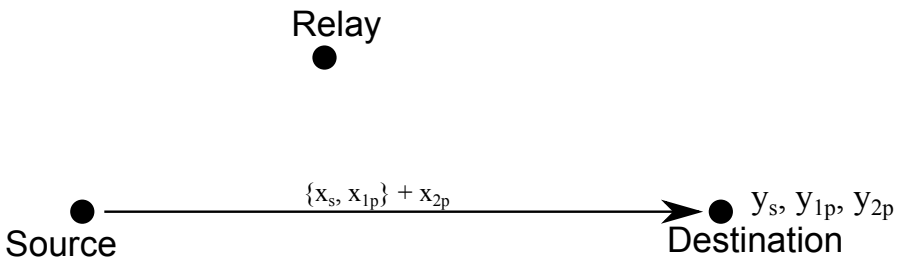

Figure 4.4: Option 2: turbo codes from the source.

- Option 3: The source firstly broadcasts a RSC code $\{x_s, x_{1p}\}$ to the destination and the relay. We assume that the relay decodes the received signal without error for simplification purpose. Then the relay sends the interleaved and re-encoded signal $\{x'_s, x'_{2p}\}$ to the destination. The destination decodes the signal sent from the relay $\{y'_s, y'_{2p}\}$ using Viterbi algorithm, but a deinterleaver is needed after the decoding to recover the real information. The diagram is shown in Figure 4.5.

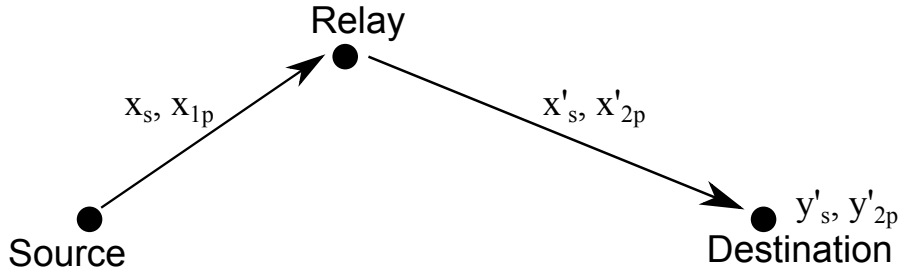

Figure 4.5: Option 3: RSC codes from the relay.

- Option 4: The source firstly broadcasts a RSC code $\{x_s, x_{1p}\}$ to the destination and the relay. We assume that the relay decodes the received signal without error for simplification purpose. Then the relay sends the interleaved and re-encoded signal $\{x'_{2p}\}$ to the destination. The destination combines the signal from the source $\{y_s, y_{1p}\}$ and the parity signal from the relay y'_{2p} to construct a turbo code $\{y_s, y_{1p}, y'_{2p}\}$. Then the BCJR MAP algorithm is employed to decode the "distributed" turbo code. The diagram is shown in Figure 4.6.

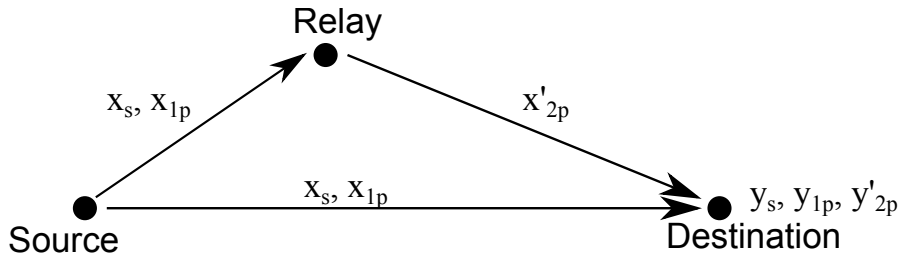

Figure 4.6: Option 4: distributed turbo codes

- Option 5: The source firstly broadcasts a RSC code $\{x_s, x_{1p}\}$ to the destination and the relay. We assume that the relay decodes the received signal without error for simplification purpose. Then the relay sends the interleaved and re-encoded signal $\{x'_s, x'_{2p}\}$ to the destination. The destination combines the signal from the relay $\{y'_s, y'_{2p}\}$ and the parity part signal from the source y_{1p} to construct a turbo code $\{y'_s, y'_{1p}, y_{2p}\}$. Then the BCJR MAP algorithm is employed to decode the "distributed" turbo code, but a deinterleaver is needed after the decoding to recover the real information. The diagram is shown in Figure 4.7.

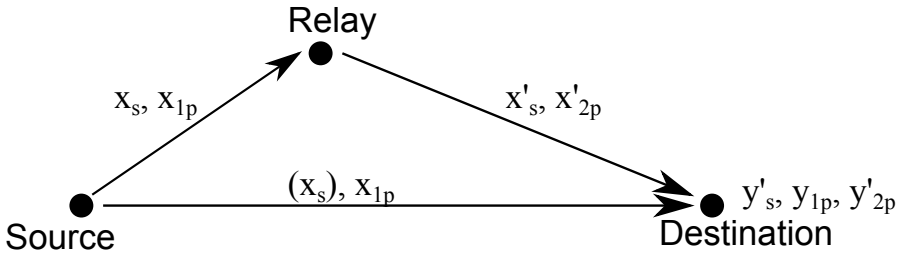

Figure 4.7: Option 5: distributed turbo codes

Now the problem is when to employ one of these options to ensure a target BER but also to minimize the energy cost. We discuss firstly for each option the energy cost problem, then a simulation based investigation indicates when to employ an appropriate option to ensure the BER with least energy cost.

4.2 Energy consumption study

Since energy consumption is one of the most important parameters in the sensor network [69], the energy saving issue shall be an interesting topic. A good choice of the above options should be a least energy consuming strategy but fulfilling the decoding performance demand. It's difficult to study deeply and roundly the energy consumption here for every option. But some experimental measurements show that, the data transmission consumes generally the most energy. The necessary energy cost for transmitting one bit data, for instance, equals approximatively millions of calculation operations [53]. Which means that the information transmission in each option will consume much more energy than signal processing operation like encoding and decoding. Hence, we will account the number of bits transmitted in each whole scheme in order to compare their energy consumption performance.

If the original signal sent from the source x_s is composed of n bits, it is easy to establish a table to compare the number of bits transmitted for each options:

From Table 4.2, it is clear that the direct link transmits the least bits, between which the option 1 using only RSC codes consume the least energy. With the help of relay, the transmitted bits are augmented to $4n$ except for the option 4, which utilize only the parity part of the RSC code x'_{2p} to forward to the destination, thus only $3n$ bit transmission is needed. If the direct link suffers more propagation impairments, is it worth employing the relay to cooperate? We will investigate the BER performance through a simulation in the next section.

Option	from source	from relay	transmitted number
1 (RSC)	$2n$	0	$2n$
2 (turbo)	$3n$	0	$3n$
3 (RSC)	$2n$	$2n$	$4n$
4 (turbo)	$2n$	$1n$	$3n$
5 (turbo)	$2n$	$2n$	$4n$

Table 4.2: Number of bits transmitted for each option in distributed channel coding scheme.

4.3 Scheme choice investigation

We have stated in section 4.1 that the signal received at relay and destination has been influenced by the slow fading, Gaussian thermal noise and SαS modelled network interference as shown in equations (4.1) and (4.2). We investigate therefore the system by configuring parameters of these communication impairments.

As it is supposed in section 4.1 that the relay can decode the signal from the source without error, thus we don't consider the channel parameter between the source and relay. The channel coefficients are set to be $h_{RD,t} = h_{SD,t} = 1$ for a slow fading character. An $\alpha = 1.5$ characteristic exponent is set for the SαS network interference. In a practical situation, the channel between the source and destination (SD) is more likely to suffer distortions than the channel between the source and relay (RD) if the relay is the one who plays the cooperative role, we assume that the strength of the interference for relay-to-destination channel is 0.8 less than that of the source-to-destination channel. In respect that the dispersion of the SαS model proportionally implies the strength of the network interference, we can interpret our assumption as $\gamma_{RD} = 0.8\gamma_{SD}$, where γ is the dispersion of the network interference. This way of interference modelling is equivalent to considering a better relay-to-destination channel than the direct link. This is however necessary if we want that the relay helps in saving energy.

The configuration can be illustrated in Figure 4.8.

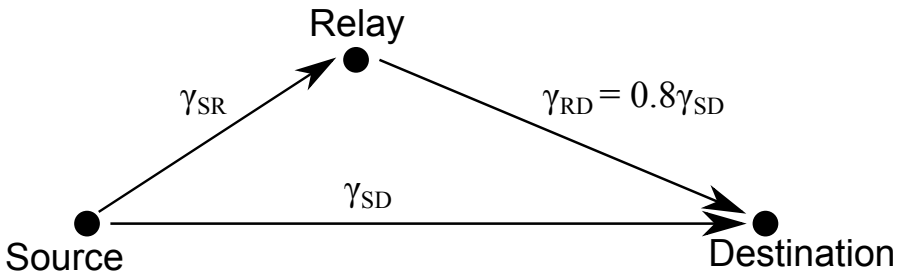

Figure 4.8: Distributed channel coding network model, $\gamma_{RD} = 0.8\gamma_{SD}$.

We let the communications take place in a very impulsive environment, the ratio of the noise-to-interference strength is defined as $\sigma^2/2\gamma = -10$ dB, where σ is the standard deviation of thermal Gaussian noise. Thus the network interference dominates the noise environment.

We evaluate the performance by measuring the BER in terms of the inverse value of γ, since the increasing of the inverse dispersion indicates the decreasing of the interference strength. Then according to the noise-to-interference strength ratio, the Gaussian noise strength can be determined as well. For RSC code, Viterbi algorithm is used and for turbo code, BCJR MAP algorithm is employed and the result is collected from the 6^{th} iteration. The p-norm replaces the Euclidean distance in all decoders.

A global illustration is exhibited in Figure 4.9, we set a threshold of BER to 10^{-3} for comparison. We notice that the options which take advantage of turbo

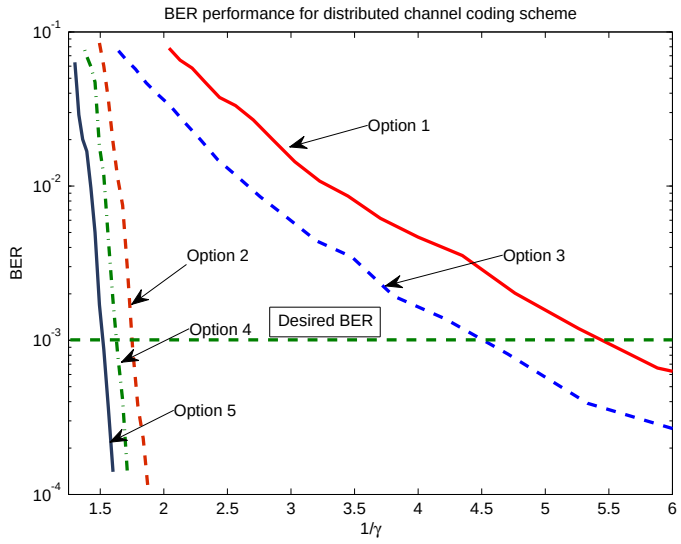

Figure 4.9: BER performance for distributed channel coding scheme.

codes (options 2, 4 and 5) perform much better than the one that utilize RSC

code (options 1 and 3). This is due to the existence of interleaver in turbo codes and its excellent concatenated structure.

A more evident prove can be found in Figure 4.10. In the same link (source-

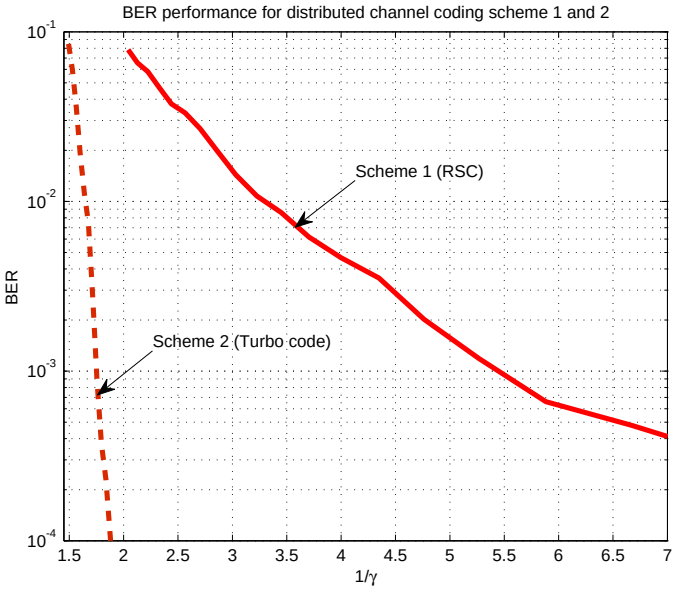

Figure 4.10: BER performance for distributed channel coding options, comparison between RSC and turbo codes.

to-destination direct link), turbo codes gain almost 8 units of $1/\gamma$ at level 10^{-3} compared with RSC codes. If the relay cooperates with the source to supply redundant information but using RSC codes as well, the performance does not improve so much as the turbo codes, as illustrated in Figure 4.11. It is obvious that only if turbo codes are employed, the performance can be greatly improved. Then with the help of relay, more improvements can be achieved, as shown in Figure 4.12. Comparing the option 4 with option 2, the relay helped option gained only 0.1 unit of $1/\gamma$. Even by changing one part of turbo code component output (from x_s to x'_s), the improvement from option 4 to option 5 is still 0.1 unit of $1/\gamma$.

For a quantitative comparison, Table 4.3 illustrates the maximum SαS interference dispersion γ with which the option can achieve a 10^{-3} BER. From Table 4.3, it is seen that option 5 has a largest tolerance for interference dispersion γ or SNR. The tolerance order for options is then $5 \rightarrow 4 \rightarrow 2 \rightarrow 3 \rightarrow 1$. Hence the turbo code decoding methods allow more tolerance than that of RSC codes.

Base on the BER demand and Table 4.3, we have a scheme selection strategy as shown in Table 4.4. The order established shows a selection strategy depending on the value of interference dispersion. If the interference dispersion is

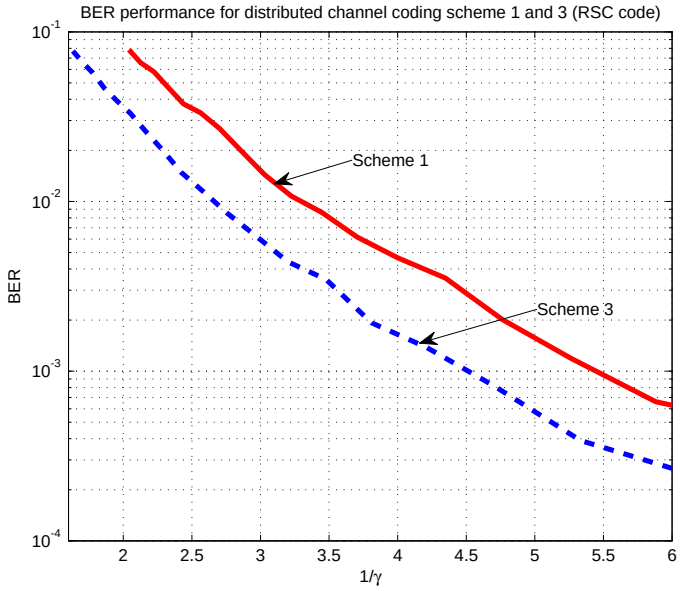

Figure 4.11: BER performance for distributed channel coding options for RSC codes.

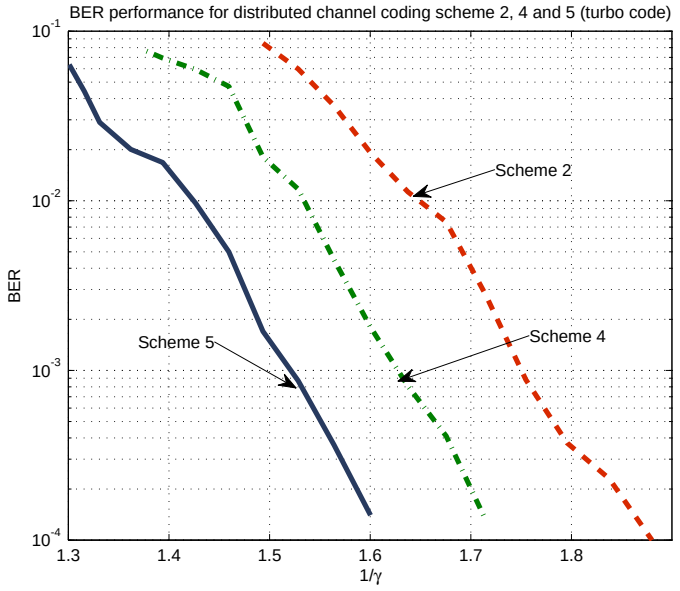

Figure 4.12: BER performance for distributed channel coding options for turbo codes.

Option	$1/\gamma$	γ
1 (RSC)	5.45	0.183
2 (turbo)	1.75	0.571
3 (RSC)	4.55	0.220
4 (turbo)	1.63	0.613
5 (turbo)	1.52	0.658

Table 4.3: Comparison of maximum interference dispersion γ to achieve 10^{-3} BER.

estimated after receiving the signal, an approximate choice of option can ensure a certain level of BER.

range of γ	option chosen
$\gamma < 0.183$	1
$\gamma < 0.220$	3
$\gamma < 0.571$	2
$\gamma < 0.613$	4
$\gamma < 0.658$	5
$\gamma > 0.658$	impossible for decoding

Table 4.4: Distributed channel coding scheme selection depending on the value of interference dispersion γ.

As the energy consumption depends very much on the data transmission, the first choice is obviously the best one, if the direct source-to-destination link has a less interfered channel that fulfils the BER performance. Then by considering Table 4.2 and 4.4, the option 4 should be a second choice when the direct link is disturbed heavily. This option allows to have a good performance by employing distributed turbo codes but raising a low energy consumption. However, option 3 does not seems to be interesting due to its poor performance compared with others except option 1 and due to its still high consumption of energy with the help of relay. If we consider that the consumption of energy is proportional to the amount of transmitted data, the use of the relay is only interesting when γ is larger than 0.571 (option 4 or option 5) to offer the best possible performance. The difference of the quality in the links involved in the communications (relayed or direct) will importantly impact on the preferred option and further studies are needed to draw general conclusions.

4.4 Conclusion

In this chapter, we have introduced distributed channel coding technique in the sense of minimising network energy consumption. With the help of relay, cooperative communications were established thus one part of encoding and decoding operations can be shared by relay. A distributed channel coding topology was proposed, with a Viterbi decoder, an interleaver and another RSC encoder at relay, and a RSC encoder at source. Depending on the different proposed distributed channel coding options, either RSC codes or turbo codes would be composed at destination, leading to different performance and energy consumption. Through a simple but illustrative simulation, the decoding and energy saving performance were studied for all the proposed options. Simulation results showed that the RSC coding for the direct source-to-destination link should be the best choice if the direct link channel was not badly interfered, according to the demanded BER performance level. Then the distributed turbo coding which benefits from the help of relay should be a best backup candidate. These proposed options and their performance comparison imply that, with a good configuration of cooperative network resources and an appropriate distributed channel coding strategy, a considerable energy saving and decoding performance improvement can be made, which leads to a flexible and "green" network.

General conclusion

In this thesis, a perspective on Internet of Things and sensor networks is investigated. The multiple-access-interference (MAI) encountered especially in dense sensor networks presents an impulsive behaviour. Conventional decoding or receiving approaches developed under the Gaussian assumption cannot deal with such an interference environment and will cause a significant performance degradation. Stable laws have proved to be accurate models for impulsive interference and its symmetric sub-family, noted as symmetric α-stable (SαS) distribution, was employed in this thesis, due to its heavy-tail property. While the second-order moments of a SαS variable is infinite when $\alpha < 2$, the geometric power framework was utilised as an alternative interference strength measurement, the geometric signal-to-noise ratio (SNR) was then defined accordingly.

The direct link was studied in the first time, by applying turbo codes as for their powerful decoding performance. The BCJR MAP decoding algorithm was chosen but the decoding metric should be replaced to adapt to the interference model and the explicit PDF expressions of general SαS random variables are lacking. The p-norm metric was proposed based on the fractional lower order moments (FLOMs) and α-stable norm, as an adapted decoding metric. Simulations were carried out for a comparison between the novel metric and the conventional Euclidean distance, the other proposed approaches such as Huber function and numerical inverse Fourier transform were compared as well. Results of simulations showed that the classical metric using the Euclidean distance in decoders exhibited a very poor bit error rate (BER) performance in either MAI only or MAI plus Gaussian thermal noise environment. The Huber function cannot deal with very impulsive cases, especially when $\alpha \leqslant 1$. The utilisation of p-norm brought a considerable BER performance improvement even when the environment is very impulsive. Its performance approached also the optimal decoder realised by numerical method, whatever the value of α is taken. The p-norm is additionally a flexible metric because no interference parameter is needed or only a rough estimate of α is sufficient for $0 < p < \alpha$.

The whole network topology was considered in the second time, and cooperative communications were adopted to improve the interference rejection perfor-

mance. With the help of relays, several receiver designs can be carried out. We studied a two-hop decode-and-forward relaying communication where a set of relays was selected among all possibilities. The chosen relays are the ones having the minimum relay-to-destination channel loss among a set of candidates. We proposed an importance sampling approach for the calculation of the optimal decision statistics and several suboptimal receiver designs. Particularly, an original approximating strategy based on the Normal Inverse Gaussian (NIG) distribution was proposed. The simulation results showed that some parametric designs like the hole-puncher and soft-limiter receivers can have good BER performance if their thresholds are appropriately configured. The NIG approximation proved to be a very efficient approach. The p-norm receiver exhibited robust performance. Both the NIG and p-norm approaches perform close to the optimal receiver no matter which noise is dominant.

When considering energy consumption issue in sensors networks, a distributed channel coding strategy was proposed with the help of relay. Cooperative communications were established in the sense that one part of the encoding and decoding operations can be shared by relay. The relay was equipped with a Viterbi decoder, an interleaver and another RSC encoder. Either RSC or turbo codes would be composed at destination depending on the different proposed distributed decoding schemes. The decoding and energy saving performance were studied through an illustrative simulation. The results showed that implementing RSC codes on direct source-to-destination link should be the best choice if the channel is of good quality, meaning that the BER performance can achieve a target level. Otherwise, a distributed turbo codes with cooperation of relay should be the most effective scheme in minimising both the error rate and energy consumption. Hence from the demonstration of network resources allocation, a good BER performance with low energy consumption strategy can be realised through a distributed channel coding scheme.

The work of this thesis proposed solutions to deal with an impulsive interference environment for both direct link and network topologies. However, we need further studies especially in the distributed coding schemes, in order that general conclusions can be drawn. It is already difficult for the interference and the cooperative channels. The impulsive nature of the network interference and the fact that stable distributions are good models do not facilitate things. For our study, it is in fact that a general framework is needed but many aspects are difficult to handle with stable interference. We can for instance mention that the dependency in time and space has important impacts when dealing with mobility and multiple antennas.

Appendix A

Power distribution

A.1 Assumptions

We consider a disc of radius R where N users are randomly placed following a uniform distribution.

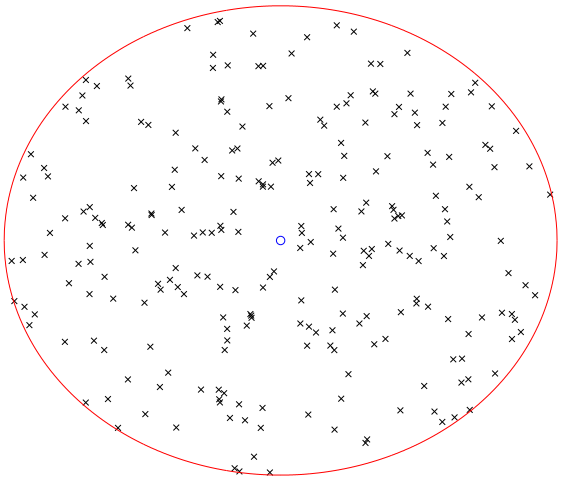

Figure A.1: Objects uniformly distributed in a circle. The object under study is in the centre of the environment.

Any of the object in the environment can be an interferer. The number κ of interferers depends on the users' density, the maximum range for a signal to be received and the activity in the network (number of simultaneous active users).

We can consider a Poisson distribution for this variable.

We ignore the near field transmission properties and consider that the received power is given by:

$$P_r \propto P_e d^{-a} \tag{A.1}$$

a is the attenuation coefficient which can take values between two and six. We can from (A.1) consider that the channel is given by:

$$\gamma = d_i^{-a} \tag{A.2}$$

A.2 Users' distribution

Let R be the radius of the considered area. If no condition is placed on the possible position of interferers, let F_d be the cumulative distribution of the distance from the considered receiver and one interferer:

$$F_d(x) = \mathbb{P}(d \leq x) = \frac{\pi x^2}{\pi R^2} = \frac{x^2}{R^2} \tag{A.3}$$

Equation (A.3) is valid for $0 \leq x \leq R$. Of course $F_d(x) = 0$ if $x < 0$ and $F_d(x) = 1$ if $x > R_M$.

The probability density function is then the derivative of $F_d(x)$:

$$f_d(x) = \frac{\mathrm{d}F}{\mathrm{d}x}(x) = \frac{2}{R^2}x \tag{A.4}$$

Equation (A.4) is valid for $0 \leq x \leq R$. Of course $f_d(x) = 0$ if $x < 0$ and $x > R_M$.

A.3 Interfering power distribution

We now consider the scenario from equation (A.2). We determine the distributions for distances d such as $0 \leq d \leq R$. Because $\gamma = d^{-\frac{a}{2}}$, this means that $R^{-\frac{a}{2}} \leq \gamma < +\infty$.

The cumulative distribution for one interfering power is then:

$$\begin{aligned} F_\gamma(x) &= \mathbb{P}(\gamma \leq x) \\ &= \mathbb{P}(d_i^{-\frac{a}{2}} \leq x) \\ &= \mathbb{P}(d_i^{\frac{a}{2}} \geq x^{-1}) \\ &= \mathbb{P}(d_i \geq x^{-\frac{2}{a}}) \\ &= 1 - F_d(x^{-\frac{2}{a}}) \\ &= 1 - \frac{x^{-\frac{4}{a}}}{R^2} \end{aligned} \tag{A.5}$$

For $x < R^{-\frac{a}{2}}$, $F_\gamma(x) = 0$.

The probability density function is then:

$$f_\gamma(x) = \frac{4x^{-\frac{4}{a}-1}}{aR^2} \tag{A.6}$$

For $x < R^{-\frac{a}{2}}$, $f_\gamma(x) = 0$.

A.4 Further remark

Let us now calculate the mean of γ in the case $a \neq 4$ which should be considered separately.:

$$\begin{aligned} \mathbb{E}[\gamma] &= \int_{R^{-\frac{a}{2}}}^{+\infty} x f_\gamma(x) \mathrm{d}x \\ &= \int_{R^{-\frac{a}{2}}}^{+\infty} x \frac{4x^{-\frac{4}{a}-1}}{aR^2} \mathrm{d}x \\ &= \int_{R^{-\frac{a}{2}}}^{+\infty} \frac{4x^{-\frac{4}{a}}}{aR^2} \mathrm{d}x \\ &= \frac{4}{aR^2} \left[\frac{x^{1-\frac{4}{a}}}{1-\frac{4}{a}} \right]_{R^{-\frac{a}{2}}}^{+\infty} \end{aligned} \tag{A.7}$$

If $a > 4$, $\mathbb{E}[\gamma]$ will tend towards infinity. If $a = 4$, we would obtain a similar conclusion. Finally, if $a < 4$, $m = \mathbb{E}[\gamma] = \frac{4R^{-\frac{a}{2}}}{4-a}$.

We now have a look on the variance of γ.

$$\begin{aligned}\mathbb{E}\left[\gamma^2\right] &= \int_{R^{-\frac{a}{2}}}^{+\infty} x^2 f_\gamma(x)\mathrm{d}x \\ &= \int_{R^{-\frac{a}{2}}}^{+\infty} x^2 \frac{4x^{-\frac{4}{a}-1}}{aR^2}\mathrm{d}x \\ &= \int_{R^{-\frac{a}{2}}}^{+\infty} \frac{4x^{-\frac{4}{a}+1}}{aR^2}\mathrm{d}x \\ &= \frac{4}{aR^2}\left[\frac{x^{2-\frac{4}{a}}}{2-\frac{4}{a}}\right]_{R^{-\frac{a}{2}}}^{+\infty}\end{aligned} \tag{A.8}$$

When $a > 2$, the variance of γ is infinite. In that case the central limit theorem does not apply and we should use the generalized central limit theorem [64, Definition 1.1.5 page 5], [58, Theorem 2 page 22]. We can then expect that the multiple access interference from 1.19 falls into the attraction domain of an α-stable distribution. This is essentially the consequence of neglecting the near field but it happens that this approximation is acceptable in many applications.

Appendix B

First limit calculation

In this appendix we want to determine the limit of the first term in (1.25).

$$\lim_{R\to+\infty} \lambda\pi R^2 \left(\phi_\psi\left(\omega R^{-\frac{a}{2}}\right) - 1\right) \tag{B.1}$$

Since ψ is a random variable with mean 0 and a finite variance σ^2_{psi}, we can give the Taylor expansion of $\phi_\psi(x)$, for x near 0, to get the approximations:

$$\phi_\psi(x) = 1 - \frac{\sigma^2_\psi}{2}x^2 + o(x^2). \tag{B.2}$$

Using (B.2), we can approximate $\phi_\psi\left(\omega R^{-\frac{a}{2}}\right)$ when $R \to +\infty$ and obtain:

$$\begin{aligned} \lambda\pi R^2 \left(\phi_\psi\left(\omega R^{-\frac{a}{2}}\right) - 1\right) &= \lambda\pi R^2 \left(1 - \frac{\sigma^2_{\phi_\psi}}{2}\left(\omega R^{-\frac{a}{2}}\right)^2 + o\left(\omega^2 R^{-a}\right) - 1\right) \\ &= \lambda\pi \left(\frac{\sigma^2_{\phi_\psi}}{2}\omega^2 R^{2-a} + \omega^2 o\left(R^{2-a}\right)\right) \end{aligned} \tag{B.3}$$

When $a > 2$, R^{2-a} tends towards 0, so:

$$\lim_{R\to+\infty} \lambda\pi R^2 \left(\phi_\psi\left(\omega R^{-\frac{a}{2}}\right) - 1\right) = 0 \tag{B.4}$$

Appendix C

Second limit existence

In this appendix we want to determine the existence of the second term in (1.25):

$$\lim_{R\to+\infty}\left(\lambda\pi\omega^{\frac{4}{a}}\int_{\omega R^{-\frac{a}{2}}}^{+\infty}\frac{d\phi_\psi}{du}(u)\,u^{-\frac{4}{a}}du\right) \tag{C.1}$$

Similarly as in annex B, using the fact that ψ is a random variable with mean 0 and a finite variance σ^2_{psi}, we can give the Taylor expansion of $\phi_\psi(x)$ in (B.2), for x near 0, to get this second approximation:

$$\frac{d\phi_\psi}{dx}(x) = -\sigma^2_{psi}x + o(x). \tag{C.2}$$

We use (C.2) to approximate $\frac{d\phi_\psi}{du}(u)$ when $R\to+\infty$ and obtain:

$$\frac{d\phi_\psi}{du}(u)\,u^{-\frac{4}{a}}du = \left(\sigma^2_{\phi_\psi}u + o(u)\right)u^{-\frac{4}{a}}du \tag{C.3}$$

We can the write the primitive of the product of $u^{-\frac{4}{a}}$ by u. If it exists in zero, the limit will exist:

$$\int u^{-\frac{4}{a}}udu = \int u^{1-\frac{4}{a}}du = \frac{u^{2-\frac{4}{a}}}{2-\frac{4}{a}} \tag{C.4}$$

If $a>2$, $2-\frac{4}{a}>0$, the primitive in (C.4) exists when R tends towards infinity ($u\to 0$) (and is equal to 0).

Appendix D

Bayes' rule and its useful expansions

For any two random variables X and Y, the joint probability of X and Y, $P(X,Y)$, can be expressed as a function of the conditional probability of X and Y, $P(X/Y)$, as

$$P(X,Y) = P(X/Y)P(Y). \tag{D.1}$$

For the joint random variables $U = \{X,Y\}$, $V = \{Y,Z\}$, the Bayes' rule and equation (D.1) lead to the following expression:

$$\begin{aligned} P(\{X,Y\}/Z) = P(U/Z) = \frac{P(U,Z)}{P(Z)} = \frac{P(X,Y,Z)}{P(Z)} = \frac{P(X,V)}{P(Z)} = \frac{P(X/V)P(V)}{P(Z)} \\ = \frac{P(X/\{Y,Z\})P(Y,Z)}{P(Z)} = P(X/\{Y,Z\})P(Y/Z). \end{aligned} \tag{D.2}$$

Bibliography

[1] S. Ambike, J. Ilow, and D. Hatzinakos. “Detection for binary transmission in a mixture of Gaussian noise and impulsive noise modeled as an alpha-stable process”. In: *Signal Processing Letters, IEEE* 1.3 (Mar. 1994), pp. 55 –57.

[2] L. R. Bahl et al. “Optimal decoding of linear codes for minimizing symbol error rate”. In: *IEEE Trans. Inform. Theory* 20.2 (Mar. 1974), pp. 284–287.

[3] Ole E. Barndorff-Nielsen and Neil Shephard. *Normal Modified Stable Processes*. Economics Series Working Papers 072. University of Oxford, Department of Economics, 2001.

[4] N. C. Beaulieu and S. Niranjayan. “New UWB receiver designs based on a Gaussien-Laplacian noise-plus-MAI model”. In: *Proc. IEEE Int. Conf. on Commum.* Glasgow, Scotland, June 2007, pp. 4128–4133.

[5] N. C. Beaulieu, H. Shao, and J. Fiorina. “P-order metric UWB receiver structures with superior performance”. In: *IEEE Trans. Commun.* 56 (Oct. 2008), pp. 1666–1676.

[6] N. C. Beaulieu and D. J. Young. “Designing Time-Hopping Ultrawide Bandwidth Receivers for Multiuser Interference Environments”. In: *Proceedings of the IEEE*. Vol. 97. 2. Feb. 2009, pp. 255–284.

[7] C. Berrou and A. Glavieux. “Near optimum error correcting coding and decoding: turbo-codes”. In: *IEEE Trans. Commun.* 44.10 (Oct. 1996), pp. 1261–1271.

[8] C. Berrou, A. Glavieux, and P. Thitimajshima. “Near Shannon limit error-correcting coding and decoding: Turbo-codes. 1”. In: *Communications, 1993. ICC 93. Geneva. Technical Program, Conference Record, IEEE International Conference on*. Vol. 2. May 1993, 1064 –1070 vol.2.

[9] P. Besbeas and B. Morgan. “Improved estimation of the stable laws”. In: *Statistics and Computing* 18.2 (2008), pp. 219–231.

[10] P.H. Borcherds. “Importance sampling: an illustrative introduction”. In: *European Journal of Physics* 21.5 (2000), p. 405.

[11] G. Bresler, A. Parekh, and D.N.C. Tse. “The Approximate Capacity of the Many-to-One and One-to-Many Gaussian Interference Channels”. In: *IEEE Trans. Inform. Theory* 56.9 (2010), pp. 4566–4592.

[12] B.W. Brorsen and S. Yang. “Maximum likelihood estimates of symmetric stable distribution parameters”. In: *Communications in statistics. Simulation and computation* 19.4 (1990), pp. 1459–1464.

[13] C.L. Brown and A.M. Zoubir. “A nonparametric approach to signal detection in impulsive interference”. In: *Signal Processing, IEEE Transactions on* 48.9 (Sept. 2000), pp. 2665 –2669.

[14] B.Zhao and M.C. Valenti. “Distributed turbo coded diversity for relay channel”. In: *Electronics letters* 39.10 (May 2003), pp. 786 –787.

[15] J. Cain, G. Clark, and J. Geist. “Punctured convolutional codes of rate (n-1)/n and simplified maximum likelihood decoding (Corresp.)” In: *Information Theory, IEEE Transactions on* 25.1 (Jan. 1979), pp. 97 –100.

[16] O.. Canpolat, M.. Uysal, and M.M. Fareed. “Analysis and Design of Distributed Space–Time Trellis Codes With Amplify-and-Forward Relaying”. In: *Vehicular Technology, IEEE Transactions on* 56.4 (2007), pp. 1649 –1660. ISSN: 0018-9545.

[17] A. B. Carleial. “Interference channels”. In: *IEEE Trans. Inform. Theory* 24.1 (Jan. 1978), pp. 60–70.

[18] A. Chakrabarti et al. “Low density parity check codes for the relay channel”. In: *Selected Areas in Communications, IEEE Journal on* 25.2 (2007), pp. 280 –291. ISSN: 0733-8716.

[19] J. M. Chambers, C. L. Mallows, and B. W. Stuck. “A method for simulating stable random variables”. In: *Journal of the American Statistical Association* 71 (1976), pp. 340–344.

[20] M. Chiani. “Analytical distribution of linearly modulated cochannel interferers”. In: *Communications, IEEE Transactions on* 45.1 (Jan. 1997), pp. 73 –79.

[21] M. A. Chitre, J. R. Potter, and S. H. Ong. “Viterbi Decoding of Convolutional Codes in Symmetric α-Stable Noise”. In: *IEEE Trans. Commun.* (Dec. 2007), pp. 2230–2233.

[22] N. Chiurtu, B. Rimoldi, and E. Telatar. “On the capacity of multi-antenna Gaussian channels”. In: *Information Theory, 2001. Proceedings. 2001 IEEE International Symposium on*. 2001, p. 53.

[23] T. C. Chuah. “Distance metric for soft-decision decoding in non-Gaussian channels”. In: *Electronics Letters* (July 2003), pp. 1062–1063.

[24] T. C. Chuah. “Robust iterative decoding of turbo codes in heavy-tailed noise”. In: *IEE Proceedings Commun.* Feb. 2005, pp. 29–38.

[25] R. Dabora, I. Maric, and A. Goldsmith. “Relay strategies for interference-forwarding”. In: *IEEE Information Theory Workshop ITW ’08*. 2008, pp. 46–50.

[26] M. Denny. “Introduction to importance sampling in rare-event simulations”. In: *European Journal of Physics* 22.4 (2001), p. 403.

[27] M. Dohler and Y. Li. *Cooperative communications: hardware, channel & phy*. Wiley & Sons, 2010.

[28] M. Dohler et al. “Near-optimum transmit power allocation for space-time block encoded wireless communication systems”. In: *Communications, IEE Proceedings-* 153.3 (2006), pp. 459 –463.

[29] W. DuMouchel. “On the Asymptotic Normality of the Maximum-Likelihood Estimate when Sampling from a Stable Distribution”. In: *Annals of Statistics* 3 (1973), pp. 948–957.

[30] T. Erseghe. “A Low-Complexity Impulse Radio Receiver Based Upon Gaussian Mixtures”. In: *IEEE Int. Conf. on Communications, ICC 2007*. June 2007, pp. 4311–4316.

[31] E. F. Fama and R. Roll. “Parameter estimates for symmetric stable distributions”. In: *Journal of the American Statistical Association* 66.334 (1971), pp. 331–338.

[32] Lisheng Fan et al. “On Distribution of SaS Noise and its Application in Performance Analysis for Linear Rake Receivers”. In: *Communications Letters, IEEE* 16.2 (2012), pp. 186 –189. ISSN: 1089-7798.

[33] J. Fiorina. “A simple IR-UWB receiver adapted to Multi-User Interferences”. In: *IEEE Global Telecommunications Conf., GLOBECOM 2006*. Nov. 2006, pp. 1–4.

[34] J. Fiorina and W. Hachem. “On the asymptotic distribution of the correlation receiver output for time-hopped UWB signals”. In: *IEEE Trans. Signal Processing* 54.7 (July 2006), pp. 2529–2545.

[35] Gerard J. Foschini. “Layered space-time architecture for wireless communication in a fading environment when using multi-element antennas”. In: *Bell Labs Technical Journal* 1.2 (1996), pp. 41–59. ISSN: 1538-7305.

[36] J. Friedmann, H. Messer, and J.F. Cardoso. “Robust parameter estimation of a deterministic signal in impulsive noise”. In: *IEEE Trans. Signal Processing* 48.4 (Apr. 2000), pp. 935–942.

[37] R.K. Ganti, F. Baccelli, and J.G. Andrews. “Series Expansion for Interference in Wireless Networks”. In: *IEEE Trans. Inform. Theory* 58.4 (Apr. 2012), pp. 2194 –2205. ISSN: 0018-9448.

[38] H. E. Ghannudi et al. “α-stable interference modeling and Cauchy receiver for an IR-UWB *ad hoc* network”. In: *IEEE Trans. Commun.* 58 (June 2010), pp. 1748–1757.

[39] H. El Ghannudi, L. Clavier, and P.A. Rolland. “Modeling Multiple Access Interference in Ad Hoc Networks Based on IR-UWB Signals Up-Converted to 60 GHz”. In: *European Conference on Wireless Technologies*. Munich, Germany, Oct. 2007, pp. 106–109.

[40] J. G. Gonzalez, J. L. Paredes, and G. R. Arce. “Zero-Order Statistics: A Mathematical Framework for the Processing and Characterization of Very Impulsive Signals”. In: *IEEE Trans. Signal Process.* 54.10 (Oct. 2006), pp. 3839–3850.

[41] T. S. Han and K. Kobayashi. “A new Achievable Rate Region for the Interference Channel”. In: *IEEE Trans. Inform. Theory* 27.1 (Jan. 1981), pp. 49–60.

[42] Y.W.P. Hong, W.J. Huang, and C.C.J. Kuo. *Cooperative Communications and Networking: Technologies and System Design*. Springer, 2010. ISBN: 9781441971937.

[43] Jun Hu and T.M. Duman. “Low Density Parity Check Codes over Wireless Relay Channels”. In: *Wireless Communications, IEEE Transactions on* 6.9 (2007), pp. 3384 –3394. ISSN: 1536-1276.

[44] P.J. Huber. *Robust Statistics*. Wiley Series in Probability and Statistics. John Wiley & Sons, 2003. ISBN: 9780471650720.

[45] M. Janani et al. “Coded cooperation in wireless communications: space-time transmission and iterative decoding”. In: *Signal Processing, IEEE Transactions on* 52.2 (2004), pp. 362 –371. ISSN: 1053-587X.

[46] D.H. Johnson. “Optimal Linear Detectors for Additive Noise Channels”. In: *IEEE Trans. Signal Processing* 44.12 (Dec. 1996), pp. 3079–3084.

[47] S. A. Kassam. *Signal Detection in Non-Gaussian Noise*. Amsterdam, The Netherlands: Springer-Verlag, 1998.

[48] Marios Kountouris and Jeffrey G. Andrews. “Downlink SDMA with Limited Feedback in Interference-Limited Wireless Networks”. In: *Wireless Communications, IEEE Transactions on* 11.8 (Aug. 2012), pp. 2730 –2741.

[49] I. A. Koutrouvelis. “Regression-type estimation of the parameters of stable laws”. In: *Journal of the American Statistical Association* 75 (1980), pp. 918–928.

[50] E. E. Kuruoglu, W. J. Fitzgerald, and P. J. W. Rayner. “Near Optimal Detection of Signals in Impulsive Noise Modeled with a Symmetric α-Stable Distribution”. In: *IEEE Commun. Lett.* 2 (1998), pp. 282–284.

[51] W. Li, J. Wei, and M. Smith. “Performance and Capacity Analysis of UWB Networks over 60GHz WPAN Channel”. In: *Journal of Communications* 3.1, Academy Publisher (Jan. 2008), pp. 51–55.

[52] Yonghui Li et al. “Distributed turbo coding with selective relaying”. In: *Personal, Indoor and Mobile Radio Communications, 2009 IEEE 20th International Symposium on*. 2009, pp. 1702 –1706.

[53] Samuel R. Madden et al. “TAG: A Tiny AGgregation service for ad-hoc sensor networks”. In: *Fifth Annual Symposium on Operating Systems Design and Implementation*. Dec. 2002, pp. 131–146.

[54] J. H. McCulloch. “Simple Consistent Estimators of Stable distribution Parameters”. In: *Communications on Satatistical Simulations* 15.4 (1986), pp. 1109–1136.

[55] A.F. Molisch, J.R. Foerster, and M. Pendergrass. “Channel models for ultrawideband personal area networks”. In: *IEEE Wireless Commun. Mag.* 10.6 (Dec. 2003), pp. 14–21.

[56] A.F. Molisch et al. “A Comprehensive Standardized Model for Ultrawideband Propagation Channels”. In: *IEEE Trans. Antennas Propagat.* 54.11, part 1 (Nov. 2006), pp. 3151–3166.

[57] J.C. Moreira and P.G. Farrell. *Essentials of Error-Control Coding*. Wiley, 2006. ISBN: 9780470035719.

[58] C. L. Nikias and M. Shao. *Signal Processing with alpha-Stable Distributions and Applications*. New York: Wiley, 1995.

[59] S. Niranjayan and N.C. Beaulieu. “BER optimal linear combiner for signal detection in symmetric alpha-stable noise: small values of alpha”. In: *Wireless Communications, IEEE Transactions on* 9.3 (Mar. 2010), pp. 886 –890.

[60] P.C. Pinto and M.Z. Win. “Communication in a Poisson Field of Interferers–Part I: Interference Distribution and Error Probability”. In: *IEEE Trans. Wireless Commun.* 9.7 (July 2010), pp. 2176–2186.

[61] P.C. Pinto and M.Z. Win. “Communication in a Poisson Field of Interferers-Part II: Channel Capacity and Interference Spectrum”. In: *IEEE Trans. Wireless Commun.* 9.7 (July 2010), pp. 2187–2195.

[62] J. G. Proakis and M. Salehi. *Communication Systems Engineering, Second Edition*. New Jersey: Prentice Hall, 2002.

[63] A. Rabbachin et al. “Cognitive Network Interference”. In: *IEEE J. Select. Areas Commun.* 29.2 (Feb. 2011), pp. 480–493.

[64] G. Samorodnitsky and M.S. Taqqu. “Stable non-Gaussian processes: Stochastic models with infinite variance”. In: (1994).

[65] H. Sato. “The capacity of the Gaussian interference channel under strong interference”. In: *IEEE Trans. Inform. Theory* 27.6 (Nov. 1981), pp. 786–788.

[66] K. Seddik and K.J.R. Liu. “Distributed Space-Frequency Coding over Broadband Relay Channels”. In: *Wireless Communications, IEEE Transactions on* 7.11 (2008), pp. 4748 –4759. ISSN: 1536-1276.

[67] M. Shafieipour, H. S. Lim, and T. C. Chuah. “Decoding of Turbo Codes in Symmetric Alpha-Stable Noise”. In: *ISRN Signal Processing* 2011 (2011).

[68] M. Shao and C.L. Nikias. “Signal processing with fractional lower order moments: stable processes and their applications”. In: *Proceedings of the IEEE* 81.7 (July 1993), pp. 986 –1010.

[69] S. K. Singh, M. P. Singh, and D. K. Singh. “Energy Efficient Transmission Error Recovery for Wireless Sensor Networks”. In: *International Journal of Grid and Distributed Computing* 3.4 (Dec. 2010), pp. 89–104.

[70] M. R. Souryal et al. “Soft-Decision Metrics for Coded Orthogonal Signaling in Symmetric Alpha-Stable Noise”. In: *IEEE Trans. Signal Process.* 56.1 (Jan. 2008).

[71] E.S. Sousa. “Performance of a spread spectrum packet radio network link in a Poisson field of interferers”. In: *IEEE Trans. Inform. Theory* 38.6 (Nov. 1992), pp. 1743–1754.

[72] A. Stefanov and E. Erkip. “Cooperative space-time coding for wireless networks”. In: *Communications, IEEE Transactions on* 53.11 (2005), pp. 1804 –1809. ISSN: 0090-6778.

[73] G.A. Tsihrintzis, C.L. Nikias, and M. Shao. “Performance of Optimum and Suboptimum Receivers in the Presence of Impulsive Noise Modeled as an Alpha-stable Process”. In: *IEEE Trans. Commun.* 43.2 (Feb. 1995), pp. 904–914.

[74] Sergio Verdu. *Multiuser Detection*. Cambridge, U.K.: Cambridge University Press, 1998.

[75] E. J. Wegman, S. C. Schwartz, and J. B. Thomas. *Topics in Non-Gaussian Signal Processing*. New York: Springer, 1989.

[76] R. Weron. *Performance of the estimators of stable law parameters*. Reserach Report HSC/95/1. Hugo Steinhaus Center for Stochastic Methods. 1991.

[77] M. Z. Win, P. C. Pinto, and L. S. Shepp. “A Mathematical Theory of Network Interference and Its Applications”. In: *Proceedings of the IEEE*. Vol. 97. 2. Feb. 2009, pp. 205–230.

[78] M.Z. Win, P.C. Pinto, and L.A. Shepp. “A Mathematical Theory of Network Interference and Its Applications”. In: *Proc. IEEE* 97.2 (Feb. 2009), pp. 205–230.

[79] J. Winters. “On the Capacity of Radio Communication Systems with Diversity in a Rayleigh Fading Environment”. In: *Selected Areas in Communications, IEEE Journal on* 5.5 (June 1987), pp. 871 –878.

[80] J. P. Woodard and L. Hanzo. “Comparative study of turbo decoding techniques: an overview”. In: *IEEE Trans. Vehicular Tech.* (Nov. 2000), pp. 2208–2233.

[81] Dong Xu et al. “A robust decoder for distributed turbo codes in relay channel”. In: *Applied Sciences in Biomedical and Communication Technologies (ISABEL), 2010 3rd International Symposium on*. Nov. 2010, pp. 1–5.

[82] Simon Yiu, R. Schober, and L. Lampe. “Decentralized distributed space-time trellis coding”. In: *Wireless Communications, IEEE Transactions on* 6.11 (2007), pp. 3985 –3993.

[83] Jinhong Yuan et al. “Distributed space-time trellis codes for a cooperative system”. In: *Wireless Communications, IEEE Transactions on* 8.10 (2009), pp. 4897 –4905.

[84] Wei Zhang et al. “Distributed Space-Frequency Coding for Cooperative Diversity in Broadband Wireless Ad Hoc Networks”. In: *Wireless Communications, IEEE Transactions on* 7.3 (2008), pp. 995–1003. ISSN: 1536-1276.

[85] Zheng Zhang and T.M. Duman. “Capacity-approaching turbo coding and iterative decoding for relay channels”. In: *Communications, IEEE Transactions on* 53.11 (2005), pp. 1895 –1905. ISSN: 0090-6778.

[86] V.M. Zolotarev. *One-dimensional stable distributions (translations of mathematical monographs, vol. 65)*. The American Mathematical Society, 1986.

[87] S. Zozor, J.M. Brossier, and P.O. Amblard. “A Parametric Approach to Suboptimal Signal Detection in α-stable Noise”. In: *IEEE Trans. Signal Processing* 54.12 (Dec. 2006), pp. 4497–4509.

Publications

Journal papers

- Gu W.; Clavier, L., "Decoding Metric Study for Turbo Codes in Very Impulsive Environment," *Communications Letters, IEEE*, vol.16, no.2, pp.256-258, February 2012.

Conference papers

- Gu, Wei; Peters, Gareth; Clavier, Laurent; Septier, Francois; Nevat, Ido;, "Receiver study for cooperative communications in convolved additive α-stable interference plus Gaussian thermal noise," *Wireless Communication Systems (ISWCS), 2012 International Symposium on*, pp.451-455, 28-31 Aug., 2012.
- Gu W.; Clavier, L.; Rolland, N.; Rolland, P.-A., "Turbo code decoding in MAI environment," *Turbo Codes and Iterative Information Processing (ISTC), 2010 6th International Symposium on*, pp.206-210, 6-10 Sept. 2010.

Abstract

Internet of Things brought great interests in recent years for its attractive applications and intelligent structure. However, the implementation of sensor networks still presents important challenges such as the generation of Multiple-Access-Interference (MAI) with impulsive nature and the relatively high energy consumption. Both the MAI and the thermal noise should be considered due to their strong impairments each may cause on the communication quality. We employ the stable and Gaussian distributions to model the MAI and the thermal noise respectively. Firstly we study the performance of turbo codes in the direct link and we propose the p-norm as a decoding metric. This metric allows a considerable error correction performance improvement which is close to the optimal decoder. Then we investigate cooperative communications. The probability densities in the decision statistic of the optimal receiver are estimated using importance sampling approach when both the stable and Gaussian noises are present. Such a method is computationally expensive. Hence we develop an approximation approach based on the Normal Inverse Gaussian (NIG) distribution. This solution is efficient for calculation and is proximate to the optimal receiver. In addition we show that the p-norm receiver has robust performance no matter what kind of noise is dominant. At last we combine the channel coding and cooperative communication works to establish a distributed channel coding strategy. Through some simulation assessments, the energy saving strategy can be realized by choosing an appropriate distributed channel coding scheme based on the direct link quality and target bit error rate.

Keywords: Sensor networks, Multiple-Access-Interference, stable distribution, turbo codes, cooperative communications, distributed channel coding

Résumé

L'Internet des objets, plus particulièrement les réseaux de capteurs, a attiré beaucoup d'attention ces dernières années. Sa mise en œuvre soulève de nombreuses difficultés, comme la génération d'interférences d'accès multiple (MAI) à caractère impulsif et la consommation d'énergie relativement forte. Les MAI et le bruit thermique doivent être considérés simultanément car ils perturbent fortement les communications. Nous modélisons les MAI et le bruit thermique respectivement par la distribution stable et gaussienne. Nous étudions tout d'abord l'effet des turbo codes sur le lien direct en utilisant la norme-p comme métrique de décodage. Cette métrique permet une performance de correction d'erreur proche du décodeur optimal. Ensuite nous nous penchons sur les communications coopératives. A l'aide de l'échantillonnage préférentiel, nous estimons les densités de probabilité de la décision statistique du récepteur optimal en présence des bruits stable et gaussien. Cette approche est coûteuse en calcul. Nous proposons donc d'approximer ces densités de probabilité par la distribution gaussienne inverse normale (NIG). Cette solution de calcul est efficace pour approcher le récepteur optimal. Nous montrons également que le récepteur utilisant la norme-p a des performances robustes, quel que soit le type de bruit dominant. A la fin nous combinons les travaux du codage canal et des communications coopératives pour établir une stratégie de codage canal distribué. Basé sur la qualité du lien direct et le niveau de taux d'erreur binaire envisagé, la stratégie d'économie d'énergie peut être mise en place via le choix d'un schéma de codage canal distribué.

Mots clés: réseaux de capteurs, interférences d'accès multiple, distribution stable, turbo-codes, communications coopératives, codage canal distribué